Netherlands organization for applied scientific research

TNO Committee on Hydrological Research

Netherlands Remote Sensing Board

Water management and remote sensing

Proceedings and information No. 42
Verslagen en Mededelingen No. 42

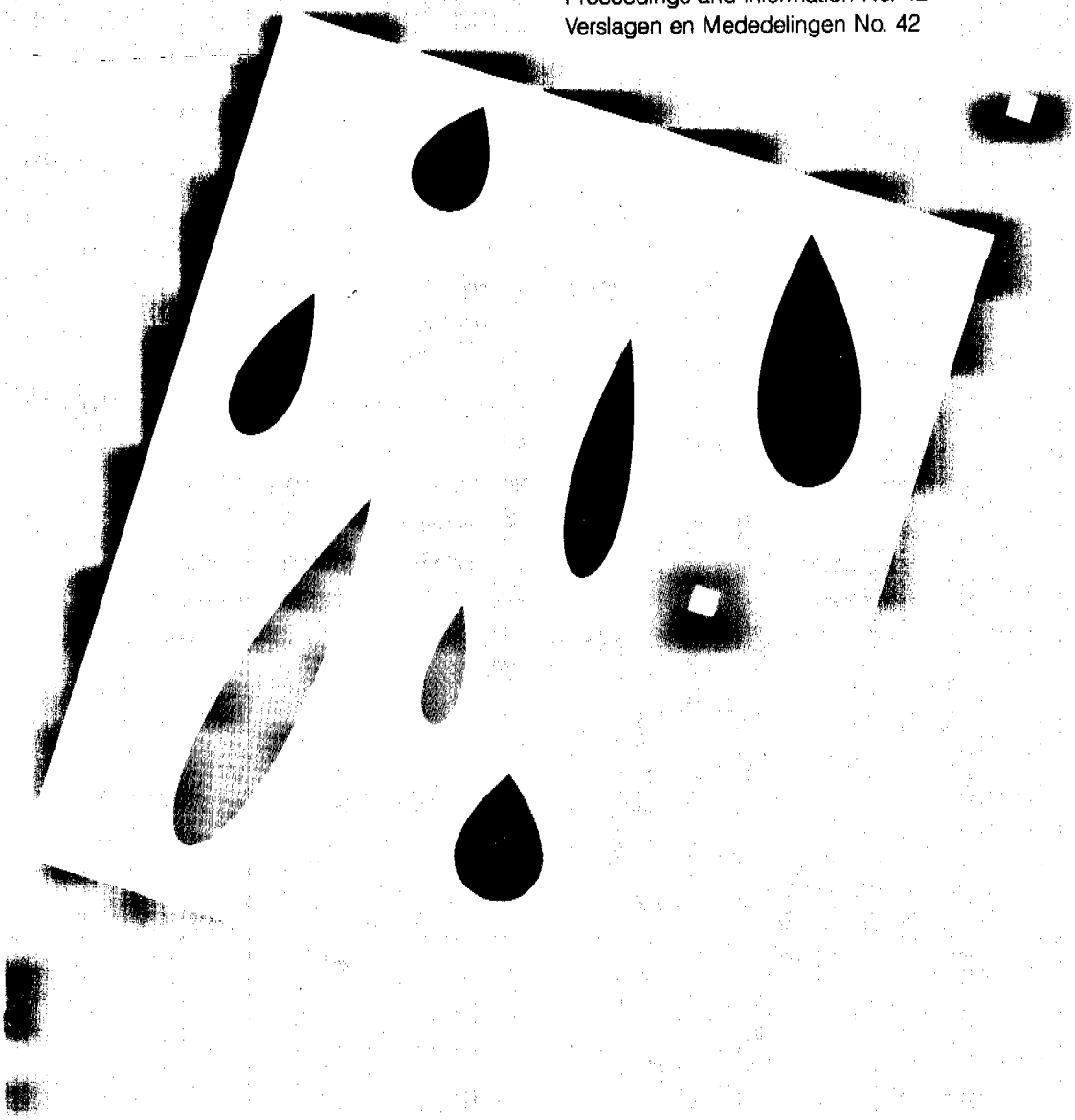

Water management and remote sensing

CIP-DATA

Water

Water management and remote sensing: Technical Meeting 47, Wageningen, The Netherlands, 7 November 1989/ ed. J.C. Hooghart -
The Hague: TNO Committee on Hydrological Research
- Illustrations - (Proceedings and information/TNO Committee on Hydrological Research; no. 42)
With index, ref.
ISBN 90-6743-170-2
SISO 573.3 UDC 528.88: 556.18
Subject heading: water management, remote sensing.

TNO Committee
on Hydrological
Research

Netherlands
Remote Sensing
Board

Water management and remote sensing

Proceedings and information No. 42
Verslagen en Mededelingen No. 42

Editor
J.C. Hooghart

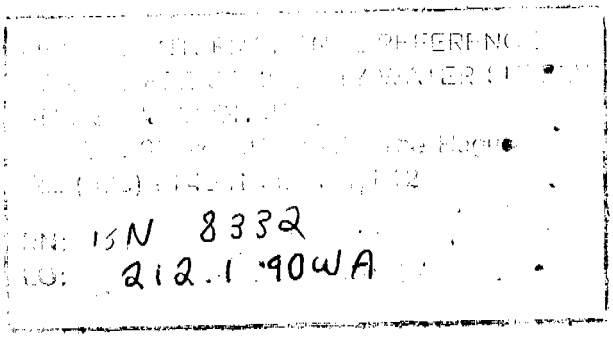

Technical Meeting 47
Wageningen, The Netherlands
7 November 1989

Published with support of the
Netherlands Remote Sensing Board

The Hague 1990

CHO

bcrs

CONTENTS

AUTHORS

S. van den Assem	Agricultural University of Wageningen, Department of Hydrology, Soil Physics and Hydraulics/Department of Meteorology, Wageningen
W.G.M. Bastiaanssen	The Winand Staring Centre for Integrated Land, Soil and Water Research, Wageningen
T.H.L. Claassen	Province of Friesland, Department of Water Management and Environment, Leeuwarden
R.A. Feddes	The Winand Staring Centre for Integrated Land, Soil and Water Research, Wageningen January 1990: Agricultural University of Wageningen, Department of Hydrology, Soil Physics and Hydraulics, Wageningen
M. Menenti	The Winand Staring Centre for Integrated Land, Soil and Water Research, Wageningen
P. Minderhoud	DHV Raadgevend Ingenieursbureau B.V., Amersfoort

G.J.A. Nieuwenhuis — The Winand Staring Centre for Integrated Land, Soil and Water Research, Wageningen

J. van Nieuwkoop — Euroconsult B.V., Arnhem

H.T.C. van Stokkom — Rijkswaterstaat, Survey Department, Delft

G.N.M. Stokman — Rijkswaterstaat, Institute for Inland Water Management and Waste Water Treatment, Lelystad

H.A.M. Thunnissen — The Winand Staring Centre for Integrated Land, Soil and Water Research, Wageningen

T.N.M. Visser — The Winand Staring Centre for Integrated Land, Soil and Water Research, Wageningen

INTRODUCTION

R.A. Feddes

In modern water management detailed information is required on processes that occur and on the state of water systems, including the way they are influenced by human activities. Remote sensing can contribute significantly to these information. For example, areal patterns of water quality parameters such as suspended solids and algae, and physical and hydrological conditions of the soil can be directly observed. Moreover, with successive synoptical images, remote sensing provides the opportunity in monitoring temporal changes over large areas.

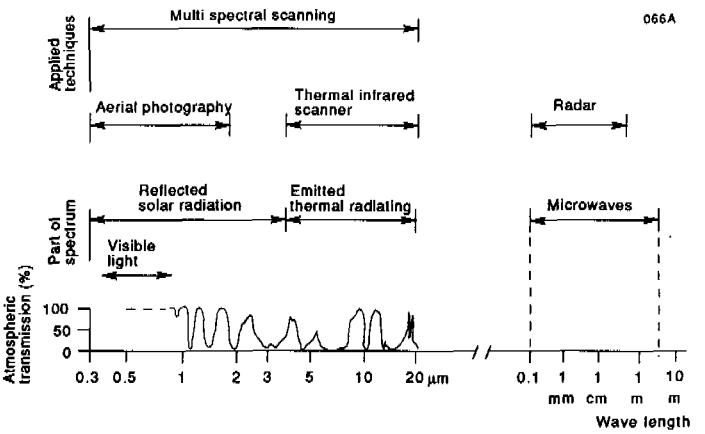

Figure 1 Overview of the electromagnetic spectrum, the transmission of the atmosphere for the different wave lenghts and the applied remote sensing techniques

1 SATELLITES

Nowadays satellites provide repetitive and continuous coverage of the earth both on a global and detailed scale. Many earth observation satellites are in use: polar satellites which turn around the poles, and geostationary satellites which have a fixed position with respect to the earth surface. An example of the latter is METEOSAT, which follows the rotation of the earth at a height of 36 000 km in the equator's plane. Every half an hour images in the reflection and thermal infrared range are taken with a detail of 5 to 10 km. Hence METEOSAT is very suitable in following fast changing processes on a global scale such as weather. A series of polar orbiting satellites which have been launched the past years, are meant for hydrological applications. For instance the American LANDSAT 5 satellite, also known as the Thematic Mapper, takes images every 16 days from a height of about 800 km with a resolution of 30 m in six bands of the reflection spectrum and of 120 m in one band of the thermal range of the spectrum. Another example is the French SPOT satellite, which has three bands in the reflection spectrum with a resolution of 20 m. For selected areas images can be taken with a frequency of about five days by positioning the mirrors of the sensor in lateral direction. Also remote sensing from aircrafts is possible. Images are taken from heights varying from 500 m to 5 km. Here the resolution of a pixel is only a few meters.

2 MEASURING TECHNIQUES

Using remote sensing techniques the weather conditions are of utmost importance. Reflection of solar radiation can only be measured during day light time under a clear sky. Thermal infrared radiation can be measured during the day as well as during the night, but only when clouds are absent. For the weather conditions in the Netherlands it means that proper images can be taken at most a few times in a year. The sun emits electromagnetic waves of different wave lengths, varying from 10^{-6} μm to a few kilometers (Fig. 1). The atmosphere around the earth absorbs most of the radiation, but through a few 'windows' radiation can reach the earth. Remote sensing take advantage of these windows. Only a small part of the solar radiation that is reflected by the earth surface is visible (0.4-0.7 μm). It is noticed that the reflection in the non-visible near-infrared range (0.7-3.5 μm) together

with the reflection in the red and green range of the electromagnetic spectrum are important to characterize the type and condition of crops. Using the so-called 'false colour' photography information from the near-infrared range can be made visible. Electromagnetic waves can also be measured emitted by the earth surface itself. One then obtains an image of the thermal radiation in the wave length range from 8-14 μm. Thermal radiation is strongly dependent on the temperature of the earth surface and on the way an object can emit the radiation (emission coefficient). Another important remote sensing technique is the radar technique which operates in the microwave range (0.1-50 cm). The measuring instrument in the aircraft or the satellite emits short pulses of electromagnetic energy. After reflection this energy is registrated by means of an antenna. Unlike the earlier mentioned systems, radar has no problems with the atmosphere: it can 'look' day and night straight through the clouds.

3 APPLICATIONS

Remotely sensed data provide information on surface water, land use, natural vegetation, crops and soils. Methods have been developed to map water quality parameters and evapotranspiration from digital reflection and thermal images. Particularly remote sensing from space supply model inputs over significant geographic areas and it offers possibilities to verify calculations with hydrological models. Moreover, with satellite systems changes in existing conditions can be monitored in a cost effective way. Consequently, remote sensing has already been a promising technique since several years. The implementation of methods based on remote sensing techniques however, has been regrettably slow. For several years remote sensing has been applied independent from conventional methods based on field observations and hydrological modelling. Nowadays different examples can be mentioned of an integrative use of remote sensing and conventional methods. It was found that remote sensing is a useful tool to achieve accurate information in water management studies. Especially thanks to the integration with geographical information systems, the significance of remote sensing in monitoring processes at the earth surface will increasingly grow in the near future.

In this publication studies dealing with the application of remote sensing in surface water management and agriculture are treated. Especially for developing countries satellite remote

sensing plays an important role. Results in irrigation management and water balance studies of desert areas are presented. A special topic deals with the detection and forecast of precipitation with radar techniques.

I hope that this publication contributes to the implementation of the discussed applications in operational water management practice.

DETECTION AND FORECAST OF PRECIPITATION WITH RADAR

S. van den Assem

ABSTRACT

Precipitation can be detected by remote sensing techniques. At non-tropical latitudes satellite data lead only to qualitative information. However, quantitative data of precipitation can be obtained by using radars, which are located at groundstations. A project is going on to investigate the possibilities of quantitative use of weather radar. Radar data are combined with data of an automatic network of raingauges in the flat southwestern part of the Netherlands. The results of a case study will be presented. Weather radars are sensitive to several sources of errors, dependent on the circumstances. Methods to reduce these errors are presented in this paper. An interpolation method is introduced to estimate mean radar reflectivities over 15 minutes; raingauge values are cumulative over 15 minutes. Correction of the radar data for attenuation with a fixed relation between rainfall and reflectivity appears to be no improvement. Adjustment of the radar by raingauges improves the results. The spatial dependence of the adjustment factor appears to be weak. In order to optimize decisions in water management and agriculture, it is important to know the confidence limits of rainfall estimates. A tentative scheme to calculate confidence limits is presented.

1 INTRODUCTION

Remote sensing by weather radar differs from the general remote sensing techniques. Normally, the sensor is positioned at an airplane or a satellite and detections are done vertically. A weather radar is generally located at a tower or at the top of a hill or mountain. The radar scans mainly in a horizontal way. The range of the weather radar is limited, due to the curvature of the earth and the wavelength used. When remote sensing is done from satellite, very large areas can be scanned. Vertical and horizontal remote sensing techniques have also several similarities: the high spatial resolution of the data, the way the data can be used (image processing), the presentation of the data, incorporation of groundtruth data, the statistical implications resulting from the comparison of point measurements (groundtruth) and areal values (remote sensing pixels). In the Netherlands two digitized C-band radars are operational to detect precipitation. One radar is situated at the airport near Amsterdam and the other at De Bilt in the centre of the country. Both radars are used qualitatively as a tool for analysis of the meteorological circumstances and short term forecasting.

In 1987 a project started to investigate the possibilities for quantitative application. Quantitative information can be obtained up to 75 km from the radar; at larger distances (up to 150 km) the radar data will be less accurate and therefore only of qualitative use, (Collinge and Kirby, 1987). In this project the data of the radar in De Bilt are used. The data are provided in a 8-bit resolution (256 intensity-levels). Accurate radar data can be very useful in rural and urban water management (Cluckie, 1987; Collier and Knowles, 1986; Scholma and Witter, 1984). To obtain reliable rainfall estimates by radar a combination is necessary with raingauges (Collier, 1986a and 1986b). Here, use of radar is combined with data of an automatic raingauge network in the western part of Noord-Brabant (southwestern part of the Netherlands). This country site is completely flat. The radar data are free of ground clutter and occultation in this area. Weather radars can be used for forecasting. This means extrapolation of the detected precipitation field in time and space. The maximum time-range of forecasting with radar is only a few hours ahead, due to the limited lifetime of systems producing precipitation. At longer time-ranges forecasts by numerical models will be more accurate than the products obtained from wheather radar(s) only. Algorithms using both types of information are under

Figure 1a Radar-image of the sw-part of the Netherlands at 24 September 1988, 15.35 UTC

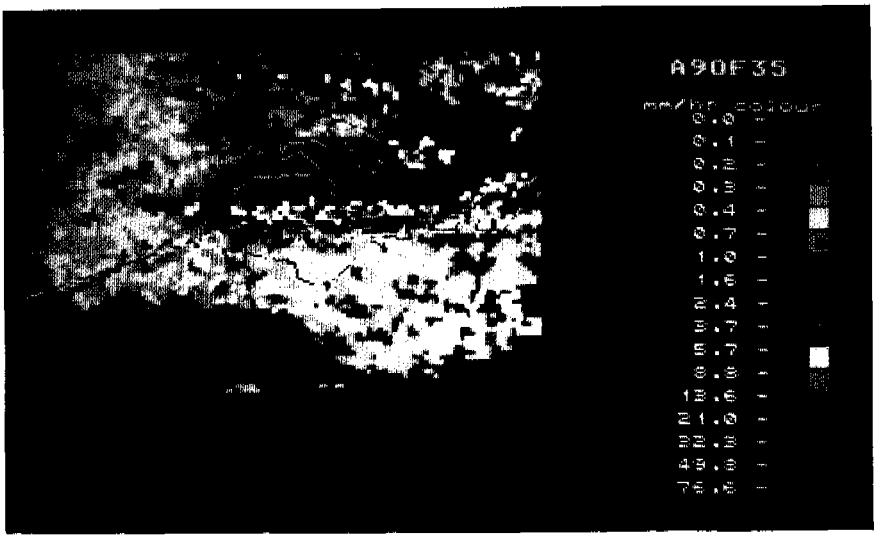

Figure 1b Radar-image of the sw-part of the Netherlands showing the mean intensities from 06.00 UTC at the 24th to 06.00 UTC, 25 September 1988

development, (Sutton and Conway, 1989).
In general, the forecasted amounts of precipitation in a certain area will show a larger uncertainty with increasing prediction time.

2 MEASUREMENT OF PRECIPITATION

2.1 Radar

The weather radar of De Bilt is a C-band radar giving its data with a spatial resolution of 2x2 km. The bundlewidth is 1 degree. Every 15 minutes the atmosphere is scanned at two elevations: .3° and 1.7°. However, within a range of 65 km distance from the radar only data of the highest beam are available; from 70 km data of the lowest beam are used. Between 65 and 70 km distance from the radar the beam with the strongest radar reflection values is chosen.

Table 1 Distance s (km) of the operational raingauges to the radar, height centre of the radar beam above the land surface h (km), and half beam width Δh (km) of the radar at the raingauge locations. The height of the radar beam is calculated by the so called 'forth-third earth approximation formula'

Location	s(km)	h(km)	Δh(km)
Zevenbergen	61.0	2.03	.530
Baarle	72.6	.691	.632
DSAS	72.9	.695	.636
Seppe	73.4	.702	.641
Steenbergen	83.2	.843	.727

In first instance, the rain intensities are derived from the well known Z-R relationship: $Z=200R^{1.6}$. Z is the reflectivity of the radar beam caused by hydrometeors (dB) and R the rainfall intensity (mm/hr). No corrections are made for groundclutter, anomalous propagation of the radar beam, melting snow causing the 'bright band', attenuation and variations in the Z-R relationship.

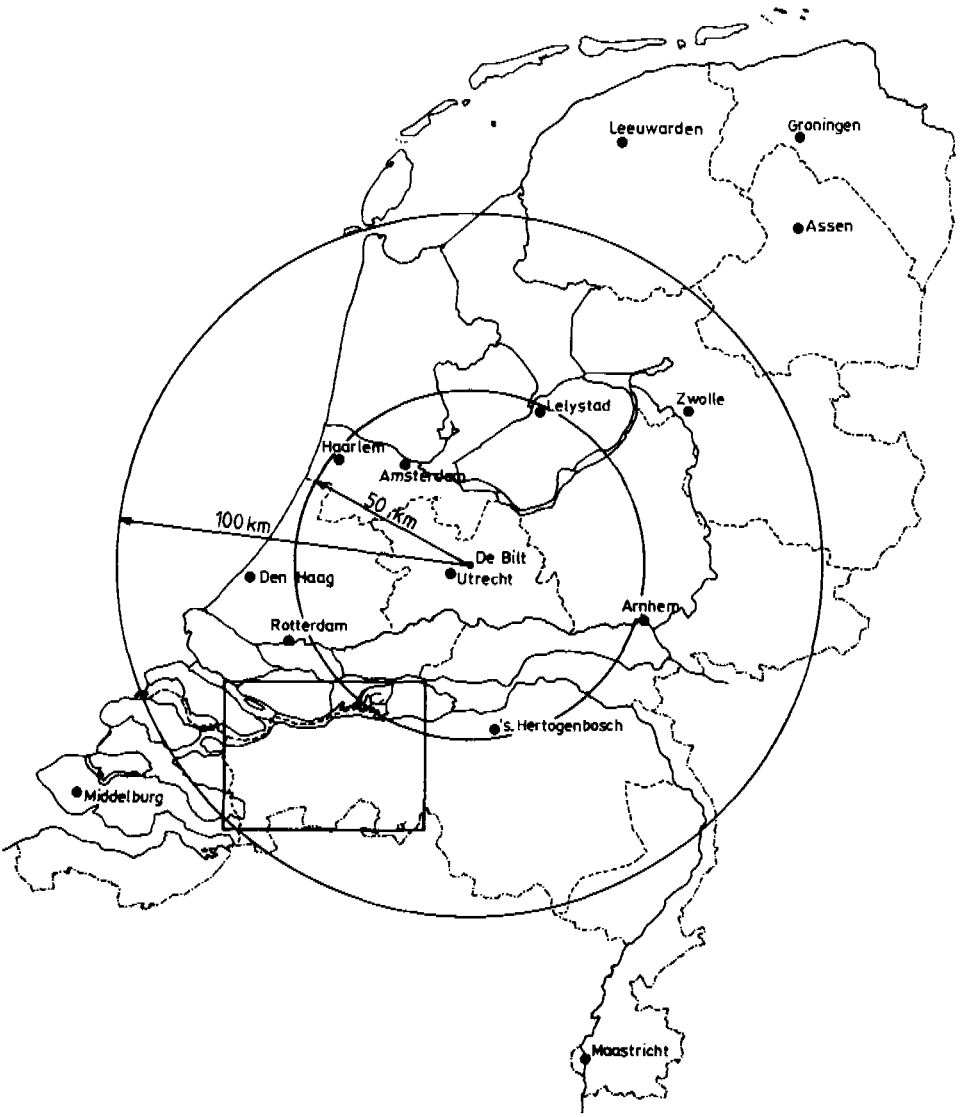

Figure 2 Map of Holland. The radar of De Bilt is situated in the centre of the circles. A raingauge network is installed in the square area SW of the radar

2.2 Raingauges

During the summer and autumn of 1988 a network of 10 automatic tipping bucket raingauges has been installed in an area of about 30x45 km at a distance of 50-100 km from the radar in De Bilt. In addition, six automatic gauges are installed temporarily to investigate:

a The distance dependency of the relation between radar estimates and raingauge values.

b Correlation structure of precipitation (semi-variogram).

The raingauges have a resolution of .16 mm. Calibration of the gauges in the laboratorium showed an intensity-dependence (Van den Assem, 1988). At extreme intensities (> 2 mm/min) the tipping value is 10-15% higher than at low intensities. The raingauge data are corrected for intensity dependence. Date and time of every tipping are archieved. Continuous precipitation values during fixed time intervals can be obtained, using a linear interpolation between tippings. This method is only possible when raingauge data are not used on real time basis.

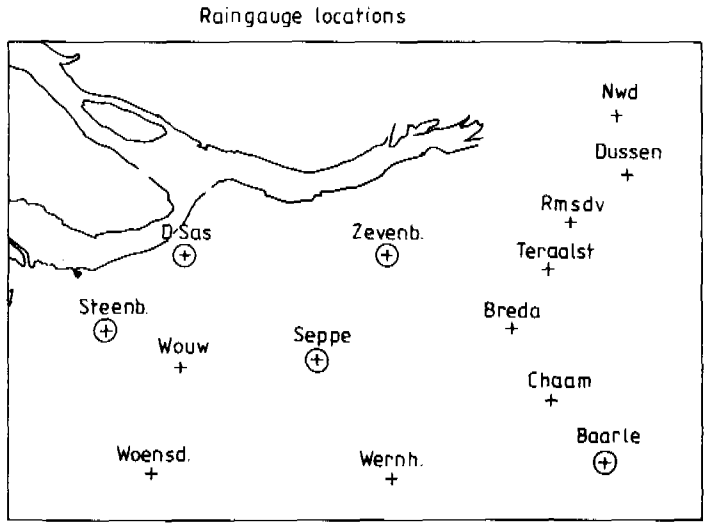

Figure 3 Map of the area in which the network of raingauges are located. ⊕: gauges operational, September 1988; + gauges not (yet) operational

3 EVENT OF 24 AND 25 SEPTEMBER 1988

3.1 Meteorological conditions

At 24 and 25 September 1988 a period occurred with more than 24 hours of continuous rain in the central and southern parts of the Netherlands. The five operative raingauges in the western part of Noord-Brabant recorded more than 50 mm of rainfall during this period. The maximum 15 minute values recorded at the 5 locations were 3 to 5 mm. A frontal system approached the Netherlands in the early morning of 24 September. The cold front followed immediately after the passage of the warm front. It progressed apparently very slowly because it was located almost parallel to the westerly 500 mbar flow. Several small scale waves were developing in the front, moving from the south of the U.K. to Germany. A conveyor belt was formed south of the front, laying from east to west over the middle and southern parts of the Netherlands. Small cells with very high intensities (> 50 mm/hr) are detected by the radar in the conveyor belt. Finally, during the evening of the 25th the front over the middle of the Netherlands retreaded under influence of a new depression from the Atlantic. Vertical soundings in De Bilt and Ukkel (Belgium) showed at 00 UTC of the 24th a O °C at 1800 m, at 12 UTC on 2400 m and at 00 UTC the 25th on 2800 m height, respectively. Bright band effects were absent during this period. In figures 1a and 1b uncorrected radar images are shown of the southwestern part of the Netherlands. The radar of De Bilt is located at the north eastern corner of the images, where groundclutter causes strong reflections. To the South-West the coastline of Zeeland and Belgium are to be seen. The first picture shows clearly an area with high intensities in Zeeland and the western part of Noord-Brabant. The second picture shows the mean intensity from 06 UTC at the 24th to 06 UTC at 25 September 1988. The scales of the colour-intensities in both images are not identical.

3.2 Interpolation of the radar data

The radar scans only once per 15 minutes. Small scale precipitation structures passing over a location of interest will likely not be noticed correctly. In order to improve the radar rainfall estimates, we developed a new interpolation scheme, which makes use of a displacement vector. The latter is obtained as follows:

On time t=0 the intensity of precipitation estimated by radar at the location P is known. The displacement vector gives the position of the precipitation cells, which will arrive at the location P at the interpolation time from t=0, up to t=15, using the radar data at t=0. When the position of a location is not centralized in a radar pixel an averaging procedure is used to include neighbouring radar pixels.

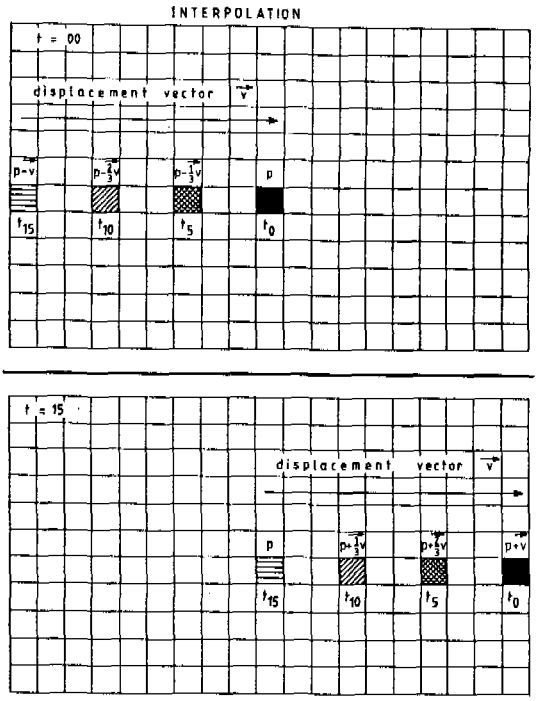

Figure 4 Forewards (a) and backwards (b) interpolation in time and space of radar data. The squares in a and b represent radar-pixels of radar scans at time t=0 and t=15 (min) respectively

At time t=15 we can calculate backwards in time, finding which precipitation cells have passed over the location P from t=0 up to t=15. When calculating backwards, the radar data at t=15 will be used. The corresponding pairs of cells at a certain interpolation time which are calculated forward and backward, can be compared with each other. The mean square difference of these pairs is an indication of the accuracy of this method, using a given set of data. A first guess of the displacement vector can be obtained from the wind-velocity at 850 and 700 mbar. An interactive procedure will provide the optimal displacement vector. The amount of precipitation which has fallen at a location will be estimated by combining forward and backward interpolated data. Weighting factors will be introduced, dependent on the elapsed time between the interpolation time and the time of both radar scans. The displacement vector appeared to be conservative for prolonged periods of time (up to several hours). This implies that the use of the displacement factor allows a rainfall forecast.

Table 2 Rainfall amounts (mm) of 15 minutes evaluated from non-interpolated (RN) and interpolated (RR) radar data compared with raingauge data at 5 locations from 06.30 UTC, 24 September 1988 up to 09.00 UTC 25 September 1988. Loc. Location; G: 15 min raingauge amount; AVG: mean value; STD: standard deviation; MAX: maximum value occurred; MIN: minimum value. The interpolation time step is 1 minute

LOC.	Zevenbergen		Baarle N.		Dintelsas		Seppe		Steenbergen	
	RN-G	RR-G	RN-G	RR-G	RN-G	RR-G	RN-G	RR-G	RN-G	RR-G
AVG	.02	- .08	.00	- .04	- .23	- .18	- .21	- .17	- .03	- .04
STD	.72	.57	.77	.76	.44	.41	.60	.52	.41	.33
MAX	4.2	3.2	4.7	4.9	0.8	1.0	1.2	1.4	1.5	1.1
MIN	-1.9	-2.1	-2.3	-2.3	-2.4	-2.2	-3.3	-2.5	-1.2	-1.0

3.3 Attenuation

A C-band radar is sensitive to attenuation, due to scattering and adsorption of the microwave, mainly caused by hydrometerors. These phenomena are well described by Battan, (1973). An estimate of the corrected reflectivity factor Z_o (dB) can be obtained with the relation:

$$Z_o(r) = Z(r) + 2 \sum_{d=1}^{r-1} k(d) \qquad [1]$$

with Z the attenuated reflectivity factor (dB), r the range (km) and k the (one way) attenuation coefficient (dB km^{-1}). The attenuation coefficient is dependent on the dropsize distribution. A relation between k and the precipitation intensity (R) is proposed by a.o. Battan, (1973) and Yoshino, (1988):

$$k = c_1 R^{c2} \qquad [2]$$

with c_1 and c_2 empirical parameters.

The data of the radar in De Bilt are not yet corrected routinely for attenuation. The data are delivered in the carthesian grid, so, in order to correct for attenuation, transformation to a polar grid must be done.

An algorithm is developed, which eliminates groundclutter at well known locations by interpolation from neighbouring pixels, transforms the radar data to a polar grid, corrects for attenuation as given by eq. (1) and retransforms the data back to the carthesian grid. The transformation method divides all pixels in sub-pixels, which amount is dependent on the refinement-factor. Here, the refinement factor is put on 4, i.e. 1 radar pixel is divided in 16 subpixels. Conversion tables are used while the transformations are executed. Both transformations cause some error in the data set, due to smoothing effects. Initially, the data in the polar grid are retransformed to the carthesian, without correction for attenuation. The ratio between the variances of the data transformed twice and the original data gives an indication of the level of smoothing. Furthermore, after the polar data are corrected for attenuation and transformed to the carthesian grid, the data are corrected for the smoothing

effect. This latter correction is an approximation, because in this smoothing correction no attenuation-correction effects are involved. The attenuation algorithm is applied on the data set of 24 and 25 September 1988. The maximum transformation error never exceeded the level of $\pm$ 4 dB in a pixel, leading to maximum errors of $\pm$ 1.5 mm. hr^{-1}. The ratio of the variances of the twice transformed and original data varied between .97 and .99.

Table 3 Rainfall amounts (mm) of 15 minutes calculated by radar data which are not corrected for attenuation (RR) and attenuation corrected radar data (RA) compared with raingauge data (G) at 5 locations from 06.30 UTC 24 September 1988 up to 09.00 UTC 25 September 1988. LOC: location; AVG: mean value; STD: standard deviation; MAX: maximum value occurred; MIN: minimal value occurred. The (one-way) attenuation coefficient k is taken at $0.003\ R^{1.0}$

LOC.	Zevenbergen		Baarle N.		Dintelsas		Seppe		Steenbergen	
	RR-G	RA-G	RR-G	RA-G	RR-G	RA-G	RR-G	RA-G	RR-G	RA-G
AVG	- .08	.00	- .04	.04	- .18	- .11	- .17	- .06	- .04	.05
STD	.57	.65	.76	.97	.41	.42	.52	.57	.33	.42
MAX	3.2	4.1	4.9	6.6	1.0	1.7	1.4	2.2	1.1	1.6
MIN	-2.1	-2.0	-2.3	-2.3	-2.2	-2.0	-2.5	-2.2		-0.9

Table 3 shows that the bias of the attenuation corrected radar data appears in general to be smaller than the bias of the non corrected data. However, the standard deviation of (RA-G) is higher than the deviation of (RR-G), leading to higher mean square errors. The correction method for attenuation seems not to improve the results.

Johnson and Brandes (1987) compared an attenuation corrected C-band radar with a S-band radar during severe weather conditions in the USA. They concluded that correction for attenuation of a C-band radar appears to be futile, because the calibration error of the attenuated reflectivity was not restricted to extreme narrow limits. Yoshino et al., (1988), compared uncorrected and corrected C-band radar data with raingauges during an extreme severe storm in Japan. The Z-R relation was adjusted in order to obtain the lowest root mean square error between radar and gauge data. Correction for attenuation leaded to an

improvement, but the results also showed that the use of an inappropriate Z-R relationship may result quickly to large errors. The Z-R relationship was fixed to the standard values ($Z=200R^{1.6}$) in the analysis of the 24 and 25 September 1988 situation. A flexible Z-R relationship combined with another attenuation coefficient might have improved the results, but should require an extreme amount of computing time.

3.4 Calibration by raingauges

Calibration of radar data by using raingauges improves the accuracy of the rainfall estimates, (Collier, 1986). During 24 and 25 September 1988 data of five raingauges were obtained in the south-western part of the Netherlands.
See Figure 2. Here, the calibration factor of location x on t=0 ($C_O(x)$) is defined by:

$$C_O(x) = \sum_{t=-60}^{-15} G_t(x) / \sum_{t=-60}^{-15} RR_t(x) \qquad [3]$$

with $G_t(x)$ the rain intensity on time t and location x measured by raingauge; $RR_t(x)$, idem, but measured by radar. An integration period of 45 minutes is introduced to avoid significant sampling errors. The most recent 15 minutes are omitted, to make it feasible to compare radar data, which are calibrated by all calibration factors. In real-time analysis it is evident that this last quarter must be implemented. The calibration factor found at several raingauge locations can be interpolated spatially by different techniques, like the Thiessen method, multiquadratic surface fitting or kriging. In this case study no spatial interpolations are executed. The radar data at the locations of the raingauges are adjusted by all five calibration factors, separately.

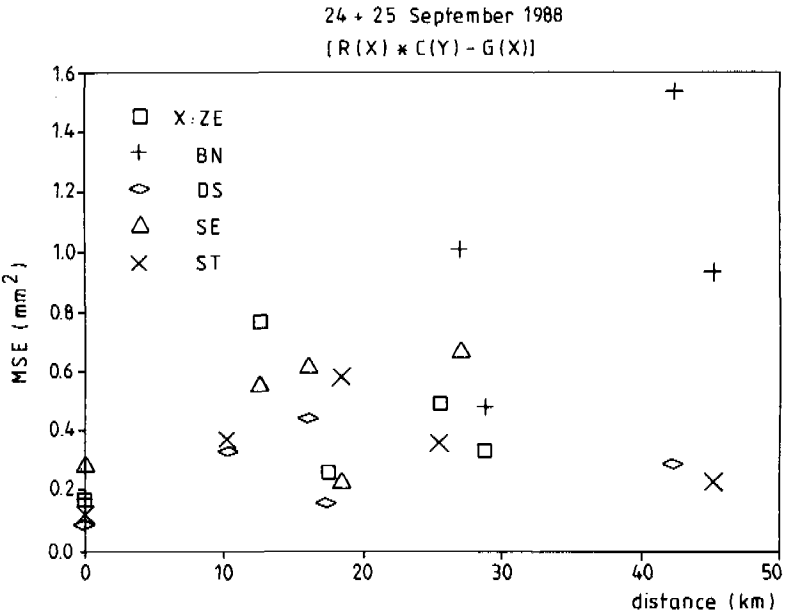

Figure 5 Mean square error (mm^2) of the radar data calibrated by calibration factors of all five raingauge locations plotted as a function of distance between the locations (km)

In figure 5 the mean square errors of the calibrated radar data are presented as a function of distance between the location of the radar pixel and the location where the calibration factor is derived. The lowest mean square errors (MSE) are obtained at the smallest distances (0 km). This can be partly due to a bias in raingauge or radar at the location of the raingauges. The relation between distance and MSE appears to be weak, partly due to the large scatter.

Table 4 Rain amounts (mm) of 15 minutes calculated by uncalibrated radar data (RR) and radar data adjusted by calibration factors of the same locations as the radar data (RC) compared with raingauge data (G) at 5 locations from 06.30 UTC 24 September 1988 up to 09.00 UTC 25 September 1988. LOC: location; AVG: mean value; STD: standard deviation; MAX: maximum value occurred; MIN: minimal value occurred

LOC.	Zevenbergen		Baarle N.		Dintelsas		Seppe		Steenbergen	
	RR-G	RC-G	RR-G	RC-G	RR-G	RC-G	RR-G	RC-G	RR-G	RC-G
AVG	- .08	.01	- .04	- .00	- .18	- .00	- .17	- .03	- .04	- .01
STD	.57	.41	.76	.41	.41	.30	.52	.54	.33	.35
MAX	3.2	1.5	4.9	2.0	1.0	1.3	1.4	2.4	1.1	1.9
MIN	-2.1	-1.6	-2.3	-2.3	-2.2	-1.0	-2.5	-2.9	-1.0	-1.0

Table 4 shows that the on site calibration of the radar improves the results at Zevenbergen, Baarle Nassau and Dintelsas. At Seppe and Steenbergen however, the bias is smaller after calibration, but the deviation is enlarged, leading to an almost unchanged mean square error.

3.5 Confidence limits

Quite often meteorological information (analysis or forecast) is considered to be free of error. This is not correct and especially concerning areal rainfall. No rainfall forecast is perfect (Einfalt, 1989). But also areal estimates of precipitation, which has already occurred, are not free of error. A network of raingauges provides a good first estimate of areal rainamounts. However, uncertainty in the data remains, due to the spatial variability of rain. Measurement-errors of the gauges themselves are thought of minor importance. A weather radar gives areal estimates, but is sensitive to several kinds of error. These errors can be partly corrected, depending on the circumstances but leaving still uncertainty in the data. Spatial interpolation of the calibration factor or (its inverse) the assessment-factor causes some inaccuracy in the interpolated points. Unforeseen development or decay of precipitation cells is a major source of inaccuracy in forecasted rainamounts.

All these errors and inaccuracies leads to areal rainfall-estimates which must be considered to have a random component. It would be desirable to quantify the uncertainty in the data.

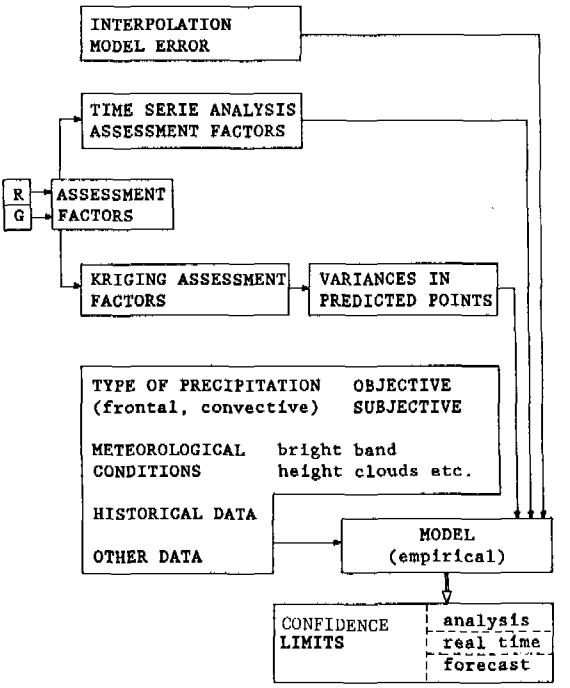

Figure 6 A tentative scheme for calculating the confidence limits of areal precipitation amounts, using radar (R) and raingauges (G)

In Figure 6 a tentative scheme is presented to calculate the confidence limits of areal rainfall amounts. Three main sources of error can be distinguished:

a model error in fore- and backwards interpolation in time and space by using an incorrect displacement vector or by non-linear development or decay of precipitation-cells;

b measurement-errors by raingauges (G) caused by spatial variability, bias, etc. and radar (R),

c errors caused by spatial interpolation of the calibration- or assessment-factor.

All these errors are interrelated. Additional information, like meteorological conditions, historical data, etc. can be introduced to optimize the model to estimate the confidence limits. Users of areal rainfall-amounts may consider the data more reliable when the

confidence limits of these data could become available as well. Confidence limits make it possible to optimize decisions which have to be taken, for instance, in water-management or agriculture.

4 CONCLUSIONS

a The accuracy of rainfall estimates obtained from radar data provided each 15 minutes is improved by an interpolation-procedure that makes use of a displacement vector of the precipitation field.

b The accuracy of precipitation measured by a C-band radar is not improved when the radar data are corrected for attenuation with a fixed Z-R relation. Adjustment of the Z-R relation or even the attenuation coefficient may lead to better results.

c Radar data calibrated by raingauges show in general an increased accuracy compared to uncalibrated radar data. The distance at which a calibration factor can still be applied will depend on the meteorological conditions. In the case study presented a weak distance dependence was to be seen. This means that a dense network of calibration raingauges will not be necessary under these circumstances.

d When quantitative rainfall estimates are used, it is important to know its confidence limits. This makes optimization of decisions possible.

ACKNOWLEDGEMENTS

The helpful advices of Han Stricker and Henk de Bruin, the technical support of the Department of Hydrology, Soil Physics and Hydraulics and data provided by the water authority 'Hoogheemraadschap West-Brabant', weather service 'Meteo Consult' and the Royal Dutch Meteorological Service 'K.N.M.I.' is gratefully acknowledged.

REFERENCES

ASSEM, S. VAN DEN; 1988. Calibration of tipping bucket raingauges. Onderzoeksverslag nr. 85, Landbouwuniversiteit Wageningen, 18 p. (in dutch).

BATTAN, L.J.; 1973. Radar observations of the atmosphere. University of Chicago Press, Chicago and London.

CLUCKIE, I.D. et al.; 1987. Some hydrological aspects of weather radar research in the United Kingdom. Hydrological Sciences - Journal des Sciences Hydrologiques, 32(3):329-346.

COLLIER, C.G.; 1986a. Accuracy of rainfall estimated by radar, part I: calibration by telemetering raingauges. J. of Hydrology, 83(4): 207-223.

COLLIER, C.G.; 1986b. Accuracy of rainfall estimates by radar, part II: comparison with raingauge network. J. of Hydrology, 83(4):225-235.

COLLIER: C.G. and KNOWLES, J.M.; 1986. Accuracy of rainfall estimates by radar, part III: application for short-term flood forecasting. J. of Hydrology, 83(4):237-249.

COLLINGE, V.K. and KIRBY, C.; 1987. Weather radar and flood forecasting. Ed. V.K. Collinge and C. Kirby, 1987. John Wiley & Sons.

EINFALT, T. and DENOEUX, T.; 1989. Never expect a perfect forecast. Preprints of International Symposium on Hydrological Applications on Weather Radar, Salford.

JOHNSON, B.C. and BRANDES, E.A.; 1987. Attenuation of a 5 cm wavelength radar signal in the Lahona-Orienta Storms. Journal of Atmospheric and Oceanic Technology, 4:512-517.

SCHOLMA, L. and WITTER, J.V.; 1984. Research on precipitation in relation to dimensioning RWZI "Bath" (in Dutch). Waterschapsbelangen, 4: 143-149.

SUTTON, G. and CONWAY, B.J.; 1989. Automating precipitation nowcasts based on satellite and radar imagery combined with numerical model products. Preprints of Seminar on 'Weather Radar Networking', Brussels.

YOSHINO, F., YOO, A. and KOUZEKI, D.; 1988. Accuracy improvement of radar raingauges by considering radar wave attenuation caused by heavy rainfall. Journal of Research, vol. 26. Public Works Research Institute.

REMOTE SENSING IN INLAND WATER MANAGEMENT

H.T.C. van Stokkom and G.N.M. Stokman

ABSTRACT

The inland water in the Netherlands is being intensively used for various purposes such as transport, drinking water supply and recreation. Besides these functions ecological and safety aspects play an important role in water management today. In order to take the right decisions in this sphere of diverse interests there is a great need for adequate information. Information which varies from very detailed and accurate at a certain spot to more general over a vast area. Knowledge is required concerning the functioning of the aquatic ecosystem and the consequences of use and measures taken. In water management optical and thermal remote sensing techniques have an evident potential in providing a part of this information. Airborne and satelliteborne imagery together with water samples enable the supply of synoptic information on a number of water parameters, such as suspended matter content, algae concentration, but also on water surface temperature and presence of water plants. Various examples will be illustrated with emphasis on the operational applications. Finally the consequences of implementation in operational inland water management, with regard to logistics and infrastructure, will be addressed.

1 INTRODUCTION

The development of remote sensing techniques originates from (military) space science and can be characterized mainly as a challenge to people active in the field of technology development. Combined with a general view on applications this incentive lead to the development of instruments which specifications predominantly were linked to the state of the art in technology at that time. During this initial stage a user community did not exist and applications were developed by scientists. However, users showed an increasing interest and became more and more involved in applications research and in the definition of new instruments. It can be clearly noticed that nowadays the incentive for activities has moved from technology-push towards the realization of information needs. This holds also for Rijkswaterstaat. Remote sensing research within Rijkswaterstaat has provided now a number of operational applications on the edge of implementation in operational daily practice.

2 INFORMATION NEED AND MEASUREMENT STRATEGY

The Netherlands can be characterized by its geographical location at the lower parts of its main rivers Rhine and Meuse combined with a dense population, intensive use of the available space for diverging purposes and a high level of industrialization. For these reasons e.g. physical planning, land reclamation, urban and rural development but also water management and construction of infrastructure are highly developed. With an increasing concern in environmental issues water management has shifted over the years from protection against water <keeping one's feet dry> towards a coherence in the concern for the condition and the use of water systems. This concept of 'integral water management' is embedded in the third National Policy Document on Water Management (Ministry of Transport and Public Works, 1989). In this concept (Fig. 1) a close connection between water systems offering possibilities and limitations for use on the one hand and various demanding waterfunctions and -interests (Table 1) on the other is recognized.

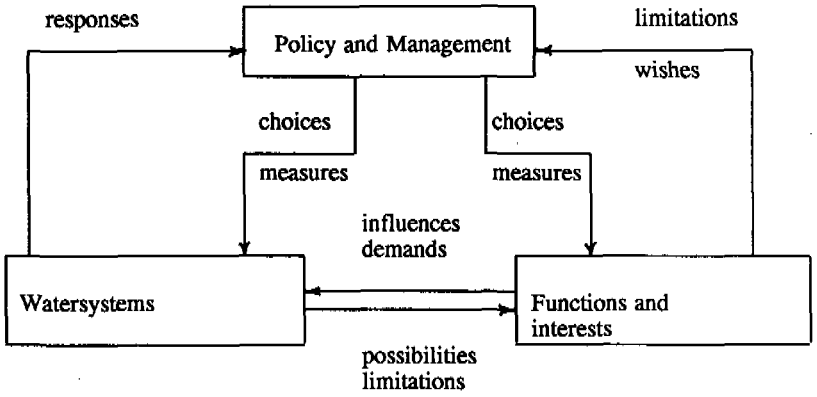

Figure 1 Integral Water Management

Table 1 Relevant functions in Integral Water Management

Social aspects
- agriculture
- shipping
- drinking water supply
- industry
- recreation
- fisheries
- minerals
Ecological aspects
- aquatic ecosystems
- terrestrial ecosystems
Safety aspects
- against flooding
- against calamities

Photograph 1
Water plant map of the Gouwzee, based on LANDSAT-TM image of 5/7/1987

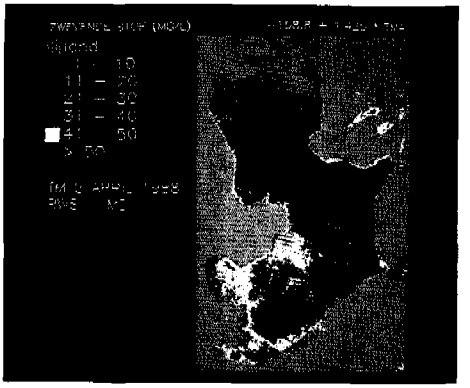

Photograph 2
Classified suspended solids map of the IJsselmeer area based on the Landsat-TM image of 2/4/1988

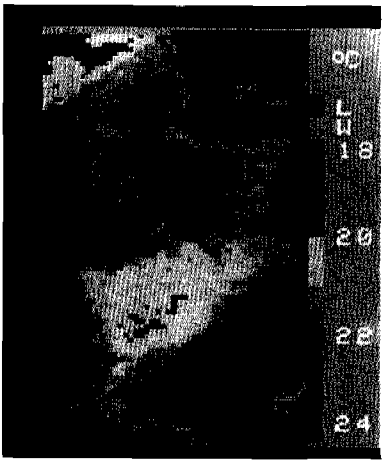

Photograph 3
Temperature map of the IJsselmeer based on the AVHRR-image of 5/7/1987

Photograph 4
Airborne thermal image of the Amsterdam harbour acquired at 26/1/1989

In a confrontation of wishes by society and capabilities of watersystems problems can be recognized. In this sphere of conflicting interests choices and measures have to be made in water policy and management. To take the right decisions a pronounced need for adequate information exists and a measurement strategy has to be set up to acquire the desired information in an efficient way.

2.1 Information need

The community defining the information needs could be distinguished in people working in operational water management (water managers) and groups involved in water research (water investigators). The demand of both groups differ in character and extent whereas at the same time it is evident that the needs are supplementary. The water manager is responsible for monitoring the developments in water systems and for maintenance and control of the use, but also for operating the water management infrastructure (locks, weirs etc.) in relation to the actual situation. Examination of these activities shows the need for adequate and timely, easily to interpret information over the area or site of interest.
The water investigator has a clear goal in building up knowledge of water systems with its physical, chemical and biological components. Spatial and temporal analysis of the processes in the aquatic ecosystem enable the optimization of the monitoring practice and the development of well-defined policies and measures. The emphasis in information requirements for knowledge development is put on time series of several mutually dependent parameters at a limited number of sites. With regard to policy preparation often very specific information is needed either on a limited number of parameters over a wide area or on a large variety of parameters on very few locations.

2.2 Measurement strategy

The confrontation of information needs of water managers and investigators and available measurement possibilities, considering factors such as available time for delivery, number and character of parameters, sample location and frequency and the required accuracy, results in the application of a certain measurement strategy. In this stage the design and optimization of monitoring networks takes place. Optimum measurement and data-processing programmes are set up and available methods and techniques, including remote

sensing, are selected on usefulness. From the measurement strategy impulses are given to the development of new methods and techniques and potential innovations are to be tested on relevance. This is also the phase to carry out a cost/benefit analysis of the measurement efforts versus the information provision. The final goal is to meet the demands for information in an efficient way.

3 THE POTENTIAL AND IMPLEMENTATION OF REMOTE SENSING

3.1 The remote sensing potential

Water management requires accurate and reliable information about the actual situation and changes in time and space to build up knowledge of water systems and to follow the actual developments. Up till now conventional techniques such as sampling by ship or from permanent stations are most frequently used to collect the required information. Data on a large variety of parameters can be obtained by laboratory analysis. However, only a limited number of locations can be investigated. Moreover, a spatial relation between the acquired data at the sample sites is commonly assumed in spite of the existing time delay in sampling, which can mount up from hours to several days. Remote sensing techniques can offer an added value in providing synoptic views over large areas, especially when satellite remote sensing is applied. Successive synoptic views show changing spatial patterns and give a deeper understanding of the processes taking place and can be used in water movement and water quality models. Information on the spatial distribution of concentrations of water parameters (concentration maps) can be derived for the following water quality parameters: phytoplankton pigments, suspended solids, yellow substances, surface temperature and waterplants. These observations support the definition and optimization of monitoring networks and contribute to the spatial interpretation of single point monitoring measurements. Subsequently, remote sensing can serve in maintaining environmental laws by the detection of (illegal) discharges, by the inspection and control of granted permits and by the control of water quality standards.

3.2 The implementation of remote sensing

In the process of developing remote sensing for operational use in the daily practice we have distinguished the following stages:

- basic research
- applications research
- operationalization research
- implementation
- operational use

The objectives of basic research are developing remote sensing instruments and acquiring fundamental knowledge of remote sensing related phenomena. Application research aims at the development of applications based on the available remote sensing techniques. During operationalization research these derived applications will be judged in the framework of envisaged implementation in daily practice. In this phase consequences of both the remote sensing and the user side are considered. Development of procedures for operational data acquisition, (pre)processing and presentation are subject of these considerations.

Within the remote sensing research community finalizing the operationalization research phase is often considered as the end of active involvement. However, our experience is that given the results of the latter phase the user has to judge costs and benefits and the impact of the use of remote sensing on his organization. The incorporation of remote sensing in the measurement strategy thus depends on whether an improvement of effectivity and efficiency in applied methods can be achieved. In order to decide on actual implementation of the developed techniques and methods the user has to consider the consequences for organization, staff and infrastructure also. Coming to this decision is part of the implementation phase and if it is positive actual implementation can be started. Involvement of remote sensing investigators by transferring knowledge and experience is considered necessary. Completion of the implementation phase means the start of operational use of remote sensing in the daily practice.

4 OPERATIONAL APPLICATIONS

Remote sensing applications may serve several purposes, such as inventory, monitoring and prediction. Whereas inventory is an activity undertaken at a certain moment in time monitoring aims at the observation of changes in time. Prediction, finally, is using remote sensing and other data together with models describing the phenomena under investigation, in order to get insight in a situation to be expected. Nowadays emphasis in operational inland water management is shifting from inventory towards monitoring and prediction.
In the following a number of operational applications will be presented.

4.1 Spaceborne remote sensing applications

At this moment products of two useful remote sensing satellites are available, namely from the Landsat and the NOAA satellite system. Until 1985 the Coastal Zone Colour Scanner (CZCS at Nimbus-7) was operated and recently the SPOT (France) and MOS (Japan) satellites were launched. Suitable products based on imagery of the latter satellite systems have not yet been developed by Rijkswaterstaat, but in principle the same approach as for Landsat and NOAA can be applied.

4.1.1 Products based on Landsat imagery

Landsat is a polar orbiting satellite system providing multi spectral scanner imagery obtained in the optical and thermal window. Landsat is operating now two satellites, Landsat-4 and -5, at an altitude of approximately 700 km above the earth. Each satellite contains two optical instruments, the Multi Spectral Scanner (MSS) and the more advanced Thematic Mapper (TM). TM was found to be the most valuable for water applications mainly because of its more fine ground resolution (30 meter) and its better radiometric resolution enabling an improved discrimination of signal differences. The main disadvantage of Landsat for water purposes is the relatively low frequency of data acquisition, once in 16 days over the same spot. Taking into account the frequent occurrence of cloud cover over the Netherlands 2 to 4 cloud free images are available per annum. It should be mentioned that the Landsatsystem is primarily aiming at land applications. Nevertheless, a number of water applications have been developed. The present situation shows products such as water plant

maps, concentration maps of optical active water parameters and synoptic images aiming at several goals.

Water plants

Water plants are an important feature characterizing the ecological functioning of watersystems. The presence of aquatic vegetation depends mainly on transparency and depth of the water body. As a result of intended water quality measures, such as nutrient reduction and biomanipulation, an improvement in water quality and an increase in transparency is to be expected. This will result in an increase of the aquatic vegetation, both in covered area and in density. For these reasons periodic information on the spatial distribution of water plants is necessary for operational water management. Water plants above (emersed), floating on or just below the water surface can be distinguished easily on TM-imagery of relatively large inland waters, such as the IJsselmeer. It is possible to obtain information on the area covered and the density of plants. Moreover, emersed water plants can be distinguished. Photograph 1 shows an example of a water plant map of the Gouwzee, a part of the IJsselmeer. Annually this lake has a dense coverage with water plants, partly emersed. Successive images make it possible to monitor the developments over the years.
Separation of plant species can not be performed by imagery from present spaceborne systems. Because of the interest of the water manager in long term changes the required frequency of information provision is ascertained at once in three years. It is found that this requirement can be met. Products are geometrically rectified and geo-referenced in order to enable water managers to compare the maps with other data. If requested a topographic map overlay can be provided. An increasing interest exist in combining above mentioned products and other data such as bottom depth, in a geographic information system (GIS) allowing efficient analyses.

Concentration maps

A method has been developed and validated to manufacture concentration maps of the following water parameters: suspended matter, algae, water transparency and surface temperature. The procedure to convert the digital imagery to concentration maps is described by Buiteveld, Meulstee and Bakker, 1989. In essence the most relevant steps are:

- taking water samples on a limited number of well-known sites at the day of satellite overflight;

- preprocessing the raw data of the digital satellite image including radiometric correction, destriping, geometric correction and resampling to a 100 meter grid;
- the preprocessing enables retrieval of the sample sites in the image. From the laboratory analysis among others the concentrations of chlorophyll (algae), suspended matter, yellow substances and Secchi depth (transparency) are ascertained at the sample sites;
- combining the concentrations and the multispectral data of the different spots a functional relation (model) can be calculated (Stokman & Van Stokkom, 1986);
- applying this functional relation subsequently to the entire satellite image provides a 'concentration map' of the respective water parameters.

It is possible to include these maps in a GIS, which offers additional analysis and presentation possibilities. The reliability of these Landsat products has been determined at: suspended matter $\pm$ 5 mg/l, algae $\pm$ 30 μg/l, transparency $\pm$ 20 cm, temperature $\pm$ 1 °C. The main advantage of the concentration maps is the overall synoptic view. With point measurements it is hardly possible to achieve this spatial image. On the whole the maps are useful in water research and management, especially where data on suspended solids, chlorophyll and Secchi depths are being used. For instance suspended matter images are used in tuning and testing of circulation models. Photograph 2 shows an image of the IJsselmeer area with a large suspended matter inflow from the river IJssel. The abrupt decrease in concentration shows a strong sedimentation in the eastern part of the IJsselmeer. The south-western Markermeer is shallow with a higher resuspension of bottom material under the prevailing weather conditions. Furthermore concentration maps may serve water quality monitoring as a contribution to the interpretation of point measurements and for the optimization of monitoring networks.

Qualitative imagery

Synoptic views of several phenomena such as the complex distribution of floating blue algae (Microcystis sp.), patterns in ice cover, qualitative flow patterns using suspended matter as a natural tracer and the coverage of water-meadows in cases of high river water levels, serve various purposes. From these synoptic images one can observe phenomena without having quantitative data available. In many cases water managers and water researchers consider those images very valuable.

4.1.2 Products based on NOAA-AVHRR imagery

Although Landsat carries more advanced instruments with regard to geometric resolution and number of spectral bands the low overflight frequency combined with Dutch weather conditions and the relatively long delivery time makes the system less suitable for 'daily' operational water management. The NOAA meteorological satellites in polar orbit are superior in this respect. Two satellites are kept in space in pairs and each passes over the Netherlands twice a day. The optical instrument, the Advanced Very High Resolution Radiometer (AVHRR), at the NOAA-satellites therefore offers a high temporal resolution of two images a day and a quick delivery. For this reason Rijkswaterstaat in collaboration with the Royal Dutch Meteorological Institute (KNMI) has developed some products based on AVHRR-imagery. By using standard procedures and fixed functional relations between ground measurements and multispectral data maps of suspended matter content, floating blue algae and surface temperature can be provided. The ground resolution is about 1 kilometre at nadir, so only broad maps can be produced. The reliability of these AVHRR-products has been determined at: for suspended matter a factor 2, for algae qualitative information on floating layers and for temperature absolute 0.6 °C and relative 0.1 °C. Temperature images are used to monitor changes in the water temperature as a measure for dispersal patterns. Suspended matter maps make it possible to monitor the transport of particles to which pollutants often adhere. Photograph 3 gives an example of a temperature map of the IJsselmeer showing various features related to water management issues. The AVHRR-products also provide valuable information for process studies. One important field is limnology, since suspended matter plays an important role in the food chain. The depth to which sunlight can penetrate the water body depends on the suspended solids concentration. The murkier the water, the less the production of algae. The virtually daily pictures of suspended matter and water temperature contain information on transport and mixing phenomena, so keeping an eye on the dynamics of large inland waters.

4.2 Airborne remote sensing applications

Considering the fixed dates and time of satellite overflights one can easily understand that flexibility in data-acquisition is rather low. Airborne remote sensing can circumvent these problems to a certain extent, but will introduce some disadvantages at the same time.

Presently, airborne remote sensing data acquisition with various sensors (aerial photography, thermal scanning, multispectral scanning, video) can be carried out by commercial firms upon request. Prices are mainly dependent to the sensor and the platform. Multi spectral scanning in the optical window using airborne instruments is still in the stage of applications research and will not be addressed. In general one may expect similar applications as using Landsat imagery but showing more details on a smaller area.

4.2.1 Aerial photography

From several studies it is known that aerial photography can provide spatial information on distribution, species composition and density of water plants. In some cases even biomass can be estimated using aerial photography (Van Urk et al., 1985, Meulstee et al., 1988). Especially true colour aerial photography is suited and preferred. In combination with Landsat TM images and field measurements the information needs of the water manager in the IJsselmeer area can be fulfilled. A combined approach is advised, which consists of following the broad developments with TM images and there where detailed information is needed aerial photography is to be applied and finally more comprehensive field surveys can be carried out. It is noted that using the mentioned remote sensing means some field checks have to be performed in order to guarantee the quality of the delivered products. By following this approach costs can be minimized (Van Oirschot et al., 1989).

For water applications aerial photography is also used to get synoptic views over relatively small areas, such as rivers, small lakes and harbours. Drifting ice on rivers, small scale behaviour of suspended matter, recreation distribution and statistics and environmental control can be subject in this respect. Knowledge concerning the procedures and methods to be used is available within Rijkswaterstaat upon request. For quick inventories, often related to environmental control programs, an alternative is found in using ultra light aircraft. Instruments applied are photography and true colour and thermal infrared video. From our experience these techniques are to be preferred for inventories where qualitative information is sufficient and no further processing is required. Although these methods are still under development an integral approach is to be recommended. This approach includes systematic airphoto coverage from time to time, regular quick inventories by ultra light aircraft or helicopters and field checks based on the acquired information. In order to achieve the full potential of this approach and to establish the required quality of the information delivered,

skilled assistance in the field of remote sensing methods and interpretation should be available.

4.2.2 Thermal scanning

Besides aerial photography airborne thermal scanning has proved to be a valuable tool ready for operational use. It is well-known that the temperature of the earth surface is directly related to the amount of emitted radiation in the thermal window of the electromagnetic spectrum. Thermal scanners measure the amount of radiation that reaches the sensor and so a thermal radiation image is being recorded. Using temperature measurements at a small number of spots the thermal image can be transformed into a surface temperature image.
As data acquisition is performed from an aircraft and by a scanning system the image can be strongly distorted due to movements of the platform during data acquisition. In order to make a proper comparison of the imagery and other data possible an adequate geometrical correction has to be carried out. De Leeuw et al., 1988 have developed a suitable method, using ground control points, which provides an image fitting well to a topographical or an other reference map.

At this moment two operational applications are fully developed, namely detection of discharges and monitoring surface current patterns and dispersion. In maintaining the Pollution of Surface Water Act airborne thermal scanning and to a lesser extend thermal video has proved to be a valuable tool in providing information on discharges of cooling water and industrial waste water. Discharges can be detected and control can be performed. Photograph 4 shows an example of the Amsterdam harbour area in which several discharges can be detected. The remote sensing tool is not suitable presently for taking transgressors in the act. This is mainly caused by the absence of on-line data processing and interpretation on board the aircraft. The latter could be an alternative, which is for several years being proved by the fully operational oil spill detection system installed in the Dutch Coast Guard aircraft. Furthermore, it is recognized that applying these techniques regularly a preventive effect exists. The relatively high costs of airborne thermal data acquisition should be mentioned.

Surface current patterns can be studied using time series of thermal images. The temperature of the surface water is being used as a natural tracer under the assumption that more or less homogeneous water bodies exist and can be distinguished during a certain time frame. For this application superimposition of multitemporal imagery is necessary, which requires accurate geometrical correction. The information is being used by the water managers to study the behaviour within regional water systems, such as river sections and harbour areas. Based on this studies permissions are granted or refused. Water researchers on the other hand use the multitemporal imagery to investigate the physical processes in water systems in order to build up knowledge needed for policy development and consultancy. Moreover, the latter category is using the imagery for verifying, improving and calibrating their surface water current models. For instance studies are presently undertaken to assimilate thermal imagery with models in order to get information on currents in the third dimension, the depth.

5 CONCLUSIONS AND RECOMMENDATIONS

In conclusion it is stated that remote sensing is providing a wide spectrum of instruments adequate for measurements with a synoptic character and a capability beyond human observation. Present remote sensing is offering a valuable contribution to the fulfilling of the information need in inland water management, especially with regard to the increase of knowledge concerning the water systems and the monitoring of changes in water systems. The contribution is mainly additional, which means that in most cases existing measurement techniques and strategies can be optimised but hardly be replaced. Furthermore, monitoring procedures can be improved by using remote sensing information. Daily operational use depends strongly on the information need and envisaged application on the one hand and the suitability of the technique, the frequency of data acquisition and costs on the other.

Deciding by the water manager or water researcher upon actual incorporation of remote sensing in the measurement strategy often is therefor a hard evaluation and judgement involving policy, organizational (infrastructure and personnel) and operational (financial consequences and added value) aspects.

REFERENCES

BUITEVELD, H., MEULSTEE, C. and BAKKER, H.; 1989. The use of satellite imagery in the IJsselmeer area (in Dutch). Netherlands Remote Sensing Board report BCRS 89-31, Delft.

MINISTRY OF TRANSPORT AND PUBLIC WORKS; 1989. Water in the Netherlands: a time for action. Summary of the national policy document on water management (in english). Information Department, The Hague.

MEULSTEE, C. and VAN STOKKOM, H.T.C.; 1985. Variation of biomass of macrophytes in the Randmeren during the growing season; field samples and aerial photography (in Dutch). Report Rijkswaterstaat Survey Department MDLK-R-8514.

MEULSTEE, C., NIENHUIS, P.H. and VAN STOKKOM, H.T.C.; 1988. Aerial photography for biomass assessment in the intertidal zone. Int.J. of Remote Sensing, Vol. 9, no. 10 & 11, pp 1859-1867.

DE LEEUW, A.J., VEUGEN, L.M.M. and VAN STOKKOM, H.T.C.; 1988. Geometric correction of remotely sensed imagery using ground control points and orthogonal polynomials. Int.J. of Remote Sensing, Vol. 9, no. 10 & 11, pp 1751-1759.

VAN OIRSCHOT, M., MEULSTEE, C., MARTEIJN, E. and STOKMAN, G.; 1989. Monitoring of aquatic vegetation in the IJsselmeer area (in Dutch). Report Rijkswaterstaat, Institute for Inland Water Management and Waste Water Treatment DBW/RIZA 89.039, Lelystad.

VAN STOKKOM, H.T.C. and DONZE, M.; 1988. Optical remote sensing and surface water nowadays (in Dutch). H_2O (21) no. 2, pp 33-42.

STOKMAN, G.N.M. and VAN STOKKOM, H.T.C.; 1986. Multi spectral scanning techniques for water quality studies in the North Sea. IAHS Publ. no. 157, pp 143-151.

VAN URK, G., VAN STOKKOM, H.T.C. and MEULSTEE, C.; 1985. Mapping and biomass estimation of aquatic macrophytes by means of aerial photography. Hungary-Dutch Seminar on Water Management Problems of Shallow Eutrophic Freshwater Lakes, Siofok, Hungary.

EUTROPHICATION OBSERVED BY REMOTE SENSING; A DISTANT POINT OF VIEW

T.H.L. Claassen

ABSTRACT

Eutrophication of surface waters, especially of lakes, is still a serious water quality problem. In summer time the water in the shallow Frisian lakes is coloured green and the phytocenoses are dominated by blue-greens, mainly *Oscillatoria agardhii*. Water quality standards for Secchi-disk transparency, chlorophyll-a and total phosphate are exceeded frequently. Two Landsat Thematic Mapper satellite images of 16 June and 3 August 1986 were studied to get insight in spatial patterns of eutrophication processes, as indicated by water colouring. The true colour images of the lakes showed great within and between lakes differences, as well as differences between both surveys. Thematic maps were made for Secchi-disk depth, chlorophyll-a and suspended matter by means of correlation of ground survey data of routine sampling stations with the corresponding satellite pixel values. The lack of simultaneous data of the groundwater sampling programme with the satellite overpass caused a limited reliability of the thematic maps. However, the use of satellite images for water quality studies, especially of eutrophication, can be a helpful instrument for water quality management.

1 INTRODUCTION

One of the main water quality problems in shallow Dutch lakes is the eutrophication. In summer time the water is coloured green, the phytocenose is dominated by blue-green algae and water quality standards are exceeded. Besides phosphate and nitrogen, also light can be one of the limiting factors for algae growth and biomass production (CUWVO, 1987). Because of the poor under water light climate water plants disappeared. Indirect effects are recorded in a changed fish-population: roughly spoken more bream (*Abramis brama)* and less pike (*Esox lucius*) were founded. Such an eutrophicated situation has been, already for many years, characteristic for the Frisian lakes, too (Claassen, 1987).

Traditionally routine water quality studies are based on samples of (fixed) stations and as such confined to (separate) point observations. In Friesland, for instance, the routine water quality monitoring programme exists of some 135 stations, which are sampled monthly. By increasing the frequency of sampling more knowledge is gathered about dynamic processes (as periodicity); by sampling many stations close together the insight in spatial patterns (as patchiness) will increase. However, routine water quality monitoring is often a compromise of both sampling strategies: limited by sampling frequency and limited by the density of sampling stations.

Remote sensing is especially useful for eliminating the spatial limitations of the routine water quality monitoring programme (Van Stokkom & Donze, 1986). For some parameters - interfering with light in one way or another - it is possible to get an area covering picture. Good results of satellite applications are reported for Secchi-disk transparency, chlorophyll-a, turbidity and suspended matter (Hilton, 1984; Lathrop & Lillesand, 1986; Stokman & Van Stokkom, 1986) and applicable for Dutch shallow lakes, i.c. Lake IJssel (RWS, 1985; Buiteveld et al., 1987).

By repeated applications remote sensing can reveal changes in water quality.

In Friesland 135 sampling stations of the routine monitoring programme are established throughout the province. In the lakes and (interconnecting) canals, together forming one vast basin water system, 75 stations are located. Of these only 15 stations are situated in the

lakes (see Fig. 1). Sampling takes place monthly in the period April till September during two separate boat trips (south-west: 1 - 8 and north-east: 9 - 15). As a consequence there is no overall picture of the water quality, in this case of the eutrophication at a given time, no more than for the whole lake surface area. Satellite remote sensing application can yield useful additional information beside the data of the routine monitoring programme.

In 1987 the project "Remote sensing of eutrophication in the basin water system in the province of Friesland, The Netherlands" was set up. In the project the possibilities were studied to use Landsat Thematic Mapper images of 1986 for water quality applications in the Frisian lakes. Reporting was carried out by Van den Brink (DHV, 1988) and published by the Netherlands Remote Sensing Board (BCRS-report 88-17). A review was given by Claassen (1989). In this article some results of the project will be presented and discussed, among others, from the perspective of the additional value of remote sensing application for (routine) water quality monitoring.

2 DESCRIPTION OF THE STUDY AREA

The province of Friesland is situated in the northern part of the Netherlands (Fig. 1). Roughly spoken the soil consists of sand in the south-eastern part, peat in the middle part and clay in the north-western part of the province. The land is bounded on the north by the Wadden Sea and on the south-west by the Lake IJssel. The whole province nearly forms - from the hydrological point of view - the unity of the Frisian basin water area (305,000 ha). The lakes and (interconnecting) canals form an uninterrupted, interconnected network of the basin water itself (14,000 ha). The lakes have a surface area of 10,000 ha. In summertime many polders whitdraw the water from the basin water system, in winter (and by water surplus also in summer) the polders drain off water into the system. The basin water system itself has - as much as possible - a constant water level of 0.52m below the reference level in the Netherlands (NAP). In summertime water level control is regulated by discharging surplus water into the Wadden Sea and by inflowing of water shortage from Lake IJssel. This daily water level control depends very much on the actual climatic conditions.

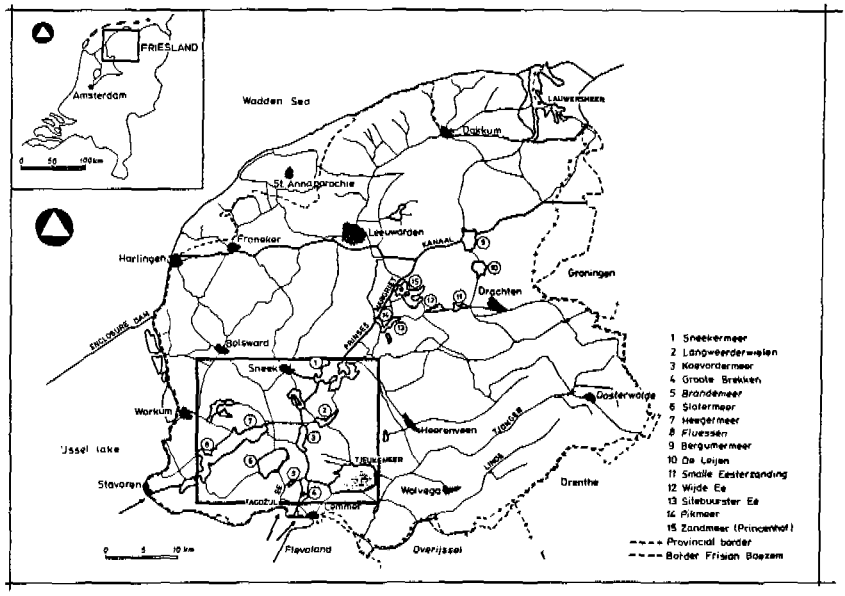

Figure 1 The province of Friesland and the catchment area of the Frisian basin water system. The 15 sampling stations in the lakes are indicated. The lakes in the framework are plotted in Figure 7

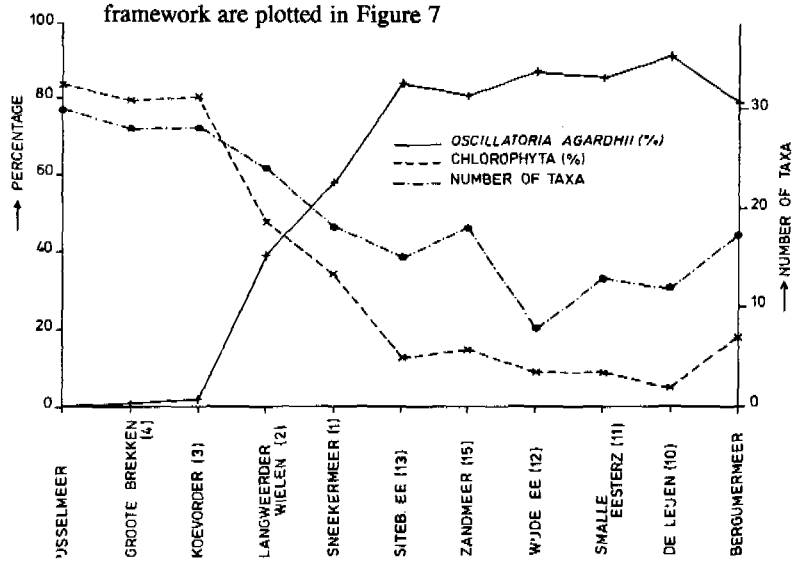

Figure 2 The percentages of *Oscillatoria agardhii* and Chlorophyta in a south-north gradient through the Frisian lake-area, August 1986

Under normal climatological/hydrological conditions the content of the basin water system ($180.10\ m^3$) is substituted 1.5-2 times by Lake IJssel water in summer and 5-6 times by polder water in winter. The inflow of Lake IJssel water is possible via Lemmer, Tacozijl en Stavoren (see arrows in Fig. 1). In the period 1970 (after locking up the Lauwersmeer)-1988 the annual mean inflow contained $246.10^6\ m^3$ via Lemmer, $39.10^6\ m^3$ via Tacozijl, and $11.10^6\ m^3$ via Stavoren. Annual maximum inflow ($695.10^6\ m^3$) took place in 1976, minimum inflow ($33.10^6\ m^3$) in 1987.

The water retention time amounts some months in summer, with clear differences for the separate lakes, among other depending on their geographical position related to the inflow-stations and on their catchment area. The lakes are eutrophic-hypertrophic. The phytoplankton is dominated by blue-greens, viz. *Oscillatoria agardhii*.

In Figure 2 the percentage of *O. agardhii* is plotted in a gradient from Lake IJssel to the north-eastern lakes. Comparable results have been found yearly, see for instance Claassen (1984) for 1983. Remarkable is the absence of *O. agardhii* and the relatively high number of taxa, including Chloraphyta in the Lake IJssel. For eight sampling stations the seasonal lapse for 1986 is presented in Figure 3.

The influence of Lake IJssel is decreasing in successive Groote Brekken, Brandemeer, Slotermeer and Heegermeer. In 1986 the Frisian basin water lakes had, in comparison with other years, a relatively small dominance of blue-greens (Anonymous, 1989). However, as a consequence water quality standards for chlorophyll-a, but also other parameters are frequently exceeded. In Table 1 some data are summarised.

Table 1 Water quality standards (avereaged values April-September) for some parameters of the so-called basic quality and the percentage of sampling stations (n = 75) in the basin water fulfilling these standards (after Anonymous, 1987; 1989)

parameter	standard	1984	1985	1986	1987	1988
Secchi-disk transparency	≥ 0.5 m	0	0	0	0	0
Chlorophyll-a	≤ 100 ug/1	25	28	36	28	40
Total phosphate	≤ 0.15 mg/1	12	0	5	3	0

The worse water quality, as expressed partly in Table 1, has not only a negative influence on the aquatic biocenoses, but also the recreational importance of the lake area is seriously threatened. Efforts already taken - like phosphate removal on treatment plants - to combat the eutrophication are still without results. A modelling study should give answers on an overall block of measures to be taken for an effective control on the still going process of eutrophication (Van Huet et al., 1987).

3 OBJECTIVES OF THE PROJECT

From the typical characteristics and qualifications of satellite remote sensing images, it looks interesting and useful to analyse the following subjects:

- To become an overall picture of the water surface of the area in study, by which the variation in colour (reflection) gives an indication of some water quality aspects. It was intended to present a true natural picture (true colour and or false colour images) of the Frisian lake area as much as possible.
- To relate and quantify patterns of some water quality parameters, registered by the satellite, with data of the routine water quality monitoring programme. It was intended to present thematic maps (Beck & Van den Brink, 1986) for the water quality parameters temperature, chlorophyll-a, Secchi-disk transparency and suspended matter.
- To analyse and interpret the mutual influence of Lake IJssel and Frisian basin water and the related development of mass algae concentrations. The management of inlet of water of Lake IJssel (related to quantity, inflow stations, period of the year, etc.) can be an important tool to combat the eutrophication in the lakes.
- To check the representativeness of the existing (15) sampling stations. After all, the study is limited to the greater surface areas (lakes) by the satellite spatial resolution.
- To give a multi-temporal analysis and interpretation of two available satellite images in one season, related to one another as well as to internal and external processes which are going on.

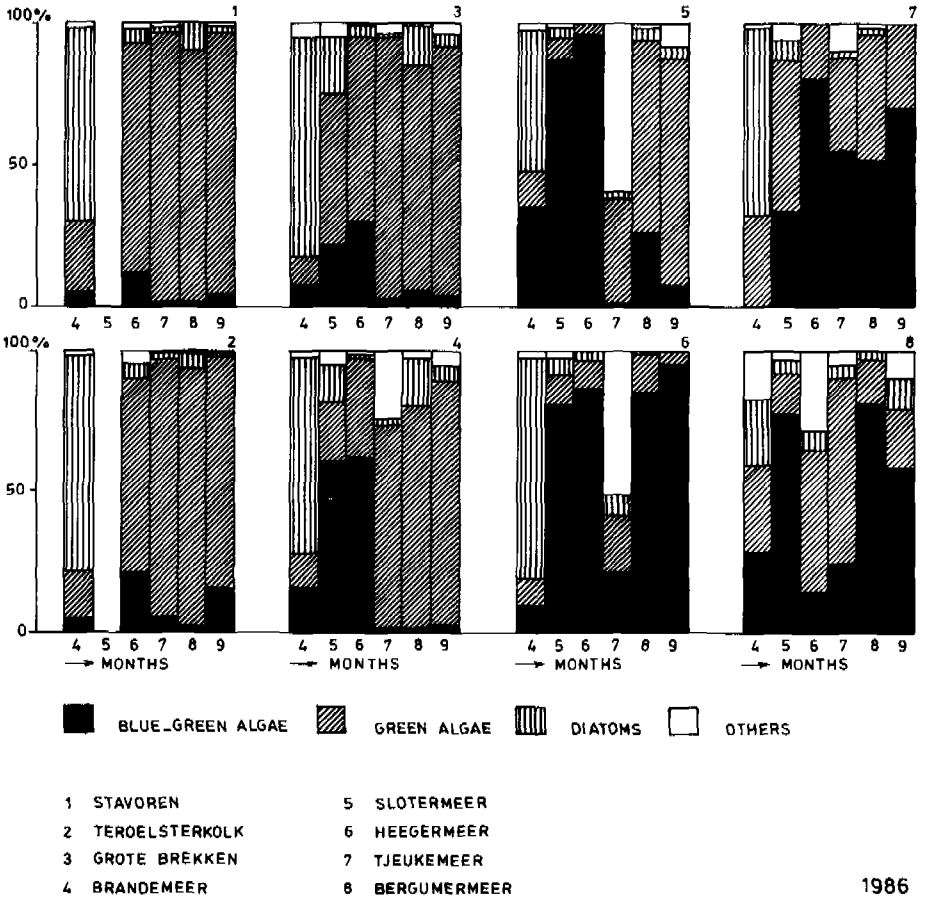

Figure 3 The percentages of the main groups of phytoplankton for eight stations in the summer of 1986

4 DATA PROCESSING

The usefulness of satellite surveys in water quality studies depends for a great deal from the weather conditions on the overpass dates, especially in the Netherlands. Above all clouds limit the number of valuable satellite borne imagery to about 4 to 5 images per year from the Landsat Thematic Mapper (Buiteveld et al., 1987), in spite of an overpass frequency of every 16 days. Two bright surveys of the Landsat Thematic Mapper (TM) have been compared, both qualitatively and quantitatively, with ground water quality data. Images of 16 June '86 and 3 August '86 were chosen, so it was possible to analyse and compare an

early and late summer situation. For Friesland it concerns Landsat 5, track 198, row 23. Only two out of four quadrants have been purchased. Data processing of the satellite images took place with the Erdas image processing system of DHV.

The ground resolution of the TM contains 30 x 30 m, so that the acquired data acquisition were only relevant to lakes. Corrections were made, among others, for atmospheric scattering, geometrical transformation (1 : 50,000) and image-noise. TM-radiance values of selected bands were related to groundwater quality data by stepwise linear regression analysis. Ground reference data consisting of Secchi-disk depth (cm), chlorophyll-a (ug/1), suspended solids (mg/1) and temperature (° C) were not available for the TM overpass-days. So most coincident data were used: for the image of 16 June '86 data of 18 June for the southern lakes (1-8 in Fig. 1) and of 25 June for the northern lakes (9-15 in Fig. 1); for the image of 3 August '86 data of 16 July and 20 August for the southern lakes and of 24 July and 27 August for the northern lakes. The data of the northern lakes had a negative influence on the significance of the regression models, therefore these lakes (9-15 in Fig. 1) were excluded in the final calculations. Furthermore regression analysis was not significant for the temperature and the Secchi-disk transparency of the August-image. Quantified relations of chlorophyll-a and Secchi-disk transparency of the June image and of chlorophyll-a and suspended matter for the August image were left over; for both dates only reliable for the southern lakes. Table 2 shows the linear regressions, used for making the thematic maps. The equations are used to calculate the geophysical parameters for each pixel from the reflectance values measured by the satellite. For more details reference is made to DHV (1988).

Table 2 Final regressions for chlorophyll-a, Secchi-disk transparency and suspended matter for the Frisian lakes and the satellite images of 16 June and 3 August 1986, used for making the thematic maps (see Fig. 7); TM_i = reflection in TM band i; after DHV (1988)

Date: 16 June 1986					
chlorophyll-a (μg/l)	=	288.41	+ 17.82TM_4	- 43.40TM_2	+10.23TM_1
Secchi-disk depth (cm)	=	159.476	- 6.851TM_3	+ 2.352TM_2	- 0.103TM_1
Date: 3 August 1986					
chlorophyll-a (μg/l)	=	-2,195.91	- 91.50TM_4	+ 123.28TM_3	+189.61TM_5
suspended matter (mg/l)	=	- 204.55	+ 5.01 TM_1	- 3.36TM_2	

Because of the initial thematic maps showed an inconvenient (16 lines) striping, a filtering was applied to remove it. This correction took place with the original digital satellite data. As a consequence unfiltered as well as filtered thematic maps were at our disposal.

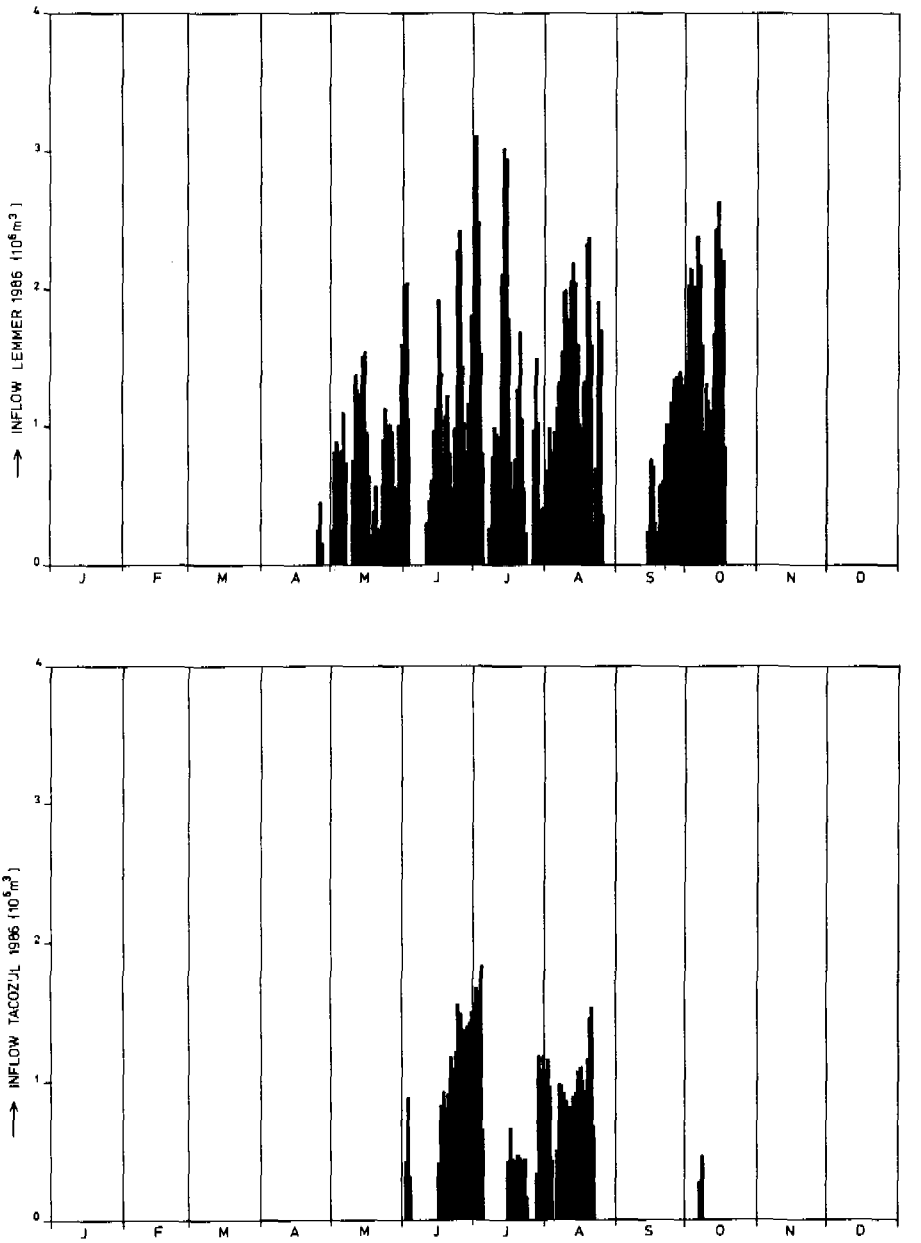

Figure 4 The daily amounts of Lake IJssel, let in in the Frisian basin water system via the inflow stations Lemmer (above, 4a) and Tacozijl (below, 4b). The total amounts for both stations in 1986 were 172.10^6m3 and 55.10^6m3, respectively

For interpretation of the selected remote sensing images it is necessary to take in mind the hydrological and weather conditions just before and on the day of passing of the satellite. Via Stavoren there was no inflow of the Lake IJssel water for more than a week (13 and 10 days) before both data (16 June '86 and 3 August '86, respectively).

The inflow of Lake IJssel water via Lemmer and Tacozijl is presented in Figure 4. In the period before 16 June '86 there was no inflow via Tacozijl. Via Lemmer the inflow started 11 June '86 and increased up to 16 June '86. In the period before 3 August '86 inflow took place continuously on both locations for a week. The amounts of water are summarized in Table 3. Here certain climatological data, as wind, are also presented. Wind can have a dramatic influence on water movements, transport and resuspension in these lakes (Leenen, 1982).

Table 3 Amounts of inflow of Lake IJssel water, wind and rainfall for the Frisian basin area, before and on the passage of the satellite on 16 June '86 and 3 August '86

date 1986	inflow of water (10^6m3) Lemmer	Tacozijl	Stavoren	wind (8 a.m.) direction	speed ($m.sec^{-1}$)	water-mark (cm NAP)	rain fall (mm)
12-06	0.461	-	-	N	3.5	-53.3	0
13-06	0.610	-	-	var.	0.5	-53.8	0
14-06	0.962	-	-	E	2	-53.7	0
15-06	1.125	-	-	E	4	-53.9	0
16-06	1.920	0.416	-	E	6	-54.6	0
30-07	0.390	1.075	-	WSW	3	-53.0	0.2
31-07	0.406	1.191	-	S	4	-52.4	0
01-08	0.392	1.086	-	WSW	6	-52.0	0.1
02-08	0.683	1.169	-	SSE	5.5	-52.3	0
03-08	0.988	0.970	-	S	2.5	-53.2	0.1

Before 16 June '86 it was dry weather, it got still warmer by a weak to moderate eastern wind; before 3 August '86 there was a fluctuating but low rainfall by a preponderating weak to moderate southern wind.

6 RESULTS

For visualisation of the digital satellite data various images were made of three out of six bands of the TM in the colours blue, green and red. The combination TM_1 (0.45 - 0.52 um) in blue, TM_2 (0.52-0.60 um) in green and TM_3 (0.63-0.69 um) in red, gives as a so called true colour image, a most reliable true to nature view of high altitude. These images of both dates are reprinted in the photographs of Figure 5.

The true colour image of 16 June '86 shows little variation within and between the lakes, while the contrast for 3 August '86 is remarkable. Slotermeer (6) and Sneekermeer (1) are dark, while Heegermeer (7) and Fluessen (8) are greenish. Tjeukemeer has a striking heterogeneity, with dark colours in the south-western and greenish colours in the north-eastern part of the lake. So these TM images hold - in combination with the different hydrological situation on both dates of satellite overpass, see Figure 4 and Table 3 - great expectations.

Coloured thematic maps have been made for the south-western lakes, as indicated in Fig. 1 The following widths of classes were used: for chlorophyll-a 20 ug/1, for Secchi-disk transparency 5 cm and for suspended matter 5 mg/1, all from zero values. In this way values below and above the water quality standards for chlorophyll-a ($\leq$ 100 ug/1) and Secchi-disk depth ($\geq$ 50 cm) are immediately visible. For the whole water surface area processed, the covering percentage of every class was given. This resulted in an impression of the range of found values as well as of the most abundant classes. In Figure 7 these overall percentages are presented for the four maps, based on unfiltered as well as filtered prints.

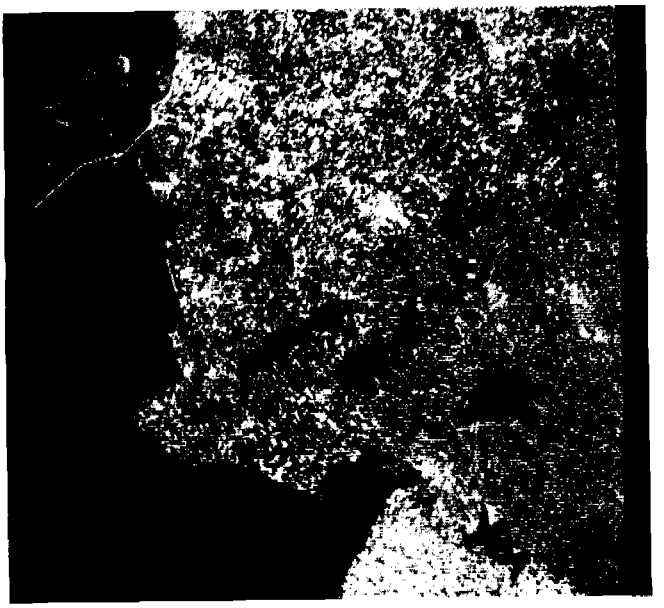

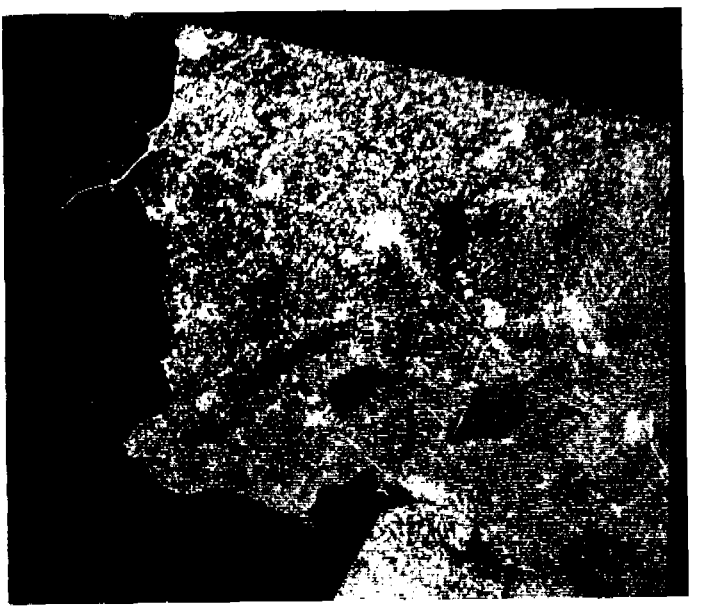

Figure 5 Overall picture of the true colour satellite images of June 16 (above, 5a) and August 3 (below, 5b)

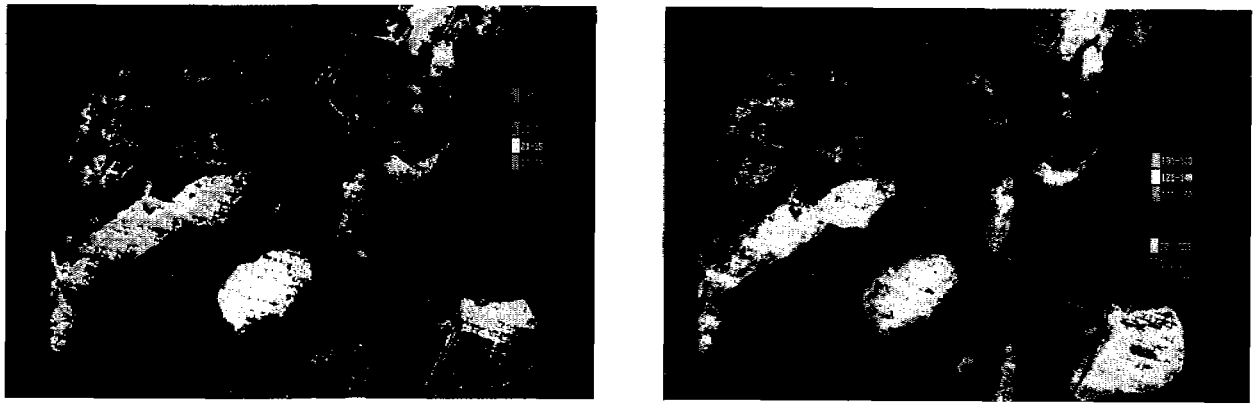

Figure 6a Thematic maps (unfiltered) for the southern lake area for Secchi-disk transparency and chlorophyll-a on 16 June 1986

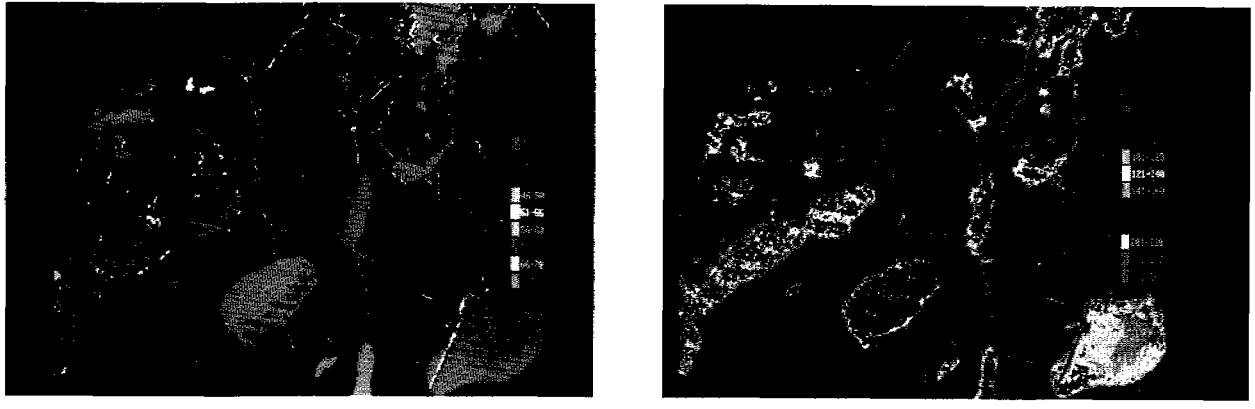

Figure 6b Thematic maps (unfiltered) for the southern lake area for suspended matter and chlorophyll-a on 3 August 1986

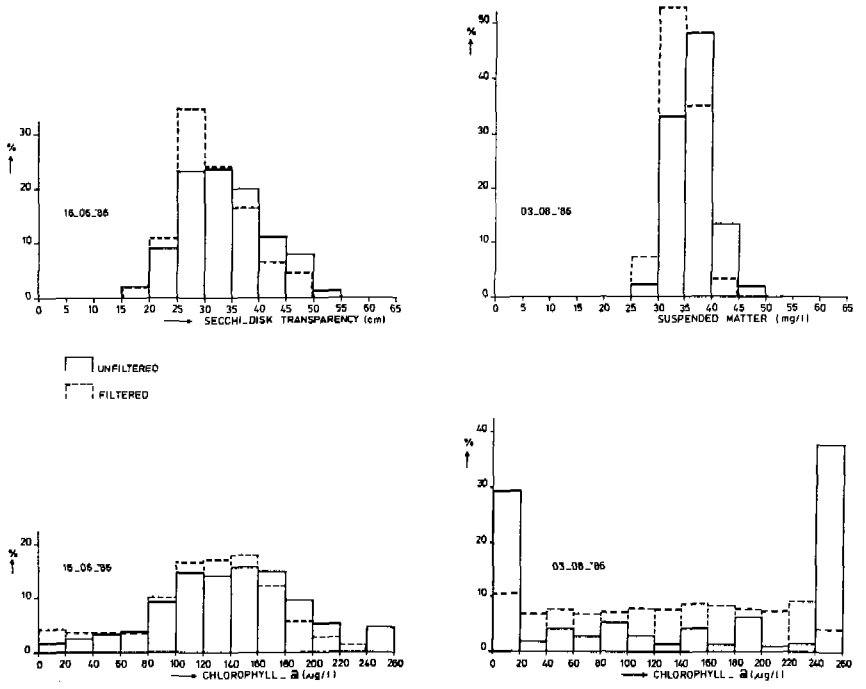

Figure 7 Percentages of cover area per class for transparency, suspended matter and chlorophyll-a for the whole lake area, bounded in Figure 1 and presented in Figure 6

For the unfiltered Secchi-disk transparency map 78.4% of the points fall in the range of 26-45 cm; for the suspended matter map 81.6% fall in the range of 31-40 mg/1. By filtering there is a remarkable shift to lower values for both parameters. Moreover it is clear that the standard for transparency has nearly never been reached. For chlorophyll-a the printed ranges on both dates are very large and the distribution for the August image seems to point to artefacts rather than to reality. This makes it hard to draw conclusions for the chlorophyll-a thematic maps. However, in Figure 6 the thematic maps are visualised for the south-western lakes, all based on the unfiltered prints. The southern and south-eastern part

of the lakes show a greater transparency than the north-western parts. This can be induced by the prevailing eastern wind just before and on the moment of the satellite overpass on 16 June '86 (see Table 3). The fact that lakes Groote Brekken, Koevordermeer and parts of Tjeukemeer in general have a greater transparency than lakes Slotermeer, Heegermeer, Fluessen and Sneekermeer seems to be related to the inflow of relatively clear water from Lake IJssel via Lemmer. All lakes except Tjeukemeer, Slotermeer en Heegermeer fall in one class regarded to suspended matter. For the three lakes mentioned two neighbouring classes are distinguished. Slotermeer has the lowest levels and as such this corresponds with the dark colour on the true colour photograph of
3 August '86. Neither the transparency map, nor the suspended matter map show a fringe effect.

For chlorophyll-a the most remarkable facts are the great within-lake variation with patchy patterns of colours. In general - except Tjeukemeer on 3 August '86 - the values are increasing, coming up to be shore of the lakes. Especially on 3 August '86 there is a pronounced fringe effect. For this date Slotermeer and Tjeukemeer have very different levels of chlorophyll-a, as expressed in the first and last bars of Figure 7, too.

In Table 4 the within-lake variability is - roughly considered - given for five lakes, as illustrated in Figure 7. The chlorophyll-a values of 3 August '86 varied extremely, in fact from 0-260 ug/1, in all lakes, so that data are not mentioned in Table 4. The ranges are greater for the unfiltered than for the filtered data of Secchi-disk depth and suspended matter. No difference is found for chlorophyll-a.

Table 4 Ranges in levels of transparency (cm), suspended matter (mg/1) and chlorophyll-a (ug/1) for five lakes as deduced from the satellite data for 16 June and 3 August 1986 and plotted in the thematic maps (Fig. 6), after DHV (1988)

	transparency 16-6-86		suspended matter 3-8-86		chlorophyll-a 16-6-86	
Lake	unfiltered	filtered	unfiltered	filtered	unfiltered	filtered
Groote Brekken	31-50	36-45	31-35	26-35	121-220	121-220
Koevordermeer	21-50	26-45	31-40	31-35	101-220	101-220
Brandemeer	31-45	31-40	31-35	31-35	181-220	101-240
Slotermeer	16-40	16-35	26-35	26-35	81-220	81-200
Tjeukemeer	21-50	21-45	31-45	31-40	41-220	61-200

Table 5 Mean values and ranges of Secchi-disk transparency (cm) for five lakes in June and August 1986. n = number of sampling stations in a lake; - = all the same values; ranges in brackets, after Van Huet (in prep.)

Lake	n	9-6	16-6	23-6	28-7	4-8	11-8
Groote Brekken	3	25 (-)	25 (-)	23 (20-25)	30 (-)	25 (-)	33 30-35
Koevordermeer	3	25 (-)	20 (-)	20 (-)	25 (-)	20 (-)	30 (-)
Brandemeer	1	30 (-)	25 (-)	25 (-)	25 (-)	30 (-)	35 (-)
Slotermeer	8	19 (15-25)	19 (15-20)	16 (15-20)	29 (20-35)	23 (15-25)	30 (15-40)
Tjeukemeer	11	34 (30-40)	29 (25-35)	21 (20-25)	30 (25-35)	25 (20-30)	28 (25-30)

Available ground data for transparency and suspended matter, comparable with the presented data in Figures 6 and 7 and Table 4, are listed in Tables 5 and 6, respectively. Transparency-measurements were carried out in an intensive eutrophication study-project and are still being compiled (Van Huet, in prep.). The suspended matter data are measured in the provincial routine sampling programme from July 1986 on. Comparing Table 4 and Table 5 the measured transparency data show much less variation than indicated by the

thematic map and are - in general - obviously lower. Comparing Table 4 and Table 6 the suspended matter values fit quite well. In such a detail no comparable data of chlorophyll-a were available.

Table 6 Measured values of suspended matter (mg/l) for six lakes, July-August 1986 and June-August 1987 (Anonymous, 1989)

	1986		1987				
Lake	16-7	20-8	24-6	21-7	17-8	23-9	x
Groote Brekken	26	33	39	53	25	25	34
Koevordermeer	37	41	46	46	24	37	29
Brandemeer	34	36	41	35	22	29	33
Slotermeer	29	35	57	27	18	31	33
Heegermeer	37	42	54	36	110	29	51
Fluessen	27	42	49	38	100	27	47

7 DISCUSSION AND CONCLUSIONS

Eutrophication is still a great problem in water quality management. Water quality standards are exceeded and many functions as well as ecological values have been affected. By mass starvation of algae there are serious oxygen problems and sometimes fish mortality. Eutrophication and its effects have been characterized inherently by dynamic processes, temporarily and spationally. For an effective programme of combatting the eutrophication it is necessary to take measures at the source (e.g. phosphate removal on treatment plants) as well as in the field itself: effect-related measures, as hydrological or biological manipulations. For this it is necessary to know about patterns and processes of algae growth and mass algae occurrence. In this respect remote sensing can give additional information to the routine water quality monitoring data. Therefore two Landsat Thematic Mapper images of 1986 were studied.

The greatest shortcoming in this project seems to be the missing data of groundwater quality on the day of the satellite overpass. Nevertheless the analyses produced useful information,

for the situation in 1986 and for future planning of investigations. The remote sensing images showed differences in water quality within and between the lakes, not yet known from the routine monitoring programme. Since 1986 the sampling dates of the lakes are planned on the satellite overpasses (every 32 days).

From the compilated parameters there was a decreasing level of details and patchiness, so an increasing uniformity for chlorophyll-a, Secchi-disk transparency and suspended matter, respectively. On the other hand, when looking at the similarities and differences between the thematic maps and the available ground data, there is a decreasing reliability for the suspended matter-, Secchi-disk depth- and chlorophyll-a maps, respectively. In fact the chlorophyll-a thematic maps have no quantitative, but only qualitative value.

The true colour images (Fig. 5) and related thematic maps (Fig. 6) of both dates show remarkable differences. Explanation of the images is not simple and not at all causal. The inflow of Lake IJssel water has a distinct influence, from the hydrological part of view. On the contrary the algae growth in the Frisian lakes, has its own autonomy for the greater part: *Oscillatoria*-dominated, characteristic of shallow turbid waters. It is not impossible that there was a collapse of algae in the Slotermeer just before the August overpass, causing the dark colour in the true colour image and giving a very low chlorophyll-a level. In general much information is needed for explaining and interpreting the satellite images.
It should be sufficient to have 15 sampling stations for making correlations with satellite data. However, most of the present stations are situated in the middle of the lakes. As appeared from the thematic maps there is - in some cases - a fringe-effect. For this reason it should be better to reallocate some stations, with the intention to have the disposal of the whole range of water quality values for the parameters in question. When taking the ranges in mind of the separate lakes (Tables 4, 5 and 6) it seems that the greater the lake, the greater the within-lake variability. This should be considered when revising the monitoring programme.

The advantages and drawbacks of remote sensing application for routine water quality monitoring are listed in Table 7. A precondition in all cases is the monitoring of field-data on satellite overpass dates. At this moment remote sensing in water quality monitoring requires additional efforts in relation to the consisted routine monitoring programme.

However, in the near future remote sensing can be a helpful instrument for water quality management, especially for problems with eutrophication. It claims some efforts and flexibility of the water quality managers. This is a question of time. Besides that the specialists have to cope with practical problems and questions which are still being discussed by the water quality managers.

Table 7 Positive and negative aspects of practical application of remote sensing in water quality monitoring

advantages	drawbacks
- map-covering images	- limited to a few water quality parameters
- patterns become visual	
- give insight in the possibility of improving the monitoring network	- risk of bad weather conditions by overpass; limited useful images
	- limited resolution
- knowledge extension	- dependence of specialists

ACKNOWLEDGEMENTS

J.W. van den Brink (DHV, Amersfoort) and G.N.M. Stokman (DBW/RIZA, Lelystad) are gratefully thanked for their intensive review of the manuscript.

REFERENCES

ANONYMOUS; 1987. Waterkwaliteit Friesland 1984-1985 (in Dutch). Provincie Friesland, Leeuwarden.

ANONYMOUS; 1989. Waterkwaliteit Friesland 1986-1987-1988 (in Dutch). Provincie Friesland, Leeuwarden.

BECK, R. and VAN DEN BRINK, J.W.; 1986. Satelliet themakaarten, een nieuw hulpmiddel in planning en beheer (in Dutch). Milieutechniek Land en Water 26 (4): 59-61.

BUITEVELD, H., MEULSTEE, C. and JORDANS, R.; 1987. Het gebruik van LANDSAT opnamen voor waterkwaliteitsonderzoek in het IJsselmeergebied (in Dutch). BCRS-87-18.

CLAASSEN, T.H.L.; 1984. De invloed van Rijnwater op het beheer van boezem- en polderwater (in Dutch) in: Rijnwater in Nederland. Oecologische kring: 53-79.

CLAASSEN, T.H.L.; 1987. The Frisian lakes as a shallow hypertrophic Oscillatoria-dominated system (in Dutch). H_2O, 19 (20): 268-275, 279.

CLAASSEN, T.H.L.; 1989. Remote sensing of eutrophication in the basinwater system in the province of Friesland, The Netherlands. PAO-cursus GEOPLAN, Delft, 12 pp.

CUWVO; 1987. Vergelijkend onderzoek naar de eutrofiëring in Nederlandse meren en plassen. Werkgroep VI, Lelystad.

DHV; 1988. De toepassingsmogelijkheden van remote sensing satellietopnamen voor het waterkwaliteitsbeheer van de Friese meren. Amersfoort.

HILTON, J.; 1984. Airborne remote sensing for freshwater and estuarine monitoring. Water Res., 18 (10): 1195-1223.

HUET, H.J.W.J.; in prep. Hydrological and phosphate modelling in south-west Frisian lakes.

HUET, H.J.W.J., DE HAAN, H. and CLAASSEN, T.H.L.; 1987. Phosphorus eutrophication research in some lakes of south western Friesland. Introduction and some preliminery results. H_2O, 20 (6): 131-135.

LATHROP, R.G. and LILLESAND, T.M.; 1986. Use of thematic mapper data to assess water quality in Green Bay and Central lake Michigan. Photogrammetric engineering and remote sensing, 52 (5): 671-680.

LEENEN, J.D.; 1982 Wind induced diffusion in a shallow lake, a case study. Hydrobio. Bull., 16 (2/3): 231-240.

LINDELL, L.T.; 1981. Experiences from correlations of Landsat data versus transmission of light and chlorophyll-a. Verh. Internat. Verein. Limnol., 21: 432-441.

RWS; 1985. Remote sensing en waterkwaliteit in het IJsselmeergebied. Projectgroep "Remote Sensing IJsselmeergebied".

STOKMAN, G.N.M. and VAN STOKKOM, H.T.C.; 1986. Multispectral scanning techniques for water quality studies in the North Sea, Monitoring to Detect Changes in water Quality Series, IAHS Publ. no. 157: 143-151.

STOKKOM, H.T.C. VAN and DONZE, M.; 1988. Remote sensing in water management. H_2O 21 (2): 33-42.

MAPPING GROUNDWATER LOSSES IN THE WESTERN DESERT OF EGYPT WITH SATELLITE MEASUREMENTS OF SURFACE REFLECTANCE AND SURFACE TEMPERATURE

W.G.M. Bastiaanssen and M. Menenti

ABSTRACT

The impact of land surface processes on surface reflectance and surface temperature is outlined. These surface parameters can be observed by remote-sensing techniques. Soil water in the top layer affects the surface reflectance and consequently the net radiation budget. Atmospheric transmittance and sun zenith angle affect the reflectance likewise. Surface temperature results from the balance of incoming and outgoing energy fluxes at the soil-atmosphere interface. Surface reflectance appear to be correlated with surface temperature. The correlation can be explained based on the surface energy balance equation. An effective aerodynamic resistance can be derived from the linear trend above dry land surfaces. The relationship between surface reflectance and surface temperature can be applied to classify different soil units.

Energy fluxes above non-homogeneous land surfaces with variable properties can be obtained from satellite images when standard meteorological data such as global radiation and air temperature are available. An example of the calculation of regional evaporation losses from a huge groundwater body in the Western Desert of Egypt is presented. LANDSAT Thematic Mapper data appear to be an excellent mean to map soil units and hydrological processes of vast and inaccessible regions. Integration of satellite images with computer models is a useful tool to study land surface processes.

1 INTRODUCTION

Groundwater resources play a dominant role in the agricultural and social development of countries in arid regions. The rapid population growth in Egypt, in combination with limited existence of cultivated areas outside the Nile Valley and Delta, makes desert reclamation necessary. Reclamation of desert lands releases the population pressure on the traditional cultivated areas. The availability of groundwater is the main constraint for development. Prediction of groundwater drawdown in the extraction areas is an important issue for the long-term planning of groundwater development. Therefore, comprehensive groundwater studies are mandatory.

Several groundwater studies in the Western Desert of Egypt have been completed during the eighties (Amer et al., 1981; Euroconsult/Pacer, 1983; Brinkmann et al., 1987). An important issue is the impact of groundwater losses in natural depressions (En: playas, Ar: sebkha) and ancient oases on total groundwater balance. An investigation on natural groundwater losses by evaporation from playas was initiated in 1986. The aim was to estimate the annual natural groundwater losses using remote- sensing techniques as developed by Menenti (1984). The results will implement a data set for annual groundwater losses. The project approach consists of four main components (Fig. 1):

(i) simulation of soil water flow in the saturated zone;
(ii) simulation of soil water flow in the unsaturated zone;
(iii) field measurements of soil/atmospherical properties and partition of land surface energy fluxes;
(iv) classification of physiographic units and mapping of land surface energy fluxes with satellite images.

Satellite imagery provides information on surface properties. Most earth-observation satellites are equipped with sensors to observe reflected shortwave solar radiation (spectral reflectance) and emitted longwave radiation (temperature) through the atmospherical windows. Surface reflectance and surface temperature can be applied to classify soil units and regional energy fluxes above non-homogeneous land surfaces. Field observations are an essential component of the investigation to study in-depth the mechanisms of evaporation from nearly dry, hot structured saline soils into the atmosphere. Further, field observations

can be applied as ground truth data to obtain at-surface reflectance and temperature with at-surface values.

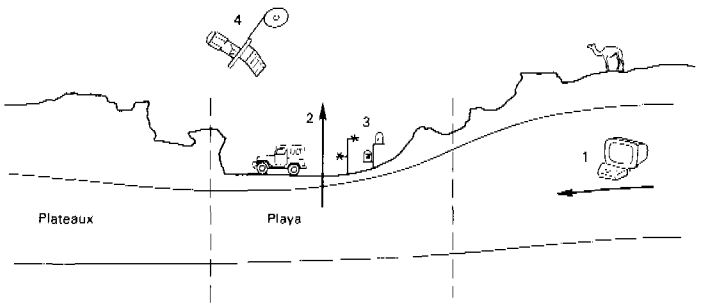

Figure 1 Project approach to map evaporation in natural desert depressions (playas). The main project components are (1) simulation of regional groundwater flow, (2) simulation of capillary rise, (3) field measurements and (4) satellite remote sensing

Aspects of the different project components are presented in this paper. The role of surface reflectance and surface temperature in the determination of regional hydrological and atmospherical processes in general is highlighted. The benefit of remote-sensing techniques towards this respect is evaluated. Results of the different components are demonstrated and interrelated for a study area in the Western Desert of Egypt.

2 THEORY ON LAND SURFACE PROCESSES AFFECTING TEMPERATURE AND REFLECTANCE

2.1 Effect of soil water content on surface reflectance and net radiation

Soil water content is an important state variable for the distribution of the surface energy fluxes. The surface energy balance equation is given in Eqn. [1]. For an explanation of all symbols used in this paper, see Annex 1.

$$Q^* = \lambda E + H + G \qquad (W.m^{-2}) \qquad [1]$$

Surface reflectance varies linearly with soil water content. Surface reflectance increases with decreasing soil water content. Atmospherical water vapour affects the scattering of incoming solar radiation. Diffuse shortwave radiation increases with the optical depth of the atmosphere. With large diffuse radiation, the soil surface behaves as a Lambertian reflector (Menenti et al., 1989a). Otherwise, surface reflectance depends strongly on sun zenith angle. So, surface reflectance varies with both water in atmosphere and soil.

To apply surface reflectance to calculate actual at-surface evaporation, a normalization procedure must be applied (Menenti et al., 1989a). The normalized surface reflectance can be applied to obtain information on the steady-state hydrological situation. With absence of rainfall, surficial soil water content is related to the existence of groundwater (Fig. 2). Deviations from the regression line in Figure 2 can be explained based on a variety of soil hydraulic properties.

The variation of surface reflectance with soil water content affects the amount of available net radiation (Fig. 3). Net radiation can be written as:

$$Q^* = (1-r)\, K^{\downarrow} + \epsilon' \sigma T_a^4 - \epsilon \sigma T_0^4 \qquad (W.m^{-2}) \qquad [2]$$

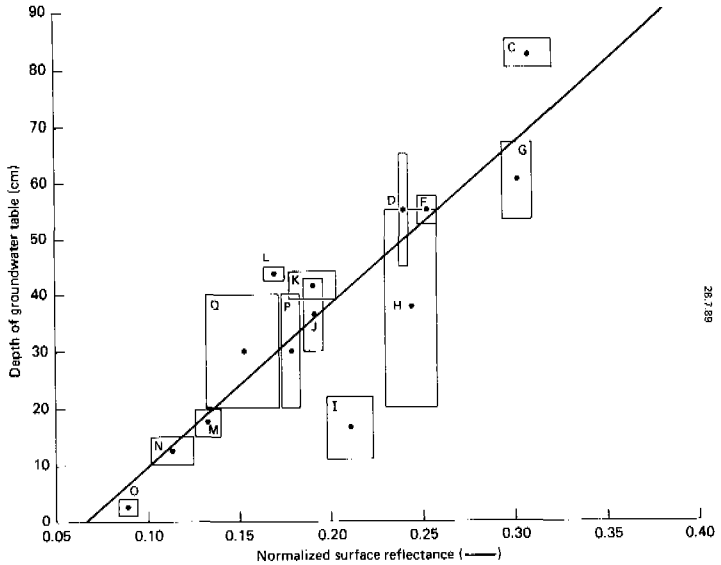

Figure 2 Observed relationship (correlation coefficient r = 0.9) between depth of the groundwater table and the normalized surface reflectance; letters indicate different soil units (after Bastiaanssen and Menenti, 1989)

Wet surfaces have a lower reflectance and absorb more shortwave solar radiation than dry surfaces. Net radiation increases with decreasing surface reflectance. The net radiation at the soil/atmosphere interface thus is controlled by the surface reflectance.

2.2 Effect of soil water content on the partition of land surface energy fluxes

The increase of net radiation with surface wetness affects the potential soil evaporation, E_{sp}. Soil evaporation is potential when the phase transfer from liquid to vapour takes place at the soil surface (Menenti, 1984). This feedback mechanism of $E_{sp} = f(Q^*)$ plays a minor role on the actual soil evaporation, E_s, when this evaporation is lower than potential, E_{sp}, i.e. when the transport capacity of the soil matrix is restricted. The capacity of the soil to conduct water through the unsaturated zone, i.e. the unsaturated hydraulic conductivity ($K(p_m)$-relationship), is a function of the degree of saturation. When the pores are

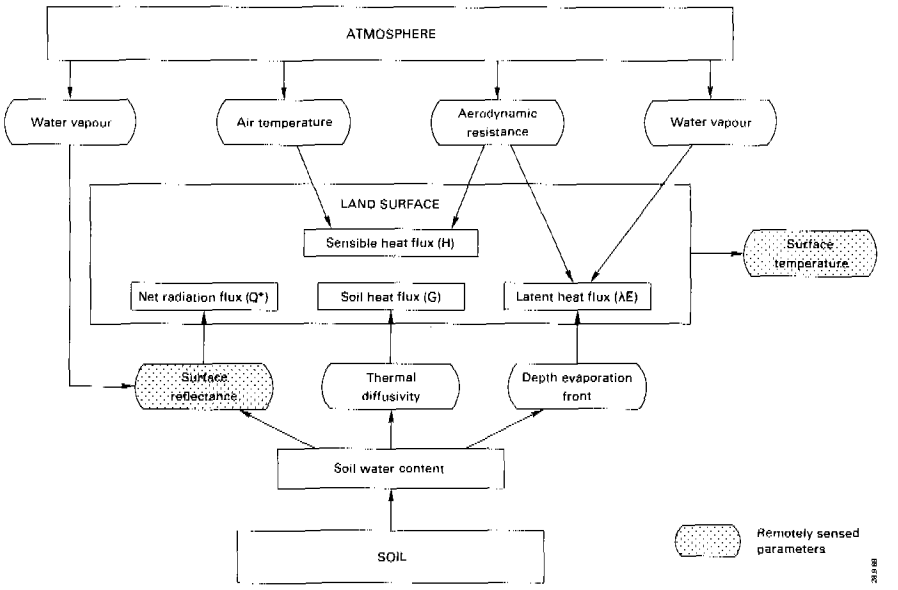

Figure 3 Schematical representation of the integration of soil and atmospherical processes. The interrelation of surface reflectance and surface temperature with soil water content is highlighted

dominantly filled with air, the liquid/vapour interface or so-called evaporation front is below the surface (Fig. 3). Vapour diffusion between the evaporation front and the soil surface lowers the upward water transport and reduces the actual soil evaporation rate. The depth of the evaporation front depends on the depth of the groundwater table, the soil hydraulic properties and the drying power of the atmosphere. So, an increase in net radiation by decreasing surface reflectance does not affect the actual soil evaporation rate. Reversibly, net radiation reduces with an increase of surface reflectance. This can be conceived as a positive feedback to any tendency in aridity. The excess of available energy will then mainly be consumed by heating of the soil, G, and air, H. The soil heat flux, G, represents the soil heat exchange component of the energy budget. Temperature waves will not penetrate equally through the soil, since most of the energy is accumulated in the top layer. The

thermal properties of the soil as a system, vary with the contribution of the different constituents. The degree of saturation is important since the thermal diffusivity of water and air are quite diverging, respectively 1.4×10^{-7} $m^2.s^{-1}$ and 2.0×10^{-5} $m^2.s^{-1}$. Although the soil heat flux increases with soil water content, the contribution on the total net energy budget is not aptly predictable since the latent heat required for evaporation plays a role too.

2.3 Effect of soil water content on surface temperature

Soil water content in the top layer thus affects the total surface energy balance. The contribution of the turbulent heat fluxes (H, λE) is directly related to soil water content. The surface temperature, which is a favourable parameter for remote sensing investigators, is a function of the ratio of all land surface energy fluxes (Fig. 3) and can be related to a specific surface flux only with drastic simplifications (Ten Berghe, 1986). Surface temperature is a dynamic equilibrium variable of the upper soil skin and describe to the physical status of the surface (Van de Griend and Gurney, 1988). The depth of the groundwater table affects the behaviour of surface temperature (Menenti, 1983).

2.4 Relationship between surface reflectance and surface temperature

Surface reflectance and surface temperature depend on soil water content and surface energy fluxes. Correlation analysis of both spaceborne and ground measurements of these variables gives a relationship of the form presented in Figure 4.

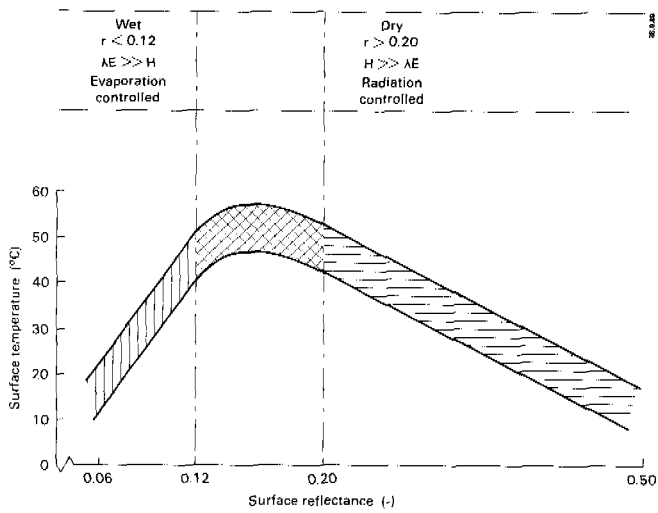

Figure 4 Surface temperature (T_0) versus surface reflectance (r) for non-homogeneous bare soil surfaces. The trend of $T_0 = f(r)$ depends on surficial soil water content and partition of surface energy fluxes

An explanation of the different trends in the relationship depicted can be given on a physical basis (Menenti et al., 1989b). For $r<0.12$, the slope between r and T_0 is positive (Fig. 4). This branch is controlled by evaporation since the surface is wet. Surface temperature increases with decreasing evaporation and soil heat flux according to Bastiaanssen and Menenti (1989):

$$T_0 = C1(C2 - r K^{\downarrow} - G - \lambda E) \qquad (K) \qquad [3]$$

$$\text{with } C1 = (4\epsilon\sigma T_0^3 + \rho_v C_p/r_{ah})^{-1} \qquad [4]$$

$$C2 = K^{\downarrow} + \epsilon'\sigma T^4 + \rho_v C_p T_a/r_{ah} + 3\epsilon\sigma T_0^{*4} \qquad [5]$$

Eqn. [3] has been derived after substitution of the transport equations of the sensible heat flux (H) and Eqn. [2] into Eqn. [1]. The following equation for H has been applied:

$$H = -\frac{\rho_v C_p}{r_{ah}} (T_0 - T_a) \qquad (W.m^{-2}) \qquad [6]$$

The slope between r and T_0 is negative when r>0.20 (Fig. 4). In this situation, the top soil is dry and evaporation is restricted by vapour diffusion between the evaporation front and the soil surface. Since $r.K^{\downarrow}$ in Eqn. [3] is larger than G and λE, surface temperature decreases with increasing reflectance. This especially holds true for high values of global radiation. Most of the energy budget is consumed as sensible heat. The variation of G and λE above non-homogeneous lands is less than the variation of H. So, under these dry conditions where E_s is some orders of magnitude lower than E_{sp}, G and λE can be assumed to be constant for land surfaces with varying net radiation budgets. This is the "radiation controlled" branch of $T_0 = f(r)$. Together with the assumption of constant global radiation and air temperature, a simplified function relating r to T_0 is obtained after rearranging Eqn. [3]:

$$r = C3 - \frac{\epsilon\sigma}{K^{\downarrow}} T_0^4 - \frac{\rho_v C_p}{r_{ah} K^{\downarrow}} T_0 \qquad (-) \qquad [7]$$

$$\text{with } C3 = 1 + \frac{\epsilon'\sigma T_a^4}{K^{\downarrow}} + \frac{\rho_v C_p T_a}{r_{ah} K^{\downarrow}} - \frac{G}{K^{\downarrow}} - \frac{\lambda E}{K^{\downarrow}} \qquad [8]$$

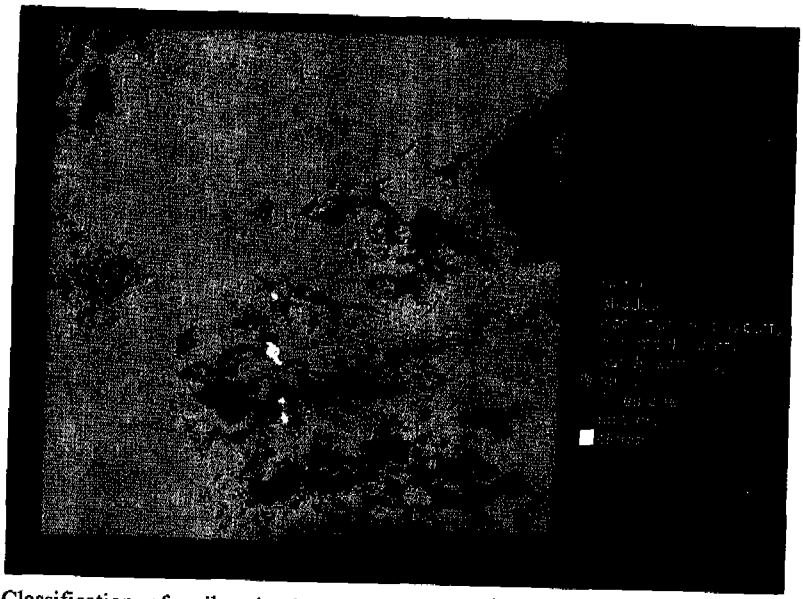

Figure 9 Classification of soil units by LANDSAT Thematic Mapper image in the Western part of the Qattara depression. Seven different soil units could be discriminated on the basis of band 6 and the total surface reflectance (after Timmerman, 1989). Path/row 179/39 and 179/40, 13 November 1987, local time 9.30 h

Figure 10 Map of latent heat flux as calculated from a LANDSAT Thematic Mapper image, showing the area around Bir Qifar in the Western part of the Qattara depression. Path/row 179/40 and 179/39, 13 November 1987, local time 9.30 h

Finally the negative slope, a, between r and T_0 can be found from Eqn. [7] after linearization by a Taylor expansion with T_0 as independent variable:

$$a = -4\epsilon\sigma T_0^3 / K^{\downarrow} - \rho_v C_p / (r_{ah} K^{\downarrow}) \qquad (K^{-1}) \qquad [9]$$

Experimental values of a can be applied to derive an effective aerodynamic resistance above non-homogeneous land types (r_{ah}). This approach is valid as long as λE forms a minor part of Q* (Fig. 5). Rocks, stones and dry sands are suitable material to meet this requirement. Under these conditions, the amount of absorbed solar radiation and turbulent sensible heat transfer are the driving forces of the time-dependent part of surface temperature patterns.

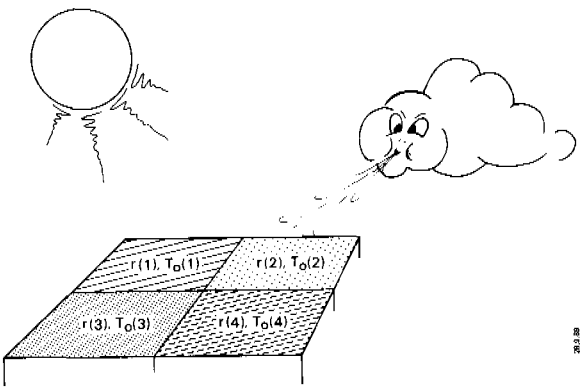

Figure 5 Aerodynamic impact on surface skin temperature for dry lands where the actual soil evaporation is some orders of magnitude lower than the potential soil evaporation and planes with different surface reflectance values

When a-values and the solar radiation are known, r_{ah} can be calculated based on Eqn. [9]. The linearized slope of $T_0 = f(r)$ can be extracted from satellite image data of r and T_0. This allows to select arbitrary area sizes and different times of the year. This promising technique can be applied to overcome the lag of information on the effective aerodynamic resistances as required for the parametrization of land surface processes as input to Global Circulation Models (Rowntree, 1988). Further, this approach of r_{ah} is an innovation to classical studies towards turbulent transfer above land surfaces. Complicated uncertainties

engaged with roughness length of heat and stability corrections for heat under non-neutral conditions of the dynamic sublayer (Kustas et al., 1989) can be solved on a two-dimensional basis.

3 METHODS

3.1 Soil classification using remote-sensing techniques

Multi-spectral scanners on board of satellites provide spectral information in narrow bands ($\sim$ 100 nm) and a high spatial resolution e.g. LANDSAT Thematic Mapper (TM): 28.5 x 28.5 m. The information extracted from multispectral sensors is dependent on the characteristics of the scanner. The LANDSAT-TM system is allocated for the classification of soils and vegetation types. Combination of multi-spectral bands into colour composites enhances the identification of different soil units. The spectral signature of soil systems differs dominantly in band 4, 5 and 7 of LANDSAT-TM (Mulders et al., 1986). Identification of hypersaline soils with these bands has given satisfactory results (Menenti et al., 1986).

In order to develop a classification procedure independent from scanner characteristics, an attempt was made to classify on the basis of total surface reflectance (albedo) and temperature (LANDSAT-TM, band 6) (Zeeman, 1989). The total surface reflectance was obtained as the weighted average from TM band 1, 2, 3, 4, 5 and 7. Advantage of this method is a standardization of classification procedures. Besides, it directly provides information on the status of surface energy fluxes.

3.2 Regional evaporation from non-homogeneous bare land surfaces

The benefit of complex formulae for bare soil evaporation varies with the availability of input data. The spatial distribution of most meteorological variables e.g. saturation deficit is the bottle-neck for the estimation of actual evaporation above non-homogeneous land surfaces. Instead of using latent heat transport equations, the principle of the remainder term has been applied:

$$\lambda E = Q^* - H - G \qquad (W.m^{-2}) \qquad [10]$$

Substituting Eqn. [2] and Eqn. [6] into Eqn. [10] relates λE to six meteorological variables:

$$\lambda E = F1(r, K^{\downarrow}, T_0, T_a, r_{ah}, G) \qquad (W.m^{-2}) \qquad [11]$$

Only r and T_0 can be directly measured from space. A method to obtain r_{ah} from $T_0 = f(r)$ has been presented in Section 2.4. With the evaporation front below surface level, G accounts on the soil heat flux at the evaporation front (G_e), which differs from the soil heat flux at the soil surface (G_0). G_0 can be conceived as the limit of G_e when the evaporation front is at surface level:

$$\lim_{z_e \to 0}(G_e) = G_0 \qquad (W.m^{-2}) \qquad [12]$$

Values of G_0 are not precisely constant for non-homogeneous land types. It was shown that G_0 varies more with thermal diffusivity than normalized surface reflectance (Bastiaanssen and Menenti, 1989). Thus the assumption of constant G-values for various dry surfaces is reasonable. Following Eqn. [11], evaporation at non-homogeneous land types (i = 1, 2...n) can be expressed by the following equation:

$$\lambda E(i) = (1-r(i))K^{\downarrow} + \epsilon' \sigma T_a^4 - \epsilon \sigma T_0(i)^4 - \rho_v C_p T_0(i)/r_{ah}(i) + \rho_v C_p T_a/r_{ah}(i) - G_e \qquad [13]$$

Combination of satellite observations of r(i), $T_0(i)$ and derived $r_{ah}(i)$-values with standard meteorological variables from ground stations ($K^{\downarrow}$, T_a, G_e), yields a solution for Eqn. [13] (Fig. 6).

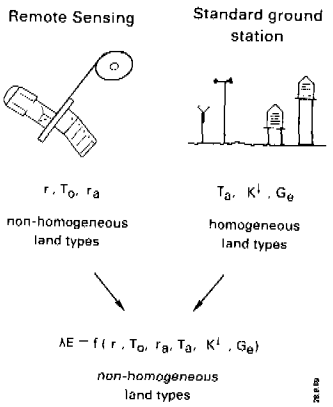

Figure 6 Procedure for the determination of evaporation from non-homogeneous land surfaces using satellite and ground-based observations. The spacial distribution of surface reflectance and surface temperature can be applied to obtain an effective aerodynamic resistance. Additional data must be collected from standard ground stations

3.3 Unsaturated soil water flow

Soil water flow under arid conditions is characterized by vapour transport through the top soil. The simulation of soil water flow under these conditions requires a coupling between the mechanisms of liquid, vapour and heat transport. A two-layer conceptual model has been developed by distinguishing an upper soil layer where water flow takes place in the vapour phase, and a lower soil layer where water flow takes place in the liquid phase (Menenti, 1984). The depth of the interface or so-called evaporation front depends among others on soil hydraulic properties e.g. $p_m(\Theta)$ and $K(p_m)$-relationships. Core samples for determination of the $p_m(\Theta)$ and $K(p_m)$-functions were collected in the Qattara depression. A cluster analysis of individual $p_m(\Theta)$ and $K(p_m)$ relationships has been carried out to classify and reduce the variation of hydraulic properties into six soil units.

Several runs with a one-dimensional numerical model (EVADES) for the simulation of the depth of the evaporation front (Bastiaanssen et al., 1989) were made. The hydraulic properties of six classified soil units were applied as input data to the EVADES-model. In this model, two boundary conditions were defined:

- the lower boundary condition, defined as the depth of the groundwater table;
- the upper boundary condition; this is the potential soil evaporation, E_{sp}.

4 CASE STUDY: REGIONAL EVAPORATION FROM THE QATTARA DEPRESSION IN THE WESTERN DESERT OF EGYPT

4.1 Hydrogeological situation

The Western Desert of Egypt consists of plateaux (max. 700 meter above mean sea level (+m.s.l.)) and deep depressions (max. 130 meter below mean sea level (-m.s.l.)) formed by wind erosion and tectonic activities. The lithological composition under the Qattara depression (20,000 km^2) is characterized by thick deposits of gravel, sand, sandstone, limestone, siltstone, clay and shales. This implies that both aquifer and aquitard systems occur. The main aquifers comprise the Moghra complex (Miocene age) and the Nubian Sandstone complex (Cretaceous age) (Fig. 7). The hydrogeology of the Northwestern desert has been investigated for the proposed Qattara Hydro Power Project by the Joint Venture Qattara (JVQ, 1979).

The multi-layered Nubian Sandstone aquifer system lies on impermeable basement rocks and belongs to the most extensive aquifer systems in the world. The groundwater reservoir of the Nubian Sandstone aquifer system (75,000 km^3) comprises almost entire Egypt and parts of Chad, Lybia and Sudan with a thickness of the groundwater bearing strata up to 3500 meter (Hesse et al., 1987). During the deposition period, some 11,000 years ago, water from the Mediterranean Sea is infiltrated so that some water-bearing layers are salty. There are indications that this process of refilling today still occurs. Tectonic movements have caused several faults and uplifts up to the surface. This discontinuity has an important impact on the hydraulic resistance of intermittent beds of clay and shale. Limestones, interbedded with shales and clayey sediments are the dominant deposits from the Upper-

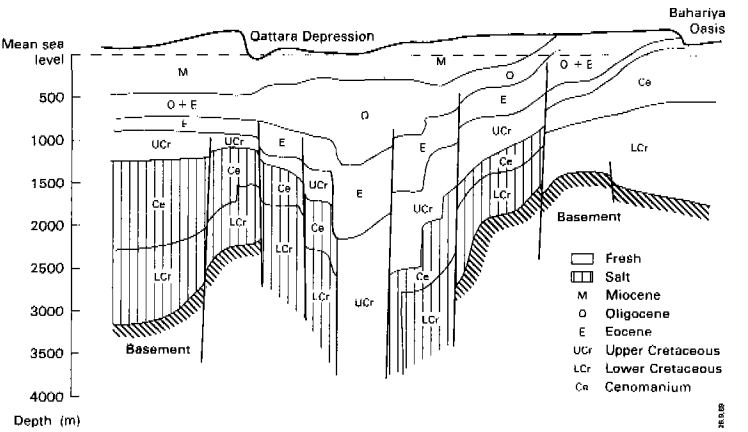

Figure 7 Generalized hydrogeological cross section between Abu Subeiha and Bahariya oasis in the Western Desert of Egypt (simplified after JVQ, 1979)

Cretaceous and Oligocene time region (Dabaa formation). Their conductance for water in absence of faults and fissures is marginal. More important for regional groundwater flow are the sands and sandstones of Miocene age, known as the Moghra and Marmarica aquifer complex. A large proportion of the floor of the Qattara depression consists of deposits of the Moghra formation. The reservoir of the Moghra complex discharges water to the playas (Sundborg and Nilsson, 1985). Permeability and storativity of groundwater depend on the porosity of intact geological units and its discontinuities. Since large areas without hydrogeological information exist, schematization of the regional hydrogeological situation is based on scarce data and interpretation (Table 1).

Table 1 Some hydrogeological parameters of the Northwestern Desert of Egypt with K = hydraulic conductivity, d = thickness and C = hydraulic resistance

Geological formation	Age	K ($m.d^{-1}$)	d (m)	C (d)
Marmarica	Middle			
Miocene		0.1-6.7	0-800	-
Moghra	Lower Miocene	0.2-17.6	0-700	-
Dabaa	Oligocene/Upper Eocene	-	0-700	5000-500,000
Abu-Roash	Eocene/Upper Cretaceous	-	500-1000	5000-400,000
Bahariya	Upper Cretaceous*	0.1-10.0	300-3500	-
Burg El-Arab	Lower Cretaceous*			
Betty	Lower Cretaceous*			

*: Nubian Sandstone aquifer system

4.2 Use of simulation models

4.2.1 Unsaturated soil water flow

A look-up table for soil specific actual evaporation can be extracted from the data set obtained by the simulations with the EVADES-model. The weather impact on the

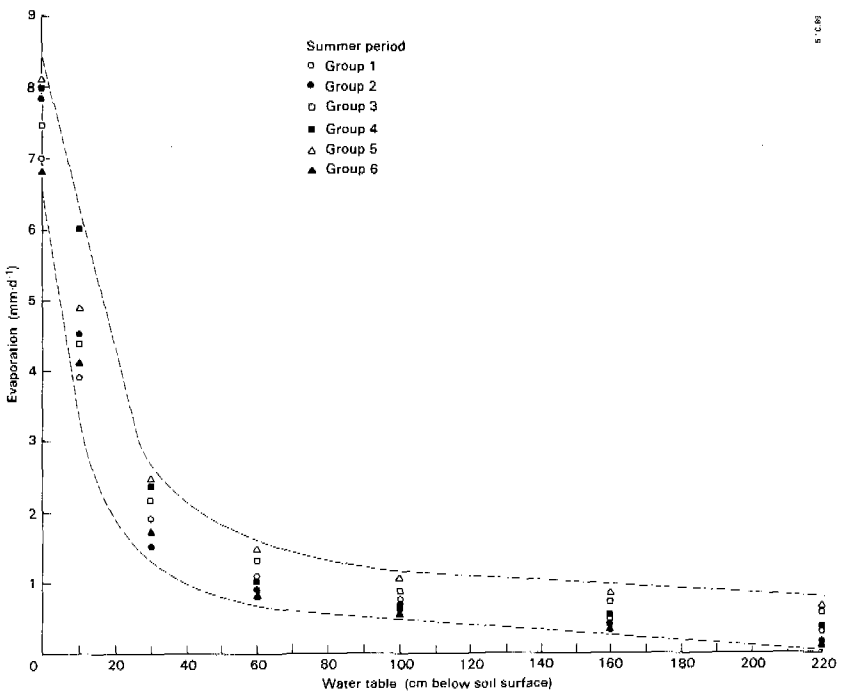

Figure 8 Look-up table for the actual soil evaporation of different Egyptian desert soils (group 1 through 6) with varying bottom boundary conditions. Calculations were done by simulation of a moving evaporation front (EVADES-model)

evaporation rate is noticeable with the presence of a shallow groundwater table (< 50 cm). Although the actual evaporation decreases rapidly when the groundwater table is deeper than 70 cm, the amount is still significant. An average depth of the groundwater table between 50 and 100 cm, which for playas is very realistic, indicates an actual evaporation between 0.45

$mm.d^{-1}$ and 1.9 $mm.d^{-1}$ (Fig. 8) which is significantly higher than figures presented in former studies e.g. E_s = 0.09-0.35 $mm.d^{-1}$ (JVQ, 1979) or E_s = 0.14-0.27 $mm.d^{-1}$ (Sundborg and Nilsson, 1985). For salt crusts and salt marshes (see Table 3, Section 4.3.1) which have an extreme shallow groundwater table (10-30 cm), the evaporation is even higher, approximately between E_s = 1.3-3.5 $mm.d^{-1}$ (Sundborg and Nilsson, 1985; E_s = 1.36-2.74 $mm.d^{-1}$).

4.2.2 Saturated soil water flow

During the study of the water balance of the Qattara depression, two fundamental questions were rosen up:

(i) Corresponds the revised regional evaporation with the possible discharge of groundwater?

(ii) How can the hydrogeological schematization of existing groundwater models be adapted in fair ranges of hydrological properties and piezometry?

In order to answer such questions, the groundwater balance was computed using three different numerical models which simulate the steady-state groundwater flow, namely FEMSATS (Querner, 1984), TRIWACO (IWACO, 1985) and AQUIFEM (Townley and Wilson, 1979).

Ad (i). Since the options of each groundwater model differ, the methodology of calculations were not uniform. The FEMSATS-model has an option to prescribe the capillary rise as a function of the groundwater table. The function depicted in Fig. 8 was generalized for homogeneous soils and applied as non-linear upper boundary condition to a five layer hydrogeological schematization. The TRIWACO-model needs the local sinks for each network element as input parameter. This includes that regional evaporation must be calculated separately first. This was done by mapping out the physiographic units, in combination with the actual evaporation values for each unit calculated by the SWATRE-model (Feddes et al., 1978). A different schematization of the aquifer systems was applied: two aquifers separated by an aquitard.

It has been concluded that groundwater flow can match the natural losses within fair ranges of K and C. This consistancy is based upon simulation runs with different schematizations of

the aquifer systems (3-5 layers), different boundary conditions (head controlled, flux

Table 2 Estimates of the annual soil evaporation from the Qattara depression as obtained by two different steady state groundwater simulation models (TRIWACO, FEMSATS)

Model Alternative		K ($m.d^{-1}$)			C (10^3 d)		Evaporation ($Mm^3.yr^{-1}$)
		Moghra	Nubian	UCE	Dabaa	Cenomanian	
TRIWACO	1	6.0	6.0	0	200		2270
	2	4.0	4.0	0	400		2270
FEMSATS	1	17.3	8.4	8.4	6-300	40-300	2244
	2	4.3	3.7	3.7	5- 85	5- 40	2080

controlled) and particularly, different estimations of the geohydrological parameters (Table 2). Taking an annual soil evaporation of 2000 $Mm^3.yr^{-1}$ for an area of 20,000 km^2, yields an average evaporation of 0.27 $mm.d^{-1}$. This average value consists of actual soil evaporation values gradually increasing from 0 $mm.d^{-1}$ for sand and limestone (67% of the area) to 3.5 $mm.d^{-1}$ and higher for soft salt marshes (1% of the area). It should be remarked that the evaporation mainly occurs in the playas (90% of the total evaporation) while vast parts of the depression floor is dry and not contributing to the natural groundwater losses. The water is mainly originating from the Nubian Sandstone aquifer system, with open connections towards the Moghra aquifer.

Ad (ii). Approving the natural losses seeks for revision of the hydrogeological schematization of the Western Desert groundwater models. The AQUIFEM-model was updated with a redesigned network and adapted sinks of groundwater (Amer et al., 1981). A new calibration of the pressure heads with other hydraulic conductivities and resistances was performed. The result was that permeabilities during previous studies were underestimated. This can be declared by the limited length of the filters for pumping tests which implies no

direct measurements of permeabilities in the deeper layers.

4.3 Results satellite observations

4.3.1 Soil classification

Seven soil units could be discriminated with a classification procedure using LANDSAT-TM images of total surface reflectance and temperature for a playa area in the Western part of the Qattara depression (Zeeman, 1989) (Fig. 9). Sand and limestone have shown overlapping r- and T_0-values. Since their existence was quite significant in the study area, band 5 of LANDSAT-TM, which is rather sensitive for vegetation- and soil water content, was added to the analysis (Timmerman, 1989). The results showed an improvement of the number of identified soil units from seven to twelve (Table 3) and decreases the standard deviation of each unit. Sand and limestone could be better discriminated.

Table 3 Classification of a LANDSAT Thematic Mapper image covering the Western part of the Qattara depression, Western Desert of Egypt. Path/row 179/39 and 179/40, 13 November 1987, 9.30 h., local time. Classification was done on the basis of total surface reflectance (albedo), band 5 (near-infrared) and band 6 (thermal infrared) (after Timmerman, 1989)

Soil unit	Total reflectance (-)		Temperature (°C)		Coverage of area
	average	range	average	range	(%)
White salt crust/marsh	0.51	0.48-0.53	18.5	17.7-19.3	0.2
Dry puffy	0.21	0.20-0.22	24.6	23.9-25.3	3.5
Hummocky	0.21	0.19-0.24	25.6	24.9-26.4	11.4
Sand plain	0.39	0.35-0.44	21.0	19.5-22.6	16.8
Darkish sand	0.34	0.31-0.37	19.9	19.3-20.6	0.4
Gravel plain/crust	0.28	0.28-0.29	24.7	24.2-25.2	4.0
Shales	0.22	0.19-0.24	29.9	29.2-30.7	3.4
Darkish limestone/sand	0.31	0.30-0.32	23.3	22.7-23.8	31.7
Lightish limestone/sand	0.33	0.32-0.34	20.2	19.8-20.5	3.4
Limestone light	0.44	0.42-0.45	22.1	21.3-23.0	3.9
Limestone dark	0.40	0.38-0.42	24.7	24.1-25.2	15.0
Water bodies	0.08	0.05-0.10	17.1	16.6-17.7	0.1
Unclassified (shadow, clouds)	-	-	-	-	6.2
				Total	100.0

4.3.2 Mapping of instantaneous latent heat flux, λE

The values of total surface reflectance and temperature as presented in Table 3 are average values for the appearance of one specific soil unit across the entire image. This methodology can perfectly be used to derive an effective r_{ah}-value for this image. The radiation controlled branch, with a negative slope between r and T_0, is found when $r > 0.22$ (see Fig. 4). Taking $K^{\downarrow} = 475$ W.m^{-2}, $G_e = 35$ W.m^{-2}, $T_a = 18.2$ °C, $\rho_v = 1.2$ kg.m^{-3} at the moment of satellite overpass, gives $r_{ah} = 119$ s.m^{-1} (Eqn. [9]), which for absence of wind (steep slope of T_0 vs r) is quite normal. Eqn. [13] can be applied to each pixel of the image. The resulting algorithm for the areal pattern of evaporation is:

$$\lambda E(i) = 3657 - r(i)475 - 5.5 \cdot 10^{-8} T_0(i)^4 - 10.1\, T_0(i) \qquad (W.m^{-2}) \qquad [14]$$

With this transformation, images of instantaneous latent heat fluxes can be obtained (Fig. 10). Additional field measurements and simulation models are required to interprete these findings to daily evaporation values.

λE-values obtained by Eqns. [9] and [13] are validated against λ E-values obtained by the Bowen-ratio energy balance method. This is a manner to validate the procedure of estimating E_s. Results of evaporation values from the Bowen-ratio energy balance approach were obtained with the help of the available set of field data. Different surface types, observed on 11, 14 and 17 June with varying aerodynamic conditions (r_{ah} = 15-103 s.m^{-1}) are considered (Table 4).

Table 4 Comparison between estimated latent heat fluxes based on non-homogeneous surface parameters, r(i) and $T_0(i)$, with field measurements of the latent heat flux according to the Bowen-ratio energy balance method

Date	Local time	Homogeneous prop.			Non-homogeneous			λE $(r(i),T_0(i))$	λE Bowen-ratio
		$K^{\downarrow}$ $(W.m^{-2})$	T_a (K)	G_e $(W.m^{-2})$	r (-)	T_0 (K)	r_{ah} $(s.m^{-1})$	$(W.m^{-2})$	$(W.m^{-2})$
11/6/88	10.00	783	26.8	101	0.20	33.6	26	148	167
11/6/88	12.00	1027	28.7	136	0.16	38.9	25	152	130
11/6/88	15.00	832	33.3	120	0.17	36.2	15	290	276
14/6/88	10.00	339	30.7	32	0.31	32.3	30	96	98
14/6/88	12.00	968	34.5	105	0.25	46.0	41	202	191
14/6/88	15.00	877	38.8	90	0.27	50.3	43	134	128
17/6/88	10.00	528	28.1	39	0.34	36.7	102	125	160
17/6/88	12.00	953	33.3	80	0.27	51.3	90	234	160
17/6/88	15.00	842	37.9	63	0.29	56.4	103	160	140

The deviation between λE = f (Bowen-ratio) and E = $f(r(i),T_0(i))$ is rather small. Hence, total surface reflectance and surface temperature can mostly be applied to estimate the aerodynamic resistance and the related instantaneous latent (and sensible heat) flux. Moreover, it is shown that the assumption of constant $K^{\downarrow}$, T_a, λE and G_e-values above drying surface with $r > 0.20$ is realistic.

4.3.3 Mapping of the daily evaporation rate, E_s

The soil specific actual daily evaporation, E_s, can be obtained using remote sensing techniques according to the following procedure:

(i) the identification of soil units (Table 3);
(ii) the estimation of the depth of the groundwater table (Fig. 2);
(iii) combining the look-up table (Fig. 8) with the results of (i) and (ii).

Table 5 Interrelation between soil unit, normalized surface reflectance and the evaporation from playas in the Qattara depression, Western Desert of Egypt

Soil unit	Normalized surface reflectance	Ground-water table from Fig. 2	Daily evapo-ration from Fig. 8	Thematic Mapper image 12/11/87 9.30 h.		
				r	T_0	λE from Fig. 10
	(-)	(cm)	($mm.d^{-1}$)	(-)	(°C)	($W.m^{-2}$)
Sand plain	0.309	69	0.6-1.4	0.39	21.0	40-130
Sandy puffy	0.302	67	0.6-1.4	0.21	24.6	100-130
Gravel plain/crust	0.240	50	0.8-1.9	0.28	24.7	70-90
Hummocky	0.179	30	1.3-2.9	0.21	25.6	75-120
Ponded puffy	0.088	6	4.7-7.2	0.08	17.1	280-320

An evaporation sequence of dry surfaces (bare coarse sand) to wet surfaces (puffy) is presented in Table 5. Although the daily evaporation differs from the instantaneous latent heat flux, the soil specific behaviour between instantaneous values and daily integrated values is identical. This phenomenon is presented in Table 5, where the range of latent heat flux is calculated from minimum and maximum pairs of (r, T_0) as depicted in Table 3 and the algorithm given in Eqn. [14].

5 CONCLUSIONS AND BENEFITS REMOTE SENSING

Satellite imagery provides information on reflected and emitted spectral radiances from the land surface. This type of information can only be applied when the knowledge between land-surface processes and spectral radiances is accurately known. The benefit of image interpretation fails or succeeds with the presence of sufficient ground-truth data and understanding of physical models.

Field observations of surface reflectance and surface temperature in combination with other soil-atmospherical parameters and surface energy fluxes, have given detailed insight in the process of evaporation from dry and structured salty soils. This was necessary to properly define algorithms which transfer information on a pixel by pixel base to thematic maps. Moreover, using remote sensing techniques, it was possible to classify dominant soil units with total surface reflectance and surface temperature. This classification procedure is independent of satellite sensor and gave enough accuracy to distinguish common soil units. Addition of LANDSAT-TM, band 5, improves the detail of classification. Considering the huge costs involved in a field soil survey in such an extensive area with salt marshes and endless sand plains, satellite remote sensing is a cheap and acceptable alternative. A normalization procedure of total surface reflectance has proven to be handy for the monitoring of the soil water status since atmospherical effects on surface reflectance are corrected. This offers the opportunity to relate surface reflectance directly to soil type and to the depth of the water table. Surface reflectance and surface temperature are mutually related and their function $T_0 = f(r)$ can be applied to derive an effective aerodynamic resistance above non-homogeneous land types. Consequently, r_{ah}-values can be extracted from satellite data on a regional basis and they can be very suitable to improve the parametrizations in General Circulation Models. Maps of instantaneous latent heat flux, based on LANDSAT-TM data, agree nicely with latent heat fluxes measured by the Bowen-ratio method. It can be concluded that playas contribute considerably to the natural evaporation of groundwater and that playas are found throughout the entire Qattara depression. Calculations with quasi three-dimensional groundwater models have shown that the revised sinks of groundwater agree with the possible discharge towards the Qattara depression and the regional distribution as observed with LANDSAT-TM data. The results have been implemented with updating of the hydrogeological schematization for

groundwater simulation models of the Western Desert of Egypt. Satellite remote sensing in combination with a proper ground truth data set appear to be an excellent tool to map regional hydrological processes.

REFERENCES

AMER, A.M., NOUR, S.E. and MISHRIKI, M.F.; 1981. A finite element model of the Nubian Aquifer system in Egypt. Water Resources Management: 327-361.

BASTIAANSSEN, W.G.M., KABAT, P. and MENENTI, M.; 1989. A new simulation model of bare soil evaporation in deserts, EVADES. Note ICW 1938. The Winand Staring Centre, Wageningen, The Netherlands. 73 pp.

BASTIAANSSEN, W.G.M. and MENENTI, M.; 1989. Surface reflectance and surface temperature in relation with soil type and regional energy fluxes. In: A.F. Bouwman (ed.). Soils and the greenhouse effect. John Wiley, Chichester, UK (in press).

BERGHE, H.F.M. TEN; 1986. Heat and water transfer at the bare soil surface. Ph.D. Thesis. Agricultural University, Wageningen, The Netherlands. 214 pp.

BRINKMANN, P.J., HEINL, M., HOLLANDER, R. and REICH, G.; 1987. Retrospective simulation of groundwater flow and transport in the Nubian aquifer system. In: E. Klitsch and E. Schrank (eds.). Berliner Geowissenschaftliche Abhandlungen, Reihe A 75.2. Dietrich Reimer Verlag, Berlin, Germany: 465-516.

EUROCONSULT/PACER; 1983. Regional development plan for New Valley. Final report. Ministry of Development. Cairo, Egypt.

FEDDES, R.A., KOWALIK, P.J. and ZARADNY, H.; 1978. Simulation of field water use and crop yield. Simulation monographs. PUDOC, Wageningen, The Netherlands. 188 pp.

GRIEND, A.A. VAN DE and GURNEY, R.J.; 1988. Satellite remote sensing and energy balance modelling for water balance assessment in (semi-) arid regions. In: I. Simmers (ed.). Estimation of natural groundwater recharge. D. Reidel Publishing Company, Dordrecht, The Netherlands: 89-116.

HESSE, K.H., HISSENE, A., KHEIR, O., SCHNACKER, E., SCHEIDER, M. and THORWEIHE, U.; 1987. Hydrological investigations in the Nubian Aquifer System, Eastern Sahara. In: E. Klitsch and E. Schrank (eds.). Berliner Geowissenschaftliche

Abhandlungen, Reihe A 75.2. Dietrich Reimer Verlag, Berlin, Germany: 397-464.

IWACO; 1985. Numerical groundwaterflow package TRIWACO, users's guide. IWACO, International Water Supply Consultant, Rotterdam, The Netherlands.

JVQ; 1979. Study Qattara Depression. Joint Venture Qattara, Ministry of Electricity and Energy, Qattara Project Authority, Cairo, Egypt.

KUSTAS, W.P., CHOUDHURY, B.J., KUNKEL, K.E. and GAY, L.W.; 1989. Estimate of the aerodynamic roughness parameters over an incomplete canopy cover of cotton. Agr. and Forest Meteo. 46: 91-105.

MENENTI, M.; 1983. A new geophysical approach using remote sensing techniques to study groundwater table depth and regional evaporation from aquifers in deserts. In: Methods and instrumentation of groundwater systems. PRoc. Int. Symp., Noordwijkerhout, mei 1983. Neth. Org. App. Sci. Res. TNO: 311-325

MENENTI, M.; 1984. Physical aspects and determination of evaporation in deserts applying remote sensing techniques. Ph.D. Thesis and Report 10 (Special Issue). The Winand Staring Centre, Wageningen, The Netherlands. p 202.

MENENTI, M., LORKEERS, A. and VISSERS, M.; 1986. An application of Thematic Mapper data in Tunesia, estimation of daily amplitude innear-surface soil temperature and discrimination on hypersaline soils. ITC-Journal 1986-1: 35-42

MENENTI, M., BASTIAANSSEN, W.G.M. and VAN EICK, D.; 1989a. Determination of surface hemispherical reflectance with Thematic Mapper data. Rem. Sens. of Env. 28:327-337

MENENTI, M., BASTIAANSSEN, W.G.M, VAN EICK, D. and ABD EL KARIM, M.H.; 1989b. Linear relationships between surface reflectance and temperature and their application to map actual evaporation of groundwater. Adv. Space Res. vol. 9(1): 165-176.

MULDERS, M.A. and EPEMA, G.F.; 1986. The Thematic Mapper: a new tool for soil mapping in arid areas. ITC-Journal 1986-1: 24-29

QUERNER, E.P.; 1984. Program FEMSATS, calculation method for steady and unsteady groundwater flow. ICW-note 1557, The Winand Staring Centre, Wageningen, The Netherlands. 24 pp.

ROWNTREE, P.R.; 1988. Land surface parametrizations - basic concepts and review of schemes, Dynamical Climatology Technical Note no. 72, Meteorological Office, Bracknell, U.K. 25 pp.

SUNDBORG, A. and NILSSON, B.; 1985. Qattara Hydrosolar Power Project Environmental Assessment, UNGI Rapport nr. 62, Uppsala University, Sweden. 194 pp.

TIMMERMAN, K.B.; 1989. Standardization of the albedo, Internal Publication no. 26, The Winand Staring Centre, Wageningen, The Netherlands. 25 pp.

TOWNLEY, L. and WILSON J.; 1979. Description and User's manual for a Finite Aquifer Flow Model, AQUIFEM-1. Technology Adaption Report 79-3. MIT, Cambridge, USA.

ZEEMAN, M.; 1989. Berekening en classificatie van oppervlakte reflectiebeelden met behulp van Landsat TM-data, case study Qattara-Depressie (Egypt). Internal Publication no. 20. The Winand Staring Centre, Wageningen, The Netherlands. 31 pp.

Symbol	Interpretation	Unit
a	slope of T_0 versus r	(K^{-1})
C	hydraulic resistance	d
C1,2,3	constant	-
C_p	air specific heat at constant pressure	$J.kg^{-1}.K^{-1}$
d	layer thickness	m
E_s	actual soil evaporation	$m.d^{-1}$
E_{sp}	potential soil evaporation	$m.d^{-1}$
g	gravitational constant	$m.s^{-2}$
G	soil heat flux	$W.m^{-2}$
G_0	soil heat flux at the land surface	$W.m^{-2}$
G_e	soil heat flux at the evaporation front	$W.m^{-2}$
H	sensible heat flux	$W.m^{-2}$
K	hydraulic conductivity	$m.d^{-1}$
$K^{\downarrow}$	incoming shortwave solar radiation	$W.m^{-2}$
$K(p_m)$	unsaturated hydraulic conductivity	$m.s^{-1}$
p_m	matric pressure head	m
Q*	net radiation	$W.m^{-2}$
r	surface reflectance	-
r_{ah}	resistance for heat transport in air	$s.m^{-1}$
T_a	air temperature	K
T_0	surface temperature	K
T_0^*	reference surface temperature	K
ϵ	surface emissivity	-
ϵ'	apparent emissivity of the atmosphere	-
Θ	soil water content	$m^3.m^{-3}$
ρ_v	density of moist air	$kg.m^{-3}$
λ	specific latent heat of vaporization	$J.kg^{-1}$
λE	latent heat flux	$W.m^{-2}$
σ	Stephan Boltzmann constant	$W.m^{-2}.K^{-4}$

APPLICATION OF REMOTE SENSING IN THE EVALUATION AND IMPROVEMENT OF IRRIGATION WATER MANAGEMENT

P. Minderhoud, J. van Nieuwkoop and T.N.M. Visser

ABSTRACT

In 1988 NEDECO, ICW, ILRI, INCYTH and DGI began cooperating on a research and demonstration project in the use of satellite images and remote sensing techniques for improved water management. This project is being financed by the BCRS, the Dutch agency for promoting commercial applications of remote sensing.

The objectives of the study are:

(1) to improve the data base for computation of crop water demands and preparation of distribution schedules

(2) to monitor irrigation management performance through mapping of areas which are effected by water shortages, salinization as well as waterlogging.

A map of cultivated and non-cultivated areas was prepared. It appeared that significant discrepancies occur between actually irrigated area and official records used by the Irrigation Agency. Next a crop type map was prepared showing areas with identical water demands. The study in Argentina shows that satellite images and remote sensing techniques have great potential for a more efficient use of irrigation water. Particularly in areas where good quality images are available and water supplies are scarce, the application of remote sensing in water management will become increasingly important.

1 INTRODUCTION

In February 1988 NEDECO, ICW, ILRI, DGI and INCYTH* began cooperating on a demonstration project in irrigation management. This project is based on results obtained from earlier projects which had been carried out cooperatively by IILA, TECNECO* and INCYTH (1977-1982) and ICW and INCYTH, and which had involved irrigation management (Chambouleyron et al., 1983; Menenti et al., 1985) and (since 1984) remote sensing (Menenti, 1988). The objective of the present project is to demonstrate and further develop a method of evaluating and optimizing water distribution on large irrigation schemes using satellite remote sensing and (numerical) modelling. The Tunuyán Irrigation Scheme, located in Mendoza Province, Argentina, was chosen as the study area (Fig. 1). A great deal of relevant data is already available for this study. Given the project objective it was not considered useful to perform all analyses over the whole area of the scheme. Most procedures were therefore applied to the command area of the Viejo Retamo, a secondary unit within the scheme. The study shows that advanced analysis tools have to be adapted to meet the local requirements of irrigation management. Local conditions define the priorities for irrigation management, which have to be taken into account carefully in order to guarantee the acceptance of advanced analysis and management tools.

* NEDECO = Association of Engineering Companies for Development, The Netherlands
ICW = Institute for Land and Water Management Research, Wageningen, (now part of The Winand Staring Centre for Integrated Land, Soil and Water Research), The Netherlands
ILRI = International Institute for Land Reclamation and Improvement, Wageningen, The Netherlands
DGI = Departemento General de Irrigación, Mendoza, Argentina
INCYTH = Instituto Nacional de Ciencia y Técnica Hidricas, Mendoza, Argentina.
IILA = Instituto Italo-Latino Americano, Italia
TECNECO = Tecnologia e Ecosistemi, Italia

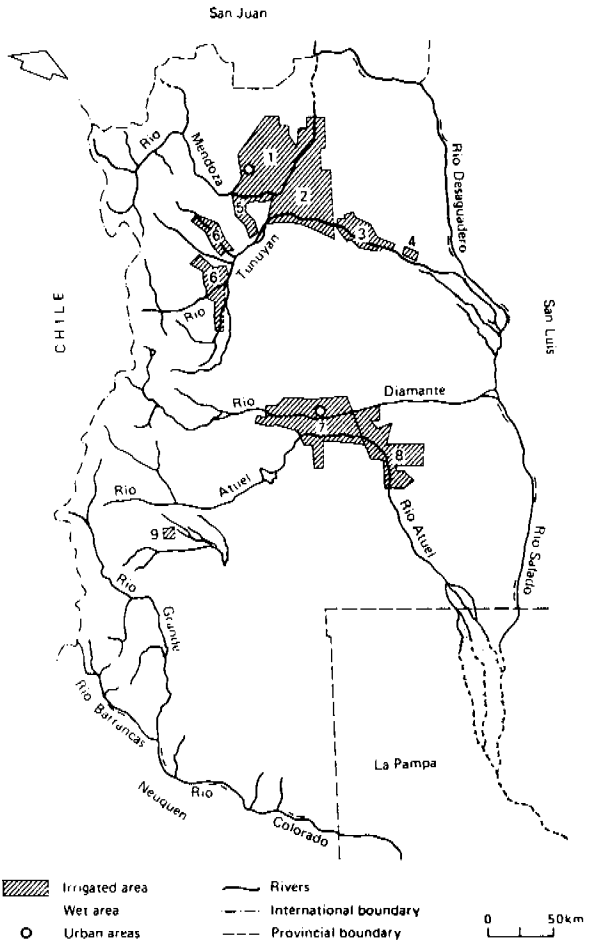

Figure 1 Main irrigation districts in the Province of Mendoza, Argentina

1 = Río Mendoza, 2 = Río Tunuyán Medio, 3 = Santa Rosa,
4 = La Paz, 5 = Ugarteche, 6 = Valle de Uco, 7 = San Rafael,
8 = General Alvear, 9 = Malargüe

This is especially relevant when considering the application of remote sensing to irrigation management. Remote sensing applications relate to a rapidly developing technology, which enables the registration of more data, with greater precision and with a greater frequency of transmission. Remote sensing involves a large number of interpretation techniques, in which various phenomena are registered through various camera systems in different spectral ranges. Data collection is usually checked and completed through terrestrial activities, checks and additional investigations in the field. In this article these general features are apparent. On the one side satellite images are made available and made best use of. On the other hand related field programmes are developed. Field programmes combined with satellite data interpretation are used to evaluate the performance of irrigation systems. Knowledge thus obtained can be used further to elaborate specific policy goals as the optimization of water supply.

2 THE Río TUNUYAN STUDY

2.1 Introduction

The province of Mendoza is situated in the central western part of Argentina. It has a long tradition in the use of water for irrigation which dates back to pre-Columbian times. When the Conquistadores came to this region they found irrigated parcels planted with crops. More than 200 years ago settlers adopted the irrigation practices of that culture. The conquest of the territory by the Spaniards and the coming of European settlers at the turn of this century, together with the construction of the railroad led to the full utilization of irrigated lands. At present the irrigated area comprises five large oases with a total area of 350,000 ha. The total average flow of all rivers is 160 m^3/s. Rainfall normally does not exceed 300 mm a year.

At present the area has been under continuous development for over one hundred years. Water management has gone through a gradual evolutionary process, coping with an increasingly modernized agriculture, enlargement of scale and changing crop patterns.
Nowadays agriculture involves extensive areas of fruit trees (grapes, peaches, etc.), and vegetable and food crops.
Water distribution is exercised through a uniform system of water-rights. Water is delivered

according to the water-rights assigned to each water-right holder. The distribution is equitable over all water-rights holders, and irrespective of the actual land use. This distribution system is simple to operate but leads to substantial losses of water.

The Río Tunuyán Medio command area is the area that has been studied in some detail in this project (Fig. 2). It covers about 70,000 ha and is partly supplied by surface water and partly by groundwater. Surface water is diverted from the Río Tunuyán by the G. Benegas Dam into the Canal Matriz Margen Derecha Reduccion (≈ 12 m^3/s) and into the Canal Matriz Margen Izquerda Matriz (≈ 60 m^3/s).
Groundwater is pumped from a confined aquifer by over 6,000 wells with a total capacity of about 50 m^3/s.

Within the areas under irrigation a variety of interrelated problems occur and these have grown in magnitude throughout the last years. On the one hand they relate to an increasing urban and industrial development with waste water emissions discharging into the agricultural areas. On the other hand they relate to sub-optimal water distribution resulting in over-irrigation, drainage problems and salinization whereas in other parts shortages of water may occur with further incentives to farmers to start exploiting groundwater resources.

This complex of institutional and managerial problems call for quantitative inventories of these phenomena, and for further planning to improve the situation.

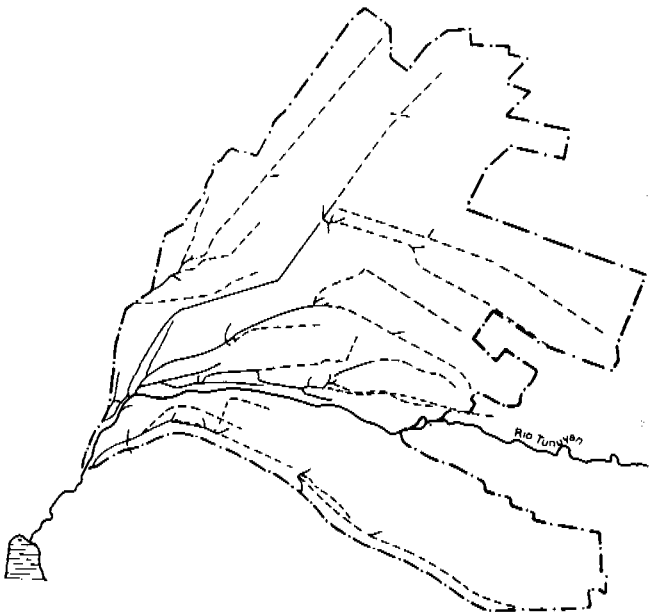

Figure 2 Layout of Río Tunuyán Irrigation Scheme showing primary canals (—), secondary canals (---) and the boundary of the command area (-.-.-) (Visser, 1989)

2.2 Outline of the study programme

Within the framework of this study various options were pursued to demonstrate how far remote sensing interpretation techniques could be used to quantify water requirements. These were combined with terrestrial data collection programmes and with the application of numerical simulation software to carry relevant computations further. Examples of the actual application of satellite data and hydrological modelling in the management of irrigation water management in the Río Tunuyán Irrigation Scheme are given.

The performance of the irrigation system is assessed on the basis of three different concepts:

1 The water allocation policy is supposed to be directed at an equitable distribution of the available surface water over the different secondary and tertiary units. Three cases are considered:
   a Each secondary and tertiary unit receives a volume of water proportional to the area with water-rights within that unit
   b Each secondary and tertiary unit receives a volume of water proportional to the actual cultivated area within that unit
   c Each secondary and tertiary unit receives a volume of water proportional to its total irrigable area.

   The performance of current water supply is assessed by calculating the ratio of the intended volume - calculated as the share of the available irrigation water that should be allocated to a certain tertiary or secondary unit - to the actual volume e.g. the volume of water that is actually supplied to that unit in any period of time.
2 The water allocation policy is supposed to be directed at matching the crop water requirements in each tertiary unit. The performance of the current water supply is assessed by determining the ratio of the crop water requirements to the actual volume for each tertiary unit.
3 In the third case the "effectiveness" of the supplied irrigation water is considered. This is done by determining the ratio of the increase in actual evapotranspiration to the actual volume supplied in any period of time.

Table 1 shows the formulae of the three ratios applying to the different concepts listed above. It also contains the land use data needed and the models used. The complexity of the calculation increases from the first to the third ratio as shown by the increasing amount and complexity of ancillary data. Moreover some of the data required e.g. to calculate the third ratio, are rather difficult to obtain; the hydraulic properties of unsaturated soil being a good example. This implies that the first ratio allows a finer spatial resolution in the appraisal of performance than the third ratio. Therefore, a trade-off has to be established in practice.

Table 1 Definition of different ratios quantifying irrigation performance; for each ratio the required land use data are indicated explicitly, with their source; the ancillary data necessary to calculate each ratio are also indicated

Ratios	Land use data needed	Source	Model	Ancillary data
1 $Ri = \frac{V_i / A_i}{V_{ij} / A_{ij}}$	area with water rights, cultivated area, total irrigable area	satellite image, field survey		discharges
2 $Ri = \sum_{k=1}^{n} \frac{ETc_k * A_{ik}}{V_i}$	crops or groups having a similar k_c	satellite image	CRIWAR	discharges, meteorological data
3 $Ri = \sum_{k=1}^{n} \frac{(ETa_k - \hat{ETa}_k) * A_{ik}}{V_i}$	crops	satellite image	SWATRE	discharges, meteorological data, soil properties

V_i = volume supplied to unit i (m^3/month)
V_{ij} = volume received at unit j, within higher order unit i (m^3/month)
A_i = irrigated area in unit i (m^2)
A_{ik} = area of crop k in unit i (m^2)
ETc_k = potential evapotranspiration of crop k (m/month)
ETa_k = actual evapotranspiration of crop k, irrigated (m/month)
$\hat{ETa}_k$ = idem, non-irrigated (m/month)
k_c = crop coefficient

The procedures and calculations presented were applied to the Viejo Retamo secondary unit.

2.3 Basic calculation procedures

As described above the values of the three ratios (see Table 1) have to be determined for the different reference units, relevant to irrigation water management. These units are defined as the command areas of the primary, secondary and tertiary irrigation canals. All input point data, such as meteorological data and soil-physical properties must be referred to the same reference units. The processing of these input data results in the following information (Visser et al., 1989):

- amount of water needed in each tertiary unit per unit of time (10 days, month)
- amount of water applied in each tertiary unit per unit of time (idem)
- different ratios of these variables.

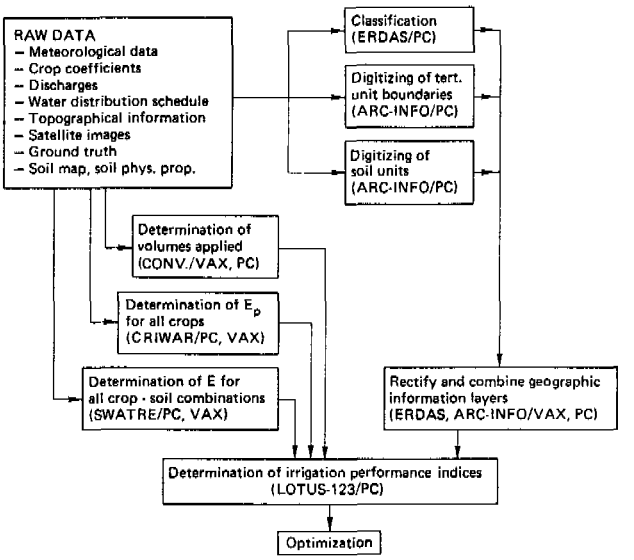

Figure 3 Chart showing raw data and operations as required to calculate ratios (Visser, 1989)

The different operations that have to be performed in order to determine the values of the three ratios are shown in Figure 3. It includes the software-hardware configurations used and the transfer of data between them. The raw data are listed in the upper left corner of the overview. The operations on the right can be characterized as Geographical Information System (GIS)-operations involving three information layers (classified image containing land use classes, map of irrigation infrastructure, soil map). They have to be rectified and

combined in order to obtain the information needed: the distribution of land use classes and soil units in the different reference units. The activities on the left consist of the calculation of the volumes applied to each reference unit and the hydrological modelling. The use of the models results in the potential (CRIWAR) and the actual (SWATRE) evapotranspiration of all crops or crop-soil combinations. All information is combined in a LOTUS-123 worksheet to calculate the values of the different ratios.
The components of Figure 3 will be discussed briefly.

- Raw data

A short list of the required input data is given to emphasize that satellites provide only part of the information. Accurate land use data are essential to improve irrigation management.
To calculate the value of the first ratio, only "basic" data on water flow, topography and the distribution of cultivated area, derived from satellite images, are needed. To calculate the value of the second ratio, additional data concerning meteorology and crop factors have to be gathered. Also the information derived from the satellite data will have to be more specific where different crops or crop types are concerned. Calculation of the third ratio can only be performed when data on the physical properties in the soil and distribution of soil types occurring in the area are available.

- Determination of volumes of water supplied to each reference unit, per unit of time

In order to determine these volumes, discharge measurement structures should be installed at the inlet of all the units. Normally the person in charge of the water distribution is also responsible for the registration of flow data. These data are mostly registered at the opening time of the structure, the closing time and the head over the weir crest at both moments. A computer programme was developed to convert these data to volumes of water applied per turn and per period of 10 days.

- Determination of potential evapotranspiration, ET_c, for all crops

To calculate the value of the second ratio (Table 1) the potential evapotranspiration of all crops occurring in the area has to be known. The potential evapotranspiration of a crop depends on the meteorological circumstances, commonly expressed in the reference evapotranspiration ET_0, and the crop properties, expressed in the crop factor k_c. The potential evapotranspiration of a crop can be determined by means of the programme

CRIWAR (VOS et al., 1988), given its k_c and some meteorological data.

- Determination of actual evapotranspiration, ET_a, for all crop-soil combinations with and without irrigation, using SWATRE

SWATRE is a numerical model of water transport in the unsaturated zone. Gathering reliable data on the soil hydraulic properties will not be easy in many cases. The programme RETC (approach described by VAN GENUCHTEN, 1986, unpublished; Salinity Laboratory, Riverside, Calif., USA) might be an adequate tool for deriving these data from basic measurements of water content at different pressure heads in a soil sample.
Once all necessary data are available SWATRE should be applied to the irrigated and non-irrigated situation in order to determine the increase in actual evapotranspiration due to the application of irrigation water.

- Classification of land use

Classification of satellite images by means of an image processing software package is necessary for mapping land use. To calculate the value of ratio 1 a classification discriminating cultivated and non-cultivated area is sufficient. Different methods to map cultivated areas using LANDSAT-TM satellite images can be applied. Potential evapotranspiration is crop-dependent so in order to obtain the value of ratio 2 a classification discriminating crop or crop type is necessary. If the classification of individual crops turns out to be unfeasible, crop types can be discriminated, each crop type having a certain crop factor (k_c) assigned to it. The map of the crop coefficient k_c is constructed by applying the following procedure:

* crops and crop varieties are mapped by means of a field survey for a number of reference plots
* mean spectral reflectances are calculated with LANDSAT-TM data for each reference plot
* reference plots are aggregated into clusters by means of unsupervised classification techniques

* the resulting clusters are applied as training set with a supervised classification technique.

  Crop coefficients k_c are assigned as a function of time to each mapped unit, which gives the required k_c map.

- Digitizing of tertiary unit boundaries

To be able to relate the land use data to the reference units mentioned in the beginning of this section, accurate information is needed on the location of the boundaries of the command areas of different tertiary, secondary and primary canals. If no such information is available, it should be gathered by means of a field survey. Aerial photographs or possibly satellite images, could be used to facilitate this. The resulting map containing these boundaries should be digitized. This should be done in such a way that the data file containing the map is compatible with the classified images to combine them. Different GIS software packages offer the possibility of doing this.

- Digitizing of soil units

The difference in actual evapotranspiration in situations with and without irrigation depends heavily on the kind of soil. Therefore the spatial distribution of the different soil units within the different reference units must be known. In order to obtain this information the boundaries of the soil units should be digitized, preferably in the same way as the map containing the reference unit boundaries.

- Rectify and combine geographical information layers

In order to obtain the value of the ratios in Table 1 the cultivated area (ratio 1), the areas of the different crops or crop types (ratio 2) or the area of each crop-soil combination (ratio 3) within each reference unit should be determined. This is done by making an overlay of all three information layers (land use map, boundaries of reference units, boundaries of soil units). Before this, the three layers should be rectified and transformed to the same coordinate system. Almost all GIS and image processing software packages offer the possibility of performing both rectification and overlay procedures.

Figure 4 Classified image showing the cultivated and not-cultivated area of the Río Tunuyán Irrigation Scheme; overlay shows the boundaries of the secondary units of the scheme (Visser, 1989)

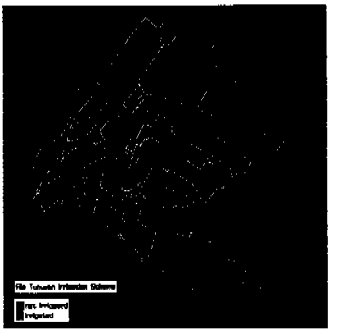

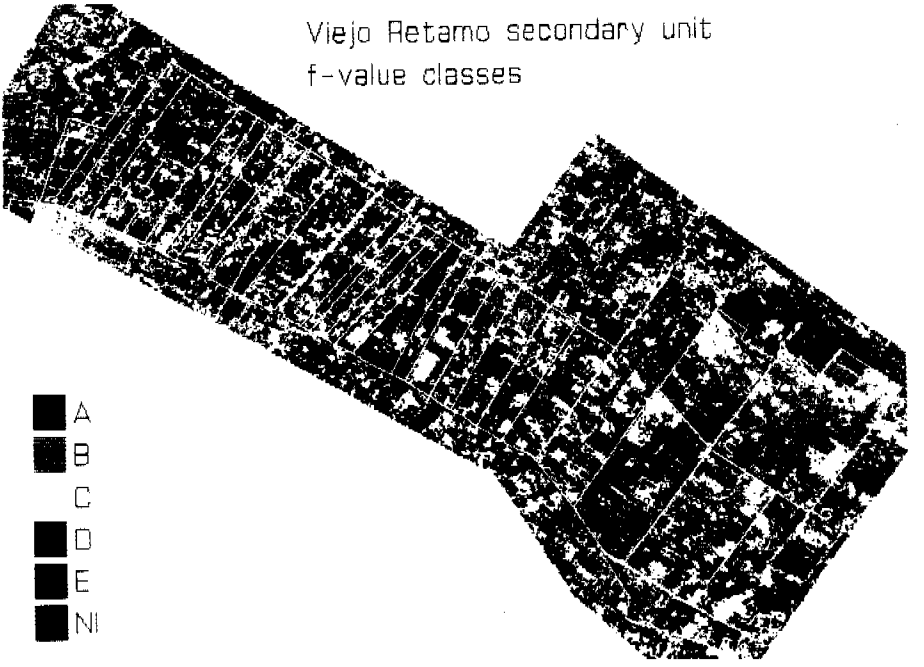

Figure 5 Classified image of Viejo Retamo secondary unit showing areas with different crop classes (A, B, C, D and E) and the not cultivated area (NI); k_c-values of crop classes A through E are given in Table 2

- Determination of ratios

All information obtained by performing the operations described above should be combined to determine the value of each performance indicator for all reference units. This is most easily done by transferring the results of both GIS operations and model calculations to a spreadsheet programme. The necessary calculations given by the formulas in Table 1 can be performed easily.

2.4 Study results

Mapping of areas under irrigation

Remote sensing images in the first instance have been analyzed with the ARC-INFO software to digitize unit boundaries and the irrigation canal system and to make these known in terrestrial coordinates after due rectification and combination with geometrical information. These results serve as a basis for quantifying irrigated and non-irrigated areas, crop distributions, (irrigated) crop water requirements and determining irrigation efficiencies.

After determination of the unit boundaries the next target is the monitoring of irrigated and non-irrigated land: traditional registration systems are often faulty and show many gaps. Satellite remote sensing could offer TM-images with spatial resolution of 30 x 30 m. Four methods were used to spatially identify the irrigated/non-irrigated areas. The so-called "detailed automatic classification" gave the best results. This conclusion was based on an analysis involving terrestrial data collection as to the status of irrigated - non-irrigated area within each of five tertiary units. The remote sensing images processing involved, through the ERDAS package, an analysis of the presence of water in leaves and soil through various manipulations with reflected radiations in bands 3, 4, 5 and 7, for each pixel. For the scheme of 70,000 ha as a whole a similar analysis was made on the basis of MSS-images (LANDSAT), with a spatial resolution of 80 x 80 m. Here an analysis of four bands was performed: two in the visible part (MSS (4), green, and MSS (5) red) and two bands in the near infrared (MSS (6) and MSS (7)).

A so-called Vegetation Index, VI, was introduced that compares the absorption in the infrared to the red and decides on the outcome whether a pixel is irrigated or not. Thus a proper image was obtained of irrigated versus non-irrigated area (Fig. 4).
The actual variation of this in respect to closeness to the surface canal system had to be assessed in relation with occurring groundwater abstraction and prevailing surface water distribution policies.

Obviously remote sensing contributes decisively to obtaining fast and reliable estimates of total irrigated area per irrigation scheme. This type of data under traditional registration systems is usually not up-to-date. Changes are not properly monitored. Once the area under irrigation is determined, overall irrigation efficiency is easily calculated if a reliable record is kept of the irrigation flow diversion towards the primary canal.

An overview of irrigation intensities in the Río Tunuyán scheme is shown in Figure 6. It is obvious from this figure that the areas with the lowest irrigation intensities are located at the periphery of the scheme indicating that irrigation supplies are not distributed equally.

2.4.2 Crop distribution

Further analysis of crops produces questions as to which crops or which groups of crops occur, in which periods, and in which pixels or tertiary units. Crop factors (k_c) and reference evapotranspiration provide the basic elements for further water requirement computations. So, identification of crops is thus essential. A classification of individual crops appeared to be impossible due to large variations in soil cover, crop age and undergrowth. Given this variability, clustering of crops with the same class of k_c-value was considered. This would only be possible if there was a relationship between this k_c-value and the spectral signature of a crop. To find out if such a relationship existed a cluster analysis was performed on the reflection data of 80 fields for which the vegetation had been mapped in March 1988. The statistical package SPSS has been used for this. Eight land use classes were distinguished, of which three contained mainly uncultivated fields and each of the remaining five classes appeared to contain crops having similar k_c-values. Therefore the

Table 2 Values of reference crop evapotranspiration, ET_0 (mm/month) and k_c-values for different crop classes

Month	ET_0 (mm/month)	k_c-values for crop classes				
		A	B	C	D	E
August	71	0.00	0.00	0.00	0.00	0.00
September	110	0.70	0.65	0.55	0.45	0.35
October	162	0.90	0.80	0.70	0.55	0.40
November	192	1.00	0.90	0.80	0.65	0.50
December	211	1.00	0.95	0.85	0.70	0.80
January	214	1.00	0.95	0.80	0.70	0.60
February	161	0.95	0.90	0.80	0.70	0.55
March	128	0.80	0.80	0.75	0.65	0.60
April	78	0.65	0.65	0.65	0.60	0.50
May	50	0.00	0.00	0.00	0.00	0.00
June	37	0.00	0.00	0.00	0.00	0.00
July	44	0.00	0.00	0.00	0.00	0.00

Figure 6 Image showing the percentage of the total irrigable area that is actually cultivated for all secondary units of the Río Tunuyán Irrigation Scheme (Visser, 1989)

relation between k_c-value and spectral signature was concluded to exist. Here again an automatic supervised classification was performed on all pixels, matching the spectral signature to those of calibrated ones. Then each pixel was assigned to a class, the spectral signature of which it matched best. This gave five crop classes with k_c-values for each month of the year (Table 2, Figure 5).

Results of water requirements computations for any one crop distribution pattern in relation to water deliveries as carried out over time contain the key components for the computations of efficiency in water delivery.

2.5 Conclusions

It is possible, given the project results achieved so far, to draw some general conclusions on the role of remote sensing in irrigation management. Conclusions can also be made which apply specifically to the situation in the Río Tunuyán Irrigation Scheme:

- Satellite remote sensing is an adequate tool for determining the actual area cultivated.
- A promising method has been found to map crop irrigation water requirements. Further research will have to be performed to find out whether this method can be applied in general.
- Combined with other necessary data, remote sensing data are very useful in allocation of irrigation water and evaluations of current irrigation water supply given different water allocation policies.
- The areas with water-rights currently used in the distribution of water in the Viejo Retamo secondary unit differ substantially from the areas actually cultivated.
- The secondary units located at the tail ends of the primary canals in the Río Tunuyán Irrigation Scheme tend to have a lower percentage of their area cultivated then the ones located at the heads of these canals. Further investigations should make clear if this is caused by the fact that not enough surface water reaches the ends of the primary canals.

3 FUTURE ROLE OF REMOTE SENSING IN IRRIGATION MANAGEMENT

The remote sensing service primarily supports activities in the field of management: "process control". These services become important as far as they serve to implement irrigation policies. Their benefit will depend on the low cost provision of new information and the introduction of innovative new methodologies. Strictly speaking remote sensing is simply a technique to gather information on different aspects of land use. Such information is particularly relevant for irrigation management if management procedures and tools are geared to the use of such data.

Remote sensing can be used to obtain information relevant to the following management components (Menenti et al., 1989 a, b):

- water : crop water requirements, waterlogging, salinization
- land : actually irrigated areas versus irrigable land
- crops : cultivated area by crop, uniformity of green biomass
- institutions : actually irrigated land versus areas having established water-rights
- finance : due versus actually paid water charges, proportional to irrigated land or by crop.

This information has to be fed into, and logically combined with, Geographical Information Systems (GIS) and Data Base Management Systems (DBMS) to obtain a common base for presentations and to link them with for instance traditional cadastral systems. This combination of methods can be of direct use in producing results useful in irrigation management.

The objectives of irrigation management are formulated at different levels:

- definition of the irrigation strategy, e.g. the overall expected outcome of a particular project
- allocation of water, e.g. a scheme per tertiary unit and by month
- actual scheduling of water deliveries to implement the original strategy.

Remote sensing can play a key role in monitoring implementation processes: actual occurrencies of water deficits, waterlogging, desalinization. It can be used for a further fine tuning of the water allocation and scheduling of water deliveries.

Satellite images and remote sensing techniques have a particular relevance in improving irrigation water management. Feasibility studies, policy formulation at an operation and management level as well as monitoring and evaluation work can all make use of the data these techniques provide.

3.1 Feasibility studies

Remote sensing makes it possible to prepare a quantitative analysis of the problems associated with poor water distribution. Inadequate distributions is clearly reflected in differences in cropping patterns, cropping intensities and crop development along irrigation canals from head to tail. Feasibility studies concerned with modernization and the effect of improved irrigation water distribution on agricultural potential in an area can make excellent use of this information. In addition remote sensing and satellite images can be used to detect the location and extent of areas affected by waterlogging and salt.

3.2 Operation and management

Irrigation managers need to know how much water is required to satisfy crop water demands and to give an optimal production. Crop water demands can be determined by establishing the type of crop, the crop development stage and the area of cropping involved. Information on the actual cropped area and the spatial distribution of cropping patterns is often unreliable. Remote sensing techniques can greatly increase the reliability of these data. An accurate lay-out map of irrigation command areas can be determined from satellite images with very little field work. A crop map can also be effectively derived in this way. With this level of reliability, irrigation schedules can be more accurately prepared. Irrigation managers concerned with the daily operation of a system need to know how much water is available. In situations where water shortages are a problem they must be able to calculate how the predicted supply can best be distributed.

3.3 Monitoring and evaluation

Monitoring and evaluation are basic to effective management. Using the results of remote sensing techniques the irrigation manager is able to check the effectiveness of system rehabilitations on improvements made in management. These will be shown in the increase in cropped areas at the tail end of canals, particularly during the dry season. Improvements may also be reflected in a reduction of water logged or salty areas.

Satellite images of the irrigation scheme can also be used to keep financing agencies well informed about the results of investments made in technical and managerial improvements.

REFERENCES

CHAMBOULEYRON, J., MENENTI, M., FORNERO, L., MORABITO, J., and STEFANINI , L.; 1983. Evaluación y optimización del uso del agua en grandes redes de riego. Instituto Italo-Latino Americano (IILA), Rome, Italy, 176 pp.

CHAMBOULEYRON, J.; 1989. The reorganization of water users' associations in Mendoza, Argentina. Irrigation and Drainage Systems 3: 000-000 (1989). Kluwer Academic Publishers.

LENTON, R.; 1988. Strategy development in IIMI. ODI/IIMI Irrigation Management Network Paper 88/1e. 23 pp.

MENENTI, M., (ED.); 1988. Mecanismos de aprovechamiento hidrico en la región andina: imagenes satelitarias y modelos de simulación. INCYTH-CRA, Mendoza, Argentina, 350 pp.

MENENTI, M., CHAMBOULEYRON, J., STEFANINI, L., MORABITO, J., and FORNERO, L.; 1985. Agricultural water use in large irrigation schemes. In: A. Perrier and C. Riou (eds.). Crop water requirements. Proc. ICID conference, 11-14 Sept. 1984, UNESCO, Paris, France: 597-610.

MENENTI, M., T.N.M. VISSER and J. CHAMBOULEYRON, 1989a. The role of remote sensing in irrigation management: case study on allocation of irrigation water. World Bank Publication, Washington DC, USA (in press).

MENENTI, M., T.N.M. VISSER, J.A. MORABITO and A. DROVANDI, 1989b. Appraisal of irrigation performance with satellite data and geo-referenced information. Proc. Intern. Conf. 'Irrigation theory and practice', 12-19 September 1989, Southampton, UK (in press).

NIEUWKOOP, J. van; 1989. Rehabilitating irrigation systems. Land & Water Vol. 64, NEDECO magazine.

VISSER, T.N.M.; 1989. Appraisal of the implementation of water allocation policies. Note No. 1963. Institute for Land and Water Management Research (ICW), Wageningen, The Netherlands, 54 pp.

VISSER, T.N.M., M. MENENTI, J.A. MORABITO and A. DROVANDI, 1989. Digital analysis of satellite data and numerical simulation applied to irrigation water management by means of a database system. Proc. Intern. Conf. 'Use of computers in scientific and technical research', 24-28 April 1989, Mendoza, Argentina: 441-453.

VOS, J., KABAT, P., BOS, M.G., and FEDDES, R.A.; 1989. CRIWAR: a simulation programme for calculating the crop irrigation water requirement of a cropped area. ILRI publication 46, 70 pp.

APPLICATION OF REMOTE SENSING IN WATER MANAGEMENT; DEVELOPMENT OF A HYDROLOGICAL INFORMATION SYSTEM

G.J.A. Nieuwenhuis and H.A.M. Thunnissen

ABSTRACT

In Dutch agricultural practise one is in particular interested in the detection of water excess in spring time and autumn and in the detection of water shortage summer time. Water excess conditions can be mapped by measuring surface reflectance in the shortwave range. The applicability of thermal images is restricted in this case. However, thermal images supply information on the occurrence of drought damage, as the temperature of crops is related to crop transpiration.

The hydrological regime in agricultural areas can also be analyzed with simulation models. With models the evolution in time can be described. Their accuracy depends on available input data and applied schematization. With geographical information systems one-dimensional model simulations can be extrapolated using existing maps, resulting in transpiration maps. In this case however, actual field conditions used as input, have to be generalized.

Remote sensing images supply detailed information about the regional spectral radiances. With the aid of physical models, this information can be translated into state variables and hydrological information. Remote sensing can be applied to verify regional transpiration values calculated with hydrological simulation models. Moreover with remote sensing actual information on land use is obtained. In general an important improvement of the

hydrological description of an agricultural area can be achieved by applying an integrative approach of remote sensing and hydrological models. In this article this is illustrated by presenting results of four different case studies.

1 INTRODUCTION

The complexity and variability of water systems and the often conflicting interests of society create a great demand for information to secure proper water management. In the past the improvement of crop production conditions was the main aim. Nowadays the interests of nature and landscape must be taken into account. The natural flora and fauna can be adversely affected by changes in the hydrological regime caused by for instance drainage and groundwater extraction for drinking water supply and sprinkler irrigation.
Information is required on the processes that occur and on the state of water systems, including the way they are influenced by human activities. Remote sensing can contribute significantly to the collection of information.

For many years remote sensing research at the Winand Staring Centre was mainly focussed on mapping of transpiration of agricultural crops under water stress conditions. This research has been resulted in a method to map crop transpiration from digital reflection and thermal images (Nieuwenhuis et al., 1985; Thunnissen and Nieuwenhuis, 1989). Due to limitations in workability and trafficability water excess in arable land in early springtime and late autumn accounts for more economical losses than water stress during summer time in the Netherlands. Moreover, water excess may cause problems with the oxygen supply and may result in low temperatures resulting in germination problems. Remotely sensed data in the visible, near and middle infrared and thermal infrared are related to the water content of bare soil (e.g. Droesen et al., in prep.). So images taken in the mentioned wavelength ranges may supply information on the occurrence of water excess conditions.

Although remote sensing was a promising technique for several years, application in practise remained restricted (e.g. Jackson, 1984). Remote sensing was applied by specialists, while only incidentally the possibilities of remote sensing techniques was investigated in relation to and integrated with conventional methods. Remote sensing image processing systems have

been developed for instance independently of geographical information systems. As far as remote sensing data were integrated with geographical data such as existing maps and model simulations, they were performed by hand. Thanks to the recent integration of both systems, important impulses have been given to the application of remote sensing techniques.

In this article, experience with remote sensing techniques in the visible, near and middle infrared and thermal infrared range of the electromagnetic spectrum will be presented. The field of investigation concerns bare soil (soil water content) and vegetation (transpiration). First the basic principles of remote sensing techniques and hydrological modelling will be treated. To demonstrate the possibilities of remote sensing in water management of rural areas some results of four case studies are presented. Especially attention will be given to the integration of GIS and remote sensing techniques in a so-called Hydrological Information System.

2 THEORY

2.1 Remote sensing in the optical and thermal range

2.1.1 Remote sensing techniques

Radiance from plants and soils is used extensively in remote sensing as an aid to characterize features at the earth surface. The most common technique to measure in the optical range of the electromagnetic spectrum deals with areal photography including false colour photography. In the latter case the applied films are sensitive in the near infrared (up to 0.9 μm). Multi Spectral Scanner (MSS) images can be taken in separated wavelength bands in both the short wave range (visible, near infrared and middle infrared) and in the thermal range. In the visible range the observed radiance is mainly related to the reflection of objects. Reflected radiance vary with leaf surface characteristics and crop structure. The "colour" of crops depends on physiological processes in the plants. This means that through the reflectance (spectral signature) information can be obtained about the type of crop and crop condition in a qualitative way (drought stresses, diseases etc).

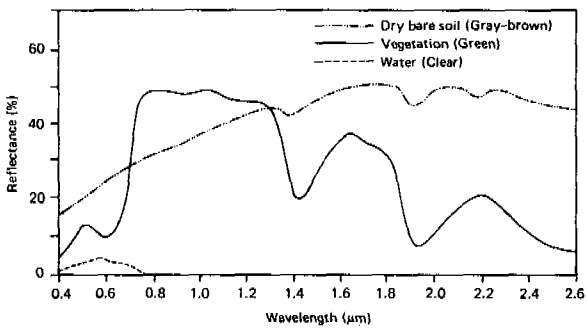

Figure 1 Typical spectral reflection curves for vegetation, soil and water (Lillesand and Kiefer, 1987)

The reflection in the near infrared is mainly determined by the structure of the plant and amount of biomass. For green vegetation the reflection in the near infrared (up to 0.9 μm) is relatively high (Fig. 1) resulting in a red colour on false colour photographs. In the middle infrared (from 1.3 up to 2.5 μm) reflection depends on absorption of radiation by water. This means that in this wavelength range surface reflection is related to the water content of crops. In the thermal range (from 8 up to 14 μm), radiation emitted by earth surface objects is observed, enabling the determination of object temperatures. Both for bare soil and vegetation covered soil through the surface temperature information on the status of energy fluxes can be obtained.

2.1.2 Soil moisture mapping for bare soil conditions

Surface reflectance of bare soil strongly depends on soil moisture conditions (Axelsson and Lunden, 1986; Droesen et al., in prep.). The decrease in shortwave reflection with increasing soil moisture content seems to proceed from internal reflection, i.e. light reflected on the surface of soil particles is re-reflected at the surface of a water film (Angstrom, 1925). Besides variation in soil moisture content, bare soil reflectance under a constant irradiation angle mainly depends on organic matter content, texture, structure and mineralogy of the soil (Baumgardner et al., 1985).

The temperature of the soil surface is determined by the instantaneous equilibrium between gains and losses of energy. In case of potential evaporation, i.e. a wet soil surface, variations in daytime surface temperature are mainly caused by variations in albedo, emissivity of the surface, roughness and thermal inertia (a measure of the response of an object to temperature changes). The influence of these parameters are all of the same order of magnitude. Variability in nighttime surface temperature is dominated by the thermal inertia (Ten Berge and Stroosnijder, 1987). The latter parameter strongly depends on soil water content (e.g. Pratt and Ellyett, 1979). In order to obtain a better measure for the thermal inertia some authors (e.g. Reginato et al., 1976) apply the diurnal temperature amplitude calculated as the difference between a day- and nighttime thermal recording.

2.1.3 Transpiration mapping of agricultural crops

Based on an energy balance approach, instantaneous transpiration values (λE) can be calculated from remotely sensed crop surface temperatures (T_c) according to Brown and Rosenberg (1973), Stone and Horton (1974), and Soer (1980):

$$\lambda E = \rho C_p (T_a - T_c)/r_{ah} + (1-r)K^{\downarrow} + \epsilon(L^{\downarrow} - \sigma T_c^4) - G \quad (W.m^{-2}) \qquad [1]$$

where: λE = latent heat flux density ($W.m^{-2}$)
ρ = density of moist air ($kg.m^{-3}$)
C_p = specific heat of moist air ($J.kg^{-1}.K^{-1}$)
T_c = crop surface temperature (K)
T_a = air temperature (K)
r_{ah} = turbulent diffusion resistance for heat transport ($s.m^{-1}$)
r = surface reflection coefficient
$K^{\downarrow}$ = incoming shortwave radiation flux ($W.m^{-2}$)
ϵ = emission coefficient
$L^{\downarrow}$ = long wave sky radiation flux ($W.m^{-2}$)
σ = constant of Stefan Boltzmann ($5.67.10^{-8}$ $W.m^{-2}.K^{-4}$)
G = heat flux into the soil ($W.m^{-2}$)

24-Hour values of λE can be calculated from only one instantaneous value by modelling the latent and sensible heat flux in the soil-plant-atmosphere system. For the interpretation of crop surface temperature and transpiration for grassland at different soil moisture conditions Soer (1977) developed the TERGRA-model. Interpretation of thermal images with the TERGRA-model is rather complicated however, because of the large number of input parameters that is required.

Jackson et al. (1977) related midday surface-air temperature differences (T_c-T_a) linearly to 24-hour transpiration and net radiation values. To estimate the slope of this relationship a crop-dependent analytical expression was derived by Seguin and Itier (1983). Nieuwenhuis et al. (1985) and Thunnissen and Nieuwenhuis (1989 and in prep.) proposed to replace the surface-air temperature difference by the temperature difference (T_c-T_c^*), existing between the crop transpiring under the restriction of the actual soil moisture condition (T_c) and the crop transpiring under the optimal soil moisture condition (T_c^*). The net radiation term was replaced by the 24-hour potential transpiration rate of the crop. With these adjustments they obtained:

$$\lambda E^{24}/\lambda E_p^{24} = 1 - B^r (T_c - T_c^*)_i \qquad [2]$$

where λE^{24} and λE_p^{24} are respectively the actual and potential 24-hour transpiration rate ($mm.d^{-1}$), B^r (K^{-1}) is an empirical coefficient and the subscript i indicates instantaneous values. Using eqn (2) differences in radiation temperature of a certain crop derived from thermal images can be transformed directly into reductions in transpiration.

Table 1 Values for the regression coefficients a and b in eqn (2) for a number of crops depending on crop height

Crop	Crop Height (cm)	a (K^{-1})	b ($s.K^{-1}.m^{-1}$)
Grass	< 15	0.050	0.010
Grass	> 15	0.050	0.017
Potatoes	60	0.050	0.023
Sugar beet	60	0.050	0.023
Cereals	100	0.090	0.030
Maize	200	0.100	0.047

From TERGRA-model calculations Thunnissen and Nieuwenhuis (1990) found that B^r can be described by a linear function of the wind velocity (u) at a height of 2.0 m above ground surface:

$$B^r = a + b.u \quad (K^{-1}) \qquad [3]$$

where a and b are regression coefficients (Table 1).

For agro-hydrological purposes thermal images are usually recorded on clear days in the summer period. We found that for such days eqns (2) and (3) can be applied for the meteorological conditions prevailing in the Netherlands.

2.2 Determination of crop transpiration with a hydrological simulation model

Remotely sensed images characterize crop conditions at one time. For several agrohydrological applications, however, determination of cumulative effects in time on the total crop yield is required. As an example one can think of the effects of groundwater extraction for domestic purposes on the growing conditions of grassland and arable crops. The amount of water available for transpiration strongly influences dry matter production. With an agrohydrological simulation model such as SWATRE (Feddes et al., 1978;

Belmans et al., 1983) the use of water by crops can be simulated during the entire growing season. SWATRE is a transient one-dimensional finite-difference soil-water-root uptake model, that applies a simple sink term and different types of boundary conditions at the bottom of the system. If the soil system remains unsaturated, one of the following three bottom boundary conditions can be used: pressure head, zero flux or free drainage. When the lower part of the system remains saturated, one can give either the groundwater level or the flux through the bottom of the system as input. In the latter case the groundwater level is computed. At the top of the system, 24-hour data on precipitation, potential soil evaporation and potential transpiration are needed.

SWATRE needs the following input:

- 24-hour meteorological data including precipitation and data necessary to calculate potential transpiration. Usually meteorological data from routine measurements are used. However, especially precipitation data may vary considerably within larger areas;
- crop characteristics such as rooting depth. The location of the different crops can usually only be derived from remote sensing images. If no images are available, the relative area of different crops per subregion taken from agricultural statistics is applied;
- soil physical parameters including (un)saturated conductivity and water retention characteristics for each soil layer. Every soil type consists of several horizons, differing in soil physical characteristics. In the Netherlands a data base of horizons was defined with characteristic hydraulic conductivity and moisture retention data (Wösten et al., 1987). These soil physical characteristics were assigned to the major soil horizons. Based on these data a simulation map was defined which presents a soil physical interpretation of the soil map, providing data for simulation of the soil water regime;
- groundwater table regime which is schematized into drainage classes.

Plate 1 Transpiration map of part of a study area near a pumping station (P) situated in the eastern part of the Netherlands as derived from reflection and thermal images of 30 July 1982. Crop relative transpiration decreases from blue (>90%), green (70-90%), yellow (50-70%), red (30-50%) to magenta (<30%). Black means forest, built-up area and short grassland. The isoline indicates a 10 cm drawdown according to the calculations reported by De Laat and Awater (1978)

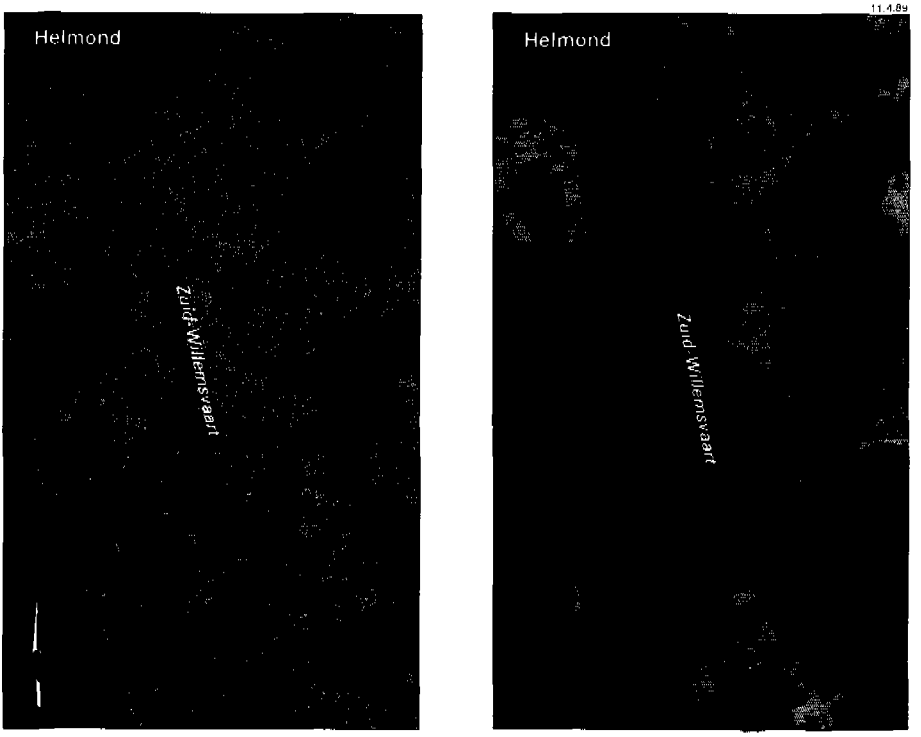

Plate 2 Transpiration maps of a study area in the province of Noord-Brabant situated in the southern part of the Netherlands as composed from reflection and thermal images of 22 July 1983 (left) and obtained by combining SWATRE simulations with a digitized soil map scale 1:50,000 (right). Crop relative transpiration decreases from dark blue (>90%), cyan (70-90%), green (50-70%), yellow (30-50%) to orange (<30%). Black means forest, built-up area and short grassland (Miltenburg and Beekman, 1989)

In this section four case studies will be treated briefly to illustrate the applicability of remote sensing in water management of rural areas.

3.1 Seepage and open-water temperatures

Generally, in summer and winter groundwater temperatures are lower respectively higher than open water temperatures. Depending on the occurrence of seepage open water temperatures are influenced consequently. With thermography surface water temperatures can be measured. To investigate the possibilities of thermography to map seepage occurrence a flight was performed in a low situated wet area in the central part of the Netherlands. In the early morning of 1 July 1986 images were taken with a thermal video camera (type Aga 782 LW). The video images were translated into calibrated temperature maps. Figure 2 shows the temperature map of the study area.

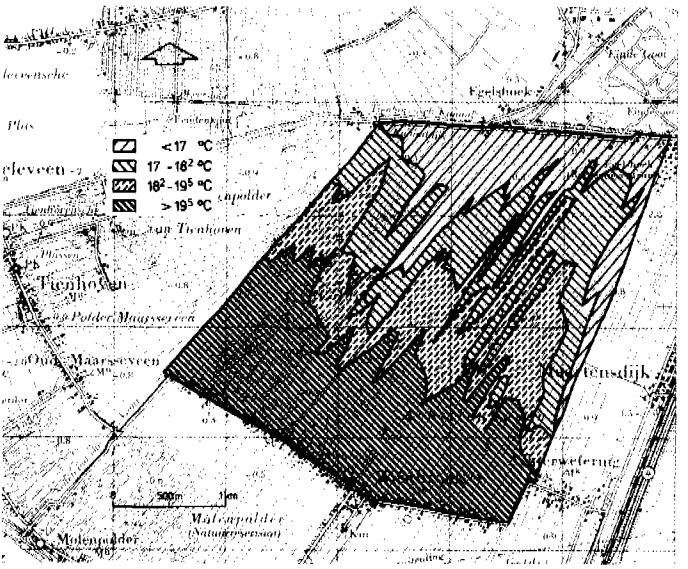

Figure 2 Map showing the distribution in open-water temperatures as derived from thermal video images taken at 1 July 1986 (Van Deursen, 1988). The image was composed from seven different tracks

In the southern part of the study area relatively high temperatures were found because of the inlet of relatively warm water from the river 'De Vecht'. In the northeastern part relatively low temperatures were found. This could be an indication for seepage occurrence.

By comparing the obtained temperature map with the available information dealing with the occurrence of seepage, Van Deursen (1988) concluded that thermal images can be very helpful to detect seepage conditions. Thermal images do not supply quantitative information about fluxes. This means that additional information from either field measurements or hydrological modelling is always indispensable. For this project Van Deursen found that remote sensing images supply information on the regional distribution of seepage occurrence. From an ecological point of view this information is very important.

3.2 Soil moisture for bare soil conditions

The possibilities of soil moisture mapping from digital reflection and thermal images were investigated in a sandy area situated in the southern part of the Netherlands (Droesen et al., in prep.). Due to limitations in workability and trafficability water excess conditions in arable land causes economical losses. To investigate the possibilities of remote sensing to detect water excess, remote sensing flights were performed at 6 April 1988 around midday and in the early morning of 7 April 1988. The remotely sensed data were correlated with field measurements. To determine the soil water content samples were taken of the 5 cm topsoil. For bare soil the relation between soil water content and remotely sensed data in the visible, near infrared and thermal infrared range of the electromagnetic spectrum was investigated (Fig. 3). Below about 20 per cent volumetric water content, the soil surface became airdry effecting a strong increase in reflectance. In this soil water content traject no relation existed between soil water content of the 5 cm topsoil and surface spectral reflectance in the "green", "red" and "near infrared". This is due to the fact that surface reflectance is only related with surface water and not with the average soil water content of the 5 cm topsoil. Therefore the statistical analysis dealt with the soil water content traject above 20 volume per cent. Green and red reflectance show the best correlation with soil water content (fig. 3: $r = -0.83$ and $r = -0.75$). In order to map soil water content with an accuracy of at least 3 volume per cent, a homogeneous topsoil type such as in this experiment, appeared to be an undispensible condition (Axelsson and Lunden, 1986). The

infrared reflectance interfered with disturbing features at the soil surface, resulting in a poor correlation with soil water content (r = -0.45). Due to an extremely low reflectance of water in the near infrared, this wavelength interval was optimal to detect waterlogged spots.

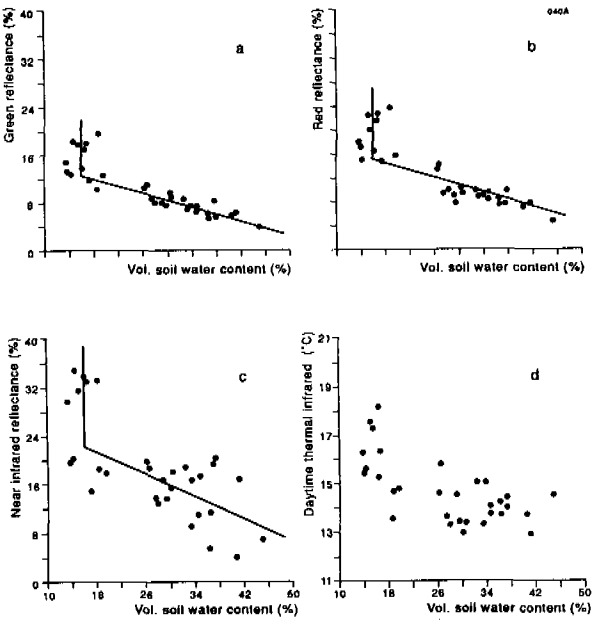

Figure 3 Relationships between measured soil water content of the 5 cm topsoil and the reflection in the green (a), red (b), near infrared (c) and emission in the thermal infrared (d) as derived from multi spectral scanner images taken at 6 april 1988 between 12.00 and 13.00 hours MET (Droesen et al., in prep)

In agricultural areas the bare soil daytime radiation temperature is useless to map soil water content of a wet soil surface. A decrease in soil water content in the wet range causes an increase in albedo resulting in a decrease in net available energy. Consequently, the different terms of the energy balance are influenced. Because of compensating effects Droesen et al. found that in the wet range the surface temperature is insensitive to changes in the soil water content. Moreover, the relation between the daily surface temperature and soil water content appeared to be specific for each plot depending on the water management practise.

Also the nighttime radiation temperature is hardly related with the soil moisture content. The bare soil nighttime radiation temperature varied over only 1.5 K. Consequently, the difference in day- and nighttime temperature hardly improved the estimation of the soil water content. So it can be concluded that thermal remote sensing does not seem to be useful for soil moisture mapping of wet soil surfaces.

The applicability of remote sensing images depends on the situation in the field at acquisition time. Recently ploughed and manured plots restrict the applicability. Nevertheless, Droesen et al. found that reflection images supply relevant information to detect water excess for arable land.

The applicability of airborne scanner images in practise is however restricted by the high acquisition costs. Although satellite imagery is relatively cheap, operational use is limited due to the low temporal and geometrical resolution. Aerial photography is a cheap alternative. The automatic processing of photographic images is however more troublesome. Due to the sensitivity of the green, red and infrared reflectance to soil water content false colour photographs give a good impression of the soil moisture status. Airdry and wet soil surfaces can be distinguished accurately. Due to the very low reflectance in the infrared, waterlogged spots can be mapped precisely. To map water excess aerial false colour photographs generally provide therefore the required inventarization accuracy.

3.3 Water excess caused by seepage

The occurrence of seepage may cause water excess effecting damage to agricultural crops. The applicability of thermal infrared scanning techniques and false colour photography for the detection of seepage along large waterways was investigated for a grassland area (Van Lieshout, 1988). Aerial photographs and thermal images were taken of a track between Lochem and Eefde along the "Twenthe kanaal". The images were taken at 22 April 1987 between 6:00 and 6:30 hours MET. The interpretation results of the images were compared with measured groundwater levels and the results obtained with the quasi three dimensional hydrological model GELGAM. With this model the saturated and unsaturated regional groundwater flow can be simulated (De Laat and Awater, 1978). Partly due to the non-optimal flight conditions a direct relationship between the surface temperature and

measured groundwater levels could not be found. However, features indicating a high water content of the topsoil like ponding, a trappled sod or a dark soil surface were clearly visible on the false colour photographs. These mapped wet areas corresponded well with the areas with a high groundwater level according to the GELGAM-model calculations. Although according to the theory thermography could be applied to detect seepage conditions (Rosema, 1975; Van Lieshout, 1988), applicability in practice was troublesome.

Seepage conditions are changing in time. Moreover surface temperatures are strongly dependent on atmospheric conditions and surface characteristics such as vegetation coverage and surface roughness, while surface temperature effects caused by seepage are relatively small. Van Lieshout found that the applicability of thermography also in this case is restricted, while false colour photographs supply information about the occurrence of water excess, relevant for mapping of seepage conditions.

3.4 Crop transpiration

To investigate the possibilities of remote sensing for the estimation of transpiration on a regional scale remote sensing flights were performed in the eastern part of the Netherlands in 1982 and 1983. Reflection and thermal images were recorded with a Daedalus digital scanner. The transpiration map shown in Plate 1, as composed with the method described in Section 2.1.3, was used to study effects of groundwater extraction by pumping stations on crop water supply. As phreatic groundwater was extracted in this region of the Netherlands, the groundwater level and therefore crop water supply were influenced. Around the centre of the extraction a more or less conical depression of the groundwater table occurred (Plate 1). Because of the conical depression of the groundwater table circular drought patterns were expected around the site of the pumping station. However, this was not observed. One of the reasons was the common practise to sprinkle grassland. Therefore numerous plots were present with crops well supplied with water and which were more or less potentially transpiring (blue in Plate 1).

Under natural conditions crop transpiration depends on meteorological conditions and total moisture availability in the root zone. The last one is determined by:

- the depth of the root zone;

- the moisture retention capacity of the root zone;
- the hydraulic conductivity of the subsoil;
- the groundwater level during the growing season.

The first three factors are mainly dependent on soil properties. To determine the effect of a lowering of the groundwater level depending on the soil properties, calculations with the SWATRE-model were performed. For the flight day in 1982 transpiration values derived from the remote sensing transpiration map were compared with the simulated values for

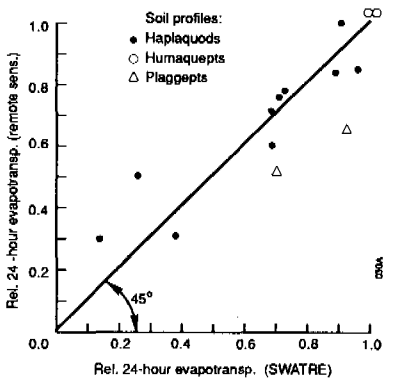

Figure 4 Relative 24-hour transpiration rates as obtained by the remote sensing approach and simulated with SWATRE for fourteen grassland plots on three different soil profiles

different locations within the study area. Different soils with varying water table were considered. Both results were in good agreement (Fig. 4). Only for Plaggept soils transpiration is probably overestimated by SWATRE (Thunnissen and Nieuwenhuis, 1989). Crop transpiration was studied in relation to the distance from the centre of the groundwater extraction. As crop transpiration depends on soil type and groundwater level, a systematic analysis was performed for each soil type and depending on the drainage conditions. Figure 5 shows two typical results. According to the remote sensing approach crop transpiration strongly decreased on 30 July 1982 in the direction of the centre of the extraction in case of shallow groundwater tables under natural conditions (Fig. 5a). Figure 6a shows that also according to SWATRE-model calculations for the concerning conditions crop transpiration

strongly decreased with lowering of the groundwater table.

Also for relatively deep groundwater tables under natural conditions both results showed good agreement (Figs. 5b and 6b). If no suppletion from groundwater occurred crop transpiration was very low on 30 July 1982 and a lowering of the groundwater table has no perceptible influence on crop transpiration (Thunnissen and Nieuwenhuis, 1989).

With remote sensing detailed information about the regional distribution of crop transpiration on flight days was obtained. With agrohydrological simulation models such as SWATRE for a restricted number of locations crop transpiration can be simulated during the entire growing season. For the explanation of drought patterns on the transpiration map determined with remote sensing, such model calculations are indispensable. The effects of groundwater extraction could not directly be determined by a visual interpretation of drought patterns on the transpiration map as derived from remote sensing images. Application of sprinkler irrigation and the variability in soil physical and hydrological properties were not taken into account. With a systematic analysis of transpiration per crop type, soil type and drainage class, however, information on effects of groundwater extraction could be obtained. The systematic analysis was performed by hand. Nowadays such an analysis can be carried out faster and more accurately using GIS techniques.

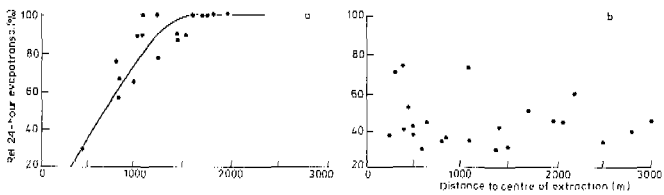

Figure 5 Relative 24 hour transpiration (λE^{24} / λE_p^{24}) on 30 July 1982 as a function of distance to the centre of the extraction. Data were derived from the transpiration map shown in Figure 4 for (a) grassland plots on Typic Haplaquod soil with a relatively shallow groundwater table and (b) maize plots on Typic Haplaquod soil with a relatively deep groundwater table. The mentioned groundwater tables apply to the situation without groundwater extraction

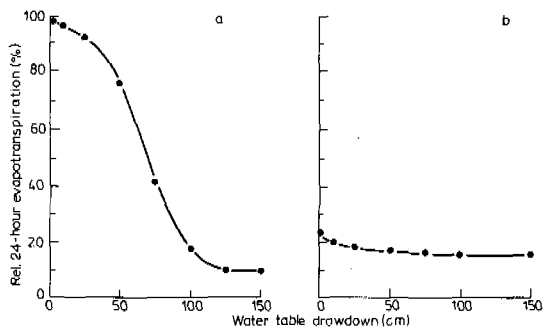

Figure 6 Relative 24 hour transpiration ($\lambda E^{24}/\lambda E_p^{24}$) on 30 July 1982 as a function of groundwater table drawdown, simulated with the model SWATRE for (a) grassland plots on Typic Haplaquod soil with a relatively shallow groundwater table and (b) maize plots on Typic Haplaquod soil with a relatively deep groundwater table. The mentioned groundwater tables apply to the situation without groundwater extraction

4 HYDROLOGICAL INFORMATION SYSTEM

4.1 Description of the information system

Remote sensing techniques and hydrological model simulations contribute both to a hydrological description of an area. Miltenburg and Beekman (1989) combined both methods in a Geographical Information System (GIS). In this system (Fig. 7) transpiration maps based on remote sensing are used to verify model simulations for a representative test area on one or two days during the growing season. Input for the GIS consists of: remote sensing images, ground truth, a digital soil/drainage map and simulation model input parameters.

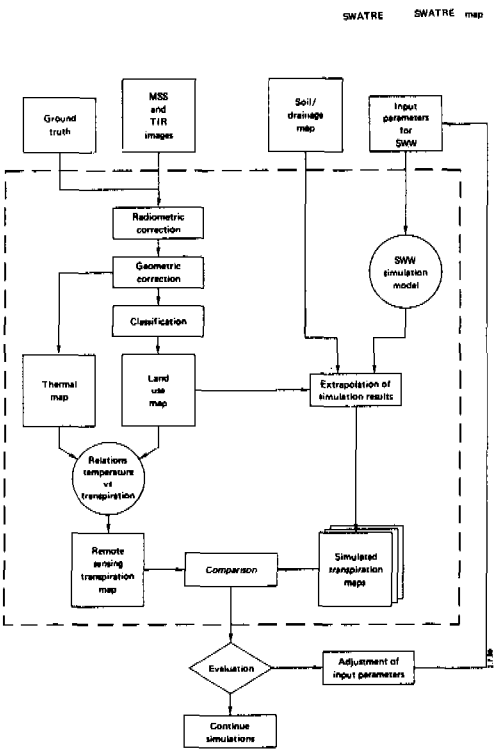

Figure 7 Flow diagram of the geographical information system in which model simulations and remotely sensed imagery are combined (Miltenburg and Beekman, 1989)

As the applied hydrological models are generally well calibrated with accurately measured soil physical, hydrological, meteorological and crop parameters, they need no verification. Actually measured input parameters are, however, usually not available over large areas, so readily available standard parameters and generalized soil/drainage maps are used. Therefore model results have to be verified. Especially the accuracy of estimated soil physical parameters, rooting depths and groundwater table depth are important because they strongly influence simulation results. Model simulations are performed for every unit on the simulation map (see Section 2.2). In practise simulation units are unique combinations of soil physical properties, crop type and drainage condition. To extrapolate model simulations it is therefore necessary to know the spatial distribution of soil types, crop types and drainage conditions. The distribution of crop types, which differs from year to year, can be extracted from classified remote sensing imagery. Soil types and drainage classes are available on digitized soil maps.

4.2 Application of the information system

The Hydrological Information System was recently used in a water management research project. The aim of this project was the development of water inlet schemes in the Province of Noord-Brabant, using model simulations (Miltenburg en Beekman, 1989). Remote sensing images from 22 July 1983 were available. They cover a test area of about 100 km² within the total study area of 4000 km². Model simulations were performed for every day of the growing season of 1983. In the southern part of the test area crops were well transpiring (Plate 2). Also in the surroundings of the indicated canal crop water supply was sufficient. Especially around forested areas soils were sensitive to drought (red colour). Plate 2 shows that transpiration maps derived from remote sensing images provided relatively detailed information, while on the basis of a generalized soil map more global information can be obtained. Miltenburg and Beekman concluded that if the remote sensing results deviate systematically from the simulation map, the applied soil physical input parameters or the groundwater table have to be adjusted.

Based on the integration of remote sensing methods and hydrological modelling, an important improvement of the hydrological description of an area can be achieved with the developed Hydrological Information System.

5 CONCLUSIONS AND DISCUSSION

The results presented in this paper demonstrate the potential of remote sensing techniques in the shortwave and thermal range of the electromagnetic spectrum to solve water management problems in humid regions such as the Netherlands. Remote sensing images supply detailed information about soil moisture conditions and the regional distribution of crop transpiration on flight days. On the other hand with agrohydrological simulation models such as SWATRE for specific soil physical and hydrological conditions crop transpiration can be simulated during the entire growing season. For the interpretation of remote sensing results such model calculations are indispensable. As a result of the successful integration of hydrological models and GIS, simulation results can be mapped automatically. Remote sensing has proven to be a valuable tool for testing models and for delivering input to information systems. Based on this concept a Hydrological Information System was developed.

The operational application of remote sensing techniques will mainly depend the availability of useful and payable images. For large scale studies images of meteorological satellites with spatial resolutions of 1 up to 10 km are of great importance. However, for water balance studies of intensively used agricultural areas the spatial resolution of meteorological satellites is not sufficient. The satellites SPOT and LANDSAT 5 provide reflection images with a reasonable spatial resolution (10 up to 30 m). The spatial resolution of thermal images obtained with the TM-scanner on board of LANDSAT 5, however, is only 120 m. Moreover, especially for humid areas the temporal resolution (16 days) is questionable and the time of acquisition (about 9.30 hrs MET) is far from optimal to detect drought damage. The increase in crop temperature because of a reduction in transpiration is maximal in the early afternoon. Consequently, for the time being application of remotely measured surface temperatures in humid regions with intensive land use, such as in the Netherlands, will mainly depend on airborne sensors.

The applicability of remote sensing techniques in the shortwave and thermal range of the electromagnetic spectrum is dependent on the prevailing weather conditions at acquisition time. With radar, however, also under cloudy conditions images can be taken. The first results of mapping water excess with radar techniques are promising (Droesen et al., in

prep.).

REFERENCES

ANGSTROM, A.; 1925. The albedo of various surfaces of ground. Geografiska Annaler 7: 323-342.

AXELSSON, S. and B. LUNDEN; 1986. Experimental results in soil moisture mapping using IR thermography. ITC Journ. 1: 43-49.

BAUMGARDNER, M.F., L.F. SILVA, L.L. BIEHL and E.R. STONER; 1985. Reflectance properties of soils. Advances in Agronomy 38: 1-44.

BELMANS, C., J.G. WESSELING and R.A. FEDDES; 1983. Simulation model of the water balance of a cropped soil: SWATRE. J. Hydrol. 63: 271-286.

BROWN, K.W. and N.J. ROSENBERG; 1973. A resistance model to predict evapotranspiration and its application to a sugar beet field. Agron. J. 65,3: 341-347.

DE LAAT, P.J.M. and R.H.C.M. AWATER; 1978. Groundwater flow and evapotranspiration: a simulation model. Part 1: Theory. Part 2: Applications. Basisrapport Commisie Bestudering Waterhuishouding Gelderland, Arnhem, The Netherlands. 64 pp.

DROESEN, W., F.P. HAGEDOORN and G.J.A. NIEUWENHUIS; (in prep.). Soil moisture mapping in a sandy agriculture area applying airborne MSS, IRLS and X-band radar imagery and false colour photography. The Winand Staring Centre for Integrated Land, Soil and Water Research, Wageningen, The Netherlands.

FEDDES, R.A., P.J. KOWALIK and H. ZARADNY; 1978. Simulation of field water use and crop yield. Simulation Monographs. PUDOC, Wageningen. 189 pp.

JACKSON, R.D., R.J. REGINATO and S.B. IDSO; 1977. Wheat canopy temperature: a practical tool for evaluating water requirements. Water Res. Res. 13: 651-656.

JACKSON, R.D.; 1984. Remote sensing of vegetation characteristics for farm management. SPIE, vol 475 Remote Sensing: 81-96.

LIESHOUT; A.M., 1988. Mapping of water excess causes by seepage along large waterways. Note 1924. Institute for Land and Water Management Research, Wageningen, The Netherlands. 66 pp.

LILLESAND, T.M. and R.W. KIEFER; 1987. Remote sensing and image interpretation.

John Wiley & Sons, New York, USA. 2nd edition. 721 pp.

MILTENBURG, J.W. and W. BEEKMAN; 1989. Evaluation of crop transpiration with remote sensing and computer simulation models. Report 1. The Winand Staring Centre, Wageningen, The Netherlands. 50 pp.

NIEUWENHUIS, G.J.A., E.H. SMIDT and H.A.M. THUNNISSEN; 1985. Estimation of regional evapotranspiration of arable crops from thermal infrared images. Int. J. Remote Sensing 6: 1319-1334.

PRATT, D. and C.D. ELLYETT; 1979. The thermal inertia approach to mapping of soil moisture and geology. Rem. Sens. Environ. 8: 151-168.

REGINATO, R.J., S.B. IDSO, J.F. VEDDER, R.D. JACKSON, M.B. BLANCHARD and R. GOETTELMAN; 1976. Soil water content and evaporation determined by thermal parameters obtained from ground-based and remote measurements. J. of Geophys. Research 81: 1617-1620.

ROSEMA, A.; 1975. A mathematical model for simulation of the thermal behaviour of bare soils based on heat and moisture transfer. NIWARS-publication 11. Delft, The Netherlands. 92 pp.

SEGUIN, B. and B. ITIER; 1983. Using midday surface temperature to estimate daily evapotranspiration from satellite thermal IR data. Int. J. Remote Sensing 4: 371-383.

SOER, G.J.R.; 1977. The TERGRA model - a mathematical model for the simulation of crop surface temperature and actual evapotranspiration. Note 1014. Institute for Land and Water Management Research, Wageningen, The Netherlands. 44 pp.

SOER, G.J.R.; 1980. Estimation of regional evapotranspiration and soil moisture conditions using remotely sensed crop surface temperatures. Remote Sensing Env. 9: 27-45.

STONE, L.R. and M.L. HORTON; 1974. Estimation of evapotranspiration using canopy temperatures: field evaluation. Agron. J. 66: 450-454.

TEN BERGE, H. and L. STROOSNIJDER; 1987. Sensitivity of surface variables to changes in physical soil properties: limitations to thermal remote sensing of bare soils. IEEE Trans. on Geosci. and R.S. GE-25: 702-708.

THUNNISSEN, H.A.M. and G.J.A. NIEUWENHUIS; 1989. An application of remote sensing and soil water balance simulation models to determine the effect of groundwater extraction on crop evapotranspiration. Agricult. Water Manage. 15: 315-332.

THUNNISSEN, H.A.M. and G.J.A. NIEUWENHUIS; (*in prep.*). A simplified method to estimate regional 24-hour evapotranspiration from thermal infrared data. The Winand

Staring Centre for Integrated Land, Soil and Water Research, Wageningen, The Netherlands.

TUCKER, C.J.; 1977. Use of near infrared/red radiance ratios for estimating vegetation biomassand physiological status. Proc. 11th Int. Symp. of Remote Sensing of Env. 1: 493-494.

VAN DEURSEN, W.; 1988. Application of thermography to map seepage in a wet area situated in the central part of the Netherlands. Note 1866. Institute for Land and Water Management Research, Wageningen, The Netherlands. 38 pp. (in Dutch).

WÖSTEN J.H.M., M.H. BANNINK and J. BEUVING; 1987. Waterretentie- en doorlatendheidskarakteristieken van boven- en ondergronden in Nederland: De Staringreeks. Rapport 18. Institute for Land and Water Management Research, Wageningen, The Netherlands. 75 pp.

Notes

Notes

TNO COMMITTEE ON HYDROLOGICAL RESEARCH

PROCEEDINGS AND INFORMATION

No. 1 Investigations into the water balance of the Rottegatspolder.
The water supply for crops I.
Observations of groundwater levels.
Investigations by drain gauges in the Netherlands.
The water supply for crops II.
The problem of the increasing salinity of ground and surface water in the Netherlands.
Proceedings of Technical Meetings 1-6 (with summaries in English), 1952.

No. 2 The study of precipitation data.
Model research on groundwater flows.
Measurements and improvement works in basin of brooks.
Geo-electrical research.
Proceedings of Technical Meetings 7-10, and
Report on the evaporation research in the Rottegatspolder 1947-1952 (with summaries in English), 1955.

No. 3 The water supply of sandy soils.
Quality requirements for surface waters.
Proceedings of Technical Meetings 11-12 (with summaries in English), and
Report on the Lysimeters in the Netherlands I (in English), 1958.

No. 4 *) Evaporation Symposium and
Report on the Lysimeters in the Netherlands II (with summaries in English), 1959.
*) Out of print.

No. 5 Groundwater levels and groundwater movement in the sandy areas of the Netherlands.
Water in unsaturated soil.
Proceedings of Technical Meetings 13-14 (with summaries in English), 1960.

No. 6 The regime of the Rhine, the Ysselmeer and Zeeland Lake.
Proceedings of Technical Meeting 15 (with summaries in English and French), 1961.

No. 7 The dry year 1959.
Proceedings of Technical Meeting 16 (with summaries in English), 1962.

No. 8 The laws of groundwater flow and their application in practice.
Proceedings of Technical Meeting 17 (with summaries in English), 1963.

No. 9 Water nuisance.
Proceedings of Technical Meeting 18 (with summaries in English), 1963.

No. 10 Steady flow of groundwater towards wells.
Compiled by the Hydrologisch Colloquium (in English), 1964.

No. 11 Geohydrological cartography.
Proceedings of Technical Meeting 19 (with summaries in French and German), 1964.

No. 12 Water balance studies.
Proceedings of Technical Meeting 20 (in English), 1966.

No. 13 Recent trends in hydrograph synthesis.
Proceedings of Technical Meeting 21 (in English), 1966.

No. 14 Precipitation data (II) and
Report on the Lysimeters in the Netherlands (III)
Proceedings of Technical Meeting 22, (with summaries in English), 1968.

No. 15 Soil - water - plant.
(In English), 1969.

No. 16 Hydrological investigations for masterplan for the future watersupply in the Netherlands.
Proceedings of Technical Meeting 29 (with summaries in English), 1975.

No. 17 Automatic processing of hydrological data.
Proceedings of Technical Meeting 25 (in English), 1973.

No. 18 Hydraulic research for water management.
Proceedings of Technical Meeting 26 (in English), 1974.

No. 19 The hydrological investigation programme in Salland (The Netherlands).
Proceedings of Technical Meeting 27 (in English), 1974.

No. 20 Salt distribution in estuaries.
Proceedings of Technical Meeting 30 (in English), 1976.

No. 21 Groundwater pollution.
Proceedings of Technical Meeting 31 (in English), 1976.

No. 22 Systems approach to the management of water resources.
Proceedings of Technical Meeting 32 (with summaries in English), 1976.

No. 23 Precipitation and measurements of precipitation.
Proceedings of Technical Meeting 33 (in English), 1977.

No. 24 Urbanization and water management.
Proceedings of Technical Meeting 34 (in English), 1978.

No. 25 The relation between water quantity and water quality in studies of surface waters.
Proceedings of Technical Meeting 35 (in English), 1979.

No. 26 Research on possible changes in the distribution of saline seepage in the Netherlands.
Proceedings of Technical Meeting 36 (in English), 1980.

No. 27 Water resources management on a regional scale.
Proceedings of Technical Meeting 37 (in English), 1981.

No. 28 Evaporation in relation to hydrology.
Proceedings of Technical Meeting 38 (in English), 1981.

No. 29a. Policy analysis for the national water management of the Netherlands.
Background papers for Technical Meeting 39 (in English), 1982.
(Netherlands contributions, related to the PAWN-study, for the ECE-seminar-1980).

No. 29b. Economic instruments for rational utilization of water resources.
Netherlands contributions, not related to the PAWN-study, for the ECE-seminar-1982 (in English), 1982.

No. 30 The role of hydrology in the United Nations Water Decade.
Proceedings of Technical Meeting 40 (in English), 1983.

No. 31 Methods and instrumentation for the investigation of groundwater systems.
Proceedings of International Symposium, Noordwijkerhout, The Netherlands (in English, with summaries in French), 1983.

No. 32*) Planning of water resources management on a regional scale.
Proceedings of Technical Meeting 41 (with Preface in English), 1985.
*) Out of print.

No. 33 Water in urban areas.
Proceedings of Technical Meeting 43 (in English), 1985.

No. 34 Water management in relation to nature, forestry and landscape management.
Proceedings of Technical Meeting 43 (in English), 1986.

No. 35 Design aspects of hydrological networks.
Published with support of the World Meteorological Organization (in English), 1986.

No. 36 Urban storm water quality and effects upon receiving waters.
Proceedings of International Conference, Wageningen,
The Netherlands (in English), 1986.

No. 37 Water in the Netherlands.
Reprint of special issue CHO-TNO 1946-1986 with annex Selection of current research topics, (in English), 1989.

No. 38 Vulnerability of soil and groundwater to pollutants.
Proceedings of the International Conference, Noordwijkerhout, the Netherlands, organized by the National Institute of Public Health and Environmental Hygiene (in English), 1987.

No. 39 Evaporation and weather.
Proceedings of Technical Meeting 44 (in English), 1987.

No. 40 Geothermal energy and heat storage in aquifers.
Proceedings of Technical Meeting 45 (in English), 1988.

No. 41 Hydro-ecological relations in the Delta Waters of the South-West Netherlands.
Proceedings of Technical Meeting 46 (in English), 1989.

No. 42 Water management and remote sensing.
Proceedings of Technical Meeting 47 (in English), 1990.

All reports are written in English except reports nos.:
1, 2, 3, 4, 6, 8, 9, 11, 14, 16, 22, 32.

For order and price information:
CHO-TNO
P.O. Box 297
2501 BD THE HAGUE
The Netherlands